diversity

MDPI

Article

A Mitogenome-Based Phylogeny of Pilargidae (Phyllodocida, Polychaeta, Annelida) and Evaluation of the Position of *Antonbruunia* †

Sonja Huč *, Avery S. Hiley, Marina F. McCowin and Greg W. Rouse *

Scripps Institution of Oceanography, University of California San Diego, La Jolla, CA 92093-0021, USA; marruda@ucsd.edu (M.F.M.)

* Correspondence: shuc@ucsd.edu (S.H.); grouse@ucsd.edu (G.W.R.)

† LSID urn:lsid:zoobank.org:pub:031E6202-C5DB-4D78-862E-07736AD07B6E.

Abstract: Pilargidae is a family of free-living and burrowing marine annelids. A lack of available molecular data for most of these species has precluded a molecular assessment of their phylogenetic relationships and has left uncertain the placement of *Antonbruunia*, which is hypothesized to be either a member of Pilargidae or its sister clade, the monotypic family Antonbruunidae. In this study, we describe the new species *Antonbruunia milenae* sp. nov., found at 845 m of depth off the coast of San Diego, California, USA, and we address the phylogeny of these organisms using 15 novel mitogenomes and multiple Sanger-sequenced loci. Our results show that *Antonbruunia* falls within Pilargidae, making Antonbruunidae a junior synonym of Pilargidae. *Glyphohesione* was transferred from Pilarginae to Synelminae, the previously unassigned genera *Otopsis* and *Antonbruunia* were shown to belong within Synelminae, and *Hermundura* was assigned to Phyllodocida *incertae sedis*. *Sigambra* was found to be non-monophyletic. Four different mitogenome gene orders were found among Pilargidae. Changes between the gene orders and the ancestral state gene order of the family were inferred. Two species have introns within the COI gene. These efforts represent a significant expansion of the available molecular resources for pilargids, as well as the basis for a more stable taxonomy.

Keywords: polychaete; deep sea; Microphthalmidae; *Hermundura*; *Antonbruunia*; marine invertebrates; whale fall; gene order; phylogenetics; mitogenomes

check for updates

Citation: Huč, S.; Hiley, A.S.; McCowin, M.F.; Rouse, G.W. A Mitogenome-Based Phylogeny of Pilargidae (Phyllodocida, Polychaeta, Annelida) and Evaluation of the Position of *Antonbruunia*. *Diversity* **2024**, *16*, 134. https://doi.org/10.3390/d16030134

Academic Editors: Michael Wink, Luc Legal and Michel Baguette

Received: 30 December 2023
Revised: 31 January 2024
Accepted: 6 February 2024
Published: 21 February 2024

Copyright: © 2024 by the authors. Licensee MDPI, Basel, Switzerland. This article is an open access article distributed under the terms and conditions of the Creative Commons Attribution (CC BY) license (https://creativecommons.org/licenses/by/4.0/).

1. Introduction

Annelids are a diverse animal group, with over 20,000 described species [1,2]. Up until the last few decades, morphology was the only way of assessing species diversity and inferring phylogenetic relationships. Now that molecular phylogenetic methods are well established and readily available, our understanding of the placement of many annelid taxa has been revised at both low [3,4] and high [5,6] taxonomic levels. This is an ongoing process, partially because it is difficult to obtain samples of many taxa due to their rarity or the inaccessibility of their habitat. Such is the case for *Antonbruunia* Hartman and Boss, 1965, a genus of inquiline phyllodocid annelid worms that live inside chemosynthetic bivalves from the families Lucinidae Fleming, 1828, Thyasiridae Dall, 1900 (1895), and Vesicomyidae Dall and Simpson, 1901 [7]. *Antonbruunia* are mostly found in the deep sea, and each species has been encountered only once [7–9]. The first species to be described, *Antonbruunia viridis* Hartman and Boss 1965, was found inhabiting the mantle cavity of *Opalocina fosteri* (Hartman and Boss 1965) (Bivalvia: Lucinidae) off the coast of Madagascar at a depth of 70 m. In each opened bivalve, there was almost always one smaller male and one larger female present.

Since its first description, the taxonomic placement of *Antonbruunia* has been a source of discussion and uncertainty. Hartman and Boss [8] speculated that their new genus was

related to but not included within Pilargidae Saint-Joseph, 1899. This is because *Antonbruunia*, like the discovered pilargids up to that point, had only simple chaetae, paired enlarged cirri on the first segment, and a simple prostomium. Unlike pilargids, *Antonbruunia* was sexually dimorphic, had parapodia that appeared uniramous despite being biramous, and they lacked eyes. Fauchald subsequently erected Antonbruunidae Fauchald, 1977, with the only differing characteristics from Pilargidae being sexual dimorphism and an inquiline lifestyle [10]. However, some have since argued that *Antonbruunia* should be classified within Pilargidae, noting the morphological disparity already included within the group [2,11–13]. Salazar-Vallejo argued that the differences Fauchald [10] listed for *Antonbruunia* are likely a result of their lifestyle and that erecting a new family was unjustified since similar morphological changes have occurred in other annelid groups [12]. Miura and Laubier considered whether *Antonbruunia* should be placed in Chrysopetalidae Ehlers, 1864, though ultimately decided the genus was more related to Pilargidae based on morphology [14]. Fitzhugh and Wolf disagreed with Salazar-Vallejo's [12] morphological interpretations and did not consider *Antonbruunia* in their cladistic analysis of Pilargidae [15]. Glasby synonymized Antonbruunidae with Pilargidae [11], while others ultimately concluded that there was not yet enough information available to confidently classify these worms using only morphology [2,16–19].

A second species, *Antonbruunia gerdesi* Quiroga and Sellanes, 2009, was discovered inside *Calyptogena gallardoi* Sellanes and Krylova, 2005 (Bivalvia: Vesicomyidae), at a depth of 750–900 m off the coast of Chile [9]. Within three of the four bivalves where the species was found, there was only a single worm, while the fourth bivalve contained three. Mackie et al. found a third species, *Antonbruunia sociabilis* Mackie, Oliver and Nygren, 2015, inside *Thyasira scotiae* Oliver and Drewery, 2014 (Bivalvia: Thyasiridae), off the coast of Scotland at a depth of 1200 m [7]. The name refers to the fact that multiple specimens were found within each dissected clam. The authors generated mitochondrial 16S rRNA (16S) and nuclear 18S rRNA (18S) sequences to assess the phylogenetic placement of *Antonbruunia*. Although the molecular phylogenies of Mackie et al. [7] included sequences of *Antonbruunia sociabilis* and representatives from fifteen other families of annelids, the position of *Antonbruunia* varied across their analyses, though the Bayesian analysis of the combined data suggested a sister group relationship to the included pilargids. The sampling of pilargids (*Ancistrosyllis* McIntosh, 1878, and *Sigambra* Müller, 1858 [7]) was insufficient to assess whether *Antonbruunia* falls within Pilargidae.

In 2020, specimens of *Antonbruunia* were found inside *Calyptogena pacifica* Dall, 1891 (Bivalvia: Vesicomyidae), from a whale fall (whale carcass on the sea floor) off the coast of California at a depth of ~845 m. This find, along with the availability of a range of pilargids in the Scripps Institution of Oceanography Benthic Invertebrate Collection (SIO-BIC), presented an opportunity to investigate the phylogenetic position of *Antonbruunia* (species overview in Table A1). This study combined newly obtained genetic and morphological data with publicly available sequences to evaluate the phylogenetic position of *Antonbruunia*, as well as determine the sub-familial classification of some yet unassessed pilargid genera, such as *Otopsis* Ditlevsen, 1917.

2. Materials and Methods

2.1. Sample Collection

Specimens of *Antonbruunia milenae* sp. nov. were recovered from inside *Calyptogena pacifica* (Bivalvia: Vesicomyidae) clams that were collected using the ROV (remotely operated vehicle) *Doc Ricketts* piloted off the R/V *Western Flyer* in 2020 at the Rosebud whale fall, 845 m depth, off the coast of San Diego, CA, USA. Fourteen pilargid taxa, one nephtyid (Figure 1), and four other members of Phyllodocida from various localities collected between 1998 and 2023 were also studied here. Live specimens were photographed, morphological voucher specimens were fixed in 5–10% formalin in sea water, rinsed, and transferred to 50% ethanol, and specimens for genetic analysis (whole animals or samples of the posterior or midsection) were fixed directly in 95% ethanol. Specimens were deposited

at SIO-BIC, La Jolla, CA, USA. Additionally, whole genomic DNA extractions of *Pilargis wolfi* Salazar-Vallejo and Harris, 2006 (USNM1499416), and *Hermundura fauveli* Berkeley and Berkeley, 1941 (USNM1643733), were borrowed from the Smithsonian Institution National Museum of Natural History (USNM), and the physical voucher (entire specimen besides what was used for the extraction) for the same specimen of *Hermundura fauveli* was borrowed from the Florida Museum of Natural History (UF). Sequences from the rest of the specimens were obtained from NCBI GenBank and the Barcode of Life Database (BOLD). Specimen details are summarized in Tables 1 and 2.

Table 1. All sequences used in the three-gene phylogeny and additional Sanger sequences. Newly obtained sequences and newly obtained samples are set in bold. The holotype is labeled with an asterisk.

Species	Voucher	Locality	Depth (m)	COI	16S rRNA	18S rRNA
Micronephthys minuta	**SIO-BIC A15537**	Disko Island, Greenland (69.2901, −53.2143)	190	**OR126034**	**OR159884**	**OR159893**
Nephtys hombergii	MB36000118 [20]	Ria Aveiro, Portugal (40.642, −8.754)	-	GU179410	-	GU179377
	MB36000136 [20]	Bohuslän, Sweden (58.217, 10.595)	-	-	GU179354	-
Nephtys sp.	AB-2017 [21]	NE Pacific (48.5, −127.0)	-	**KY972420**	**-**	**-**
Antonbruunia milenae sp. nov.	**SIO-BIC: A12278,**	San Diego, CA, USA (32.7769, −117.4881)	845	**OR126047**	**-**	**-**
	A12279,			**OR126043**	**OR159883**	**OR148950**
	A12280,			**OR126045**	**-**	**-**
	A12281 *,			**OR126046 ***	**-**	**-**
	A12283			**OR126044**	**-**	**-**
Antonbruunia sociabilis	NMW<GBR>: Z.2012.074.13 [7]	Scotland (57.9500, −15.5500)	1200	-	KP992845	KP992843
Pilargis verrucosa	**SIO-BIC A13955**	Koster, Sweden (58.895, 10.989)	-	**OR126029**	**OR159877**	**OR159892**
Pilargis wolfi	USNM1499416	Virginia, USA (37.5848, −75.6486)	-	USNM1499416	**OR159878**	**OR159891**
Pilargis cf. *cholae*	**SIO-BIC A4846**	Carrie Bow Cay, Belize (16.8134, −88.0817)	1	**OR126031**	**OR159876**	**OR159890**
Cabira pilargiformis	BIOUG06647-G01 [22]	Dongying, China (37.948, 119.361)	16	HZPLY558-13	-	-
Sigambra magnuncus	[23]	W Africa (−5.34, 3.68)		GQ426642	GQ426621	GQ426593
Sigambra hanaokai	**SIO-BIC: A5771, A15561**	Tanabe Bay, Japan (33.6997, 135.3268)	32–36	**OR126015, OR126016**	**OR159880 -**	**OR159886 -**
Sigambra parva	Vd4(c)-Pil [24]	NW India (22.3000, 69.3900)	-	KY775644	-	-

Table 1. *Cont.*

Species	Voucher	Locality	Depth (m)	COI	16S rRNA	18S rRNA
Sigambra sp. 1	**SIO-BIC: A1516,**	W Costa Rica (8.9308, −84.3072)	967–1005	**OR126027,**	**OR123440**	**PP034425**
	A9597,	W Costa Rica (9.1174, −84.8396)	1795	**OR126028,**	-	-
	A9843	W Costa Rica (8.9309, −84.3133)	999	**OR126026**	-	-
Sigambra sp. 2	**SIO-BIC A10175**	W Costa Rica (7.6802, −85.9118)	528.2	**OR126014**	**OR123444**	**PP034426**
Sigambra sp. 3	**SIO-BIC: A15568,**	Rovinj, Croatia (45.0915, 13.6244)	25	**OR126019,**	**OR159881**	**OR159887**
	A15569,			**OR126020,**	**-**	**-**
	A15570,			**OR126021,**	**-**	**-**
	A15571,			**OR126018,**	**-**	**-**
	A15572,			**OR126023,**	**-**	**-**
	A15573			**OR126022,**	**-**	**-**
	A5926	Banyuls-sur-Mer, France (42.4958, 3.1400)	24	**OR126017**	**OR159882**	**OR159888**
Sigambra sp. 4	**A16333**	Hong Kong, China (22.4692, 114.2117)	1	**PP050561**	**PP034423**	-
Litocorsa stremma	Itsastk13-P23 [25]	N Spain (44.75, −4.96)	-	KT307655	-	-
Ancistrosyllis sp.	**SIO-BIC A12326**	Santa Monica, CA, USA (33.8385, −118.6904)	711	**OR126024**	**OR123445**	**PP034427**
Ancistrosyllis breviceps	**SIO-BIC A6261**	Santa Barbara, CA, USA (34.3700, −120.0300)	400	**OR126025**	**OR159879**	**OR159889**
Ancistrosyllis groenlandica	Itsastk13-P43 [25],	N Spain, (44.75, −4.96)	-	KT307624	-	-
	[26]	-	-	-	-	DQ790075
Glyphohesione klatti	**SIO-BIC A6066**	N Trondheim, Norway (63.5086, 10.4419)	35	**OR126035**	**OR123443**	**PP034428**
Otopsis sp.	**SIO-BIC: A15574,**	Monterey, CA, USA (36.7721, −122.0831)	2892–2937	**OR126036,**	**OR123441**	**PP034429**
	A15575,			**OR126037,**	**-**	**-**
	A15576,			**OR126039,**	**-**	**-**
	A15577,			**OR126042,**	**-**	**-**
	A15578,			**OR126040,**	**-**	**-**
	A15579,			**OR126041,**	**-**	**-**
	A15580			**OR126038**	**-**	**-**
Synelmis amoureuxi	**SIO-BIC A4721**	Carrie Bow Cay, Belize (16.8032, −88.0778)	10	**OR126033**	**OR123442**	**PP034430**

Table 1. *Cont.*

Species	Voucher	Locality	Depth (m)	COI	16S rRNA	18S rRNA
Pseudexogone cf. *backstromi*	**SIO-BIC A2813**	S Pacific (−17.4904, −129.8267)	18–20	**OR126032**	**OR159875**	**OR159895**
Hermundura americana	**A16381** **A16382**	Pagan River, Chesapeake Bay, VA, USA	- -	**PP050562** **PP050563**	**PP034424** **-**	**PP033026** **PP033027**
Hermundura fauveli	USNM1643733 [27]	Bremerton, WA, USA (47.5471, −122.6620)	-	BBPS179-19	**OR159885**	**OR159894**

Table 2. All the sequences that were used for the mitogenome analysis. Newly obtained sequences and newly obtained samples are set in bold.

Species	Voucher	Locality	Depth (m)	18S rRNA	Mitochondrial Genome
Micronephthys minuta	**SIO-BIC A15537**	Disko Island, Greenland (69.2901, −53.2143)	190	**OR159893**	**OR123448**
Nephtys sp.	AB-2017 [21]	NE Pacific (48.5, −127.0)	-	-	KY972376, KY972406, KY972433, KY972447, KY972462, KY972476, KY972490, KY972504, KY972532
Antonbruunia milenae sp. nov.	**SIO-BIC A12279**	San Diego, CA, USA (32.7769, −117.4881)	845	**OR148950**	**OR123446**
Pilargis verrucosa	**SIO-BIC A13955**	Koster, Sweden (58.895, 10.989)	-	**OR159892**	**OR123439**
Pilargis wolfi	USNM1499416	Virginia, USA (37.5848, −75.6486)	-	**OR159891**	**OR123447**
Sigambra sp. 1	**SIO-BIC A1516**	W Costa Rica (8.9308, −84.3072)	967–1005	**PP034425**	**OR123440**
Sigambra sp. 2	**SIO-BIC A10175**	W Costa Rica (7.6802, −85.9118)	528.2	**PP034426**	**OR123444**
Sigambra sp. 3	**SIO-BIC A15568**	Rovinj, Croatia (45.0915, 13.6244)	25	**OR159887**	**PP035855**
Ancistrosyllis sp.	**SIO-BIC A12326**	Santa Monica, CA, USA (33.8385, −118.6904)	711	**PP034427**	**OR123445**
Glyphohesione klatti	**SIO-BIC A6066**	N Trondheim, Norway (63.5086, 10.4419)	35	**PP034428**	**OR123443**
Otopsis sp.	**SIO-BIC A15574**	Monterey, CA, USA (36.7721, −122.0831)	2892–2937	**PP034429**	**OR123441**
Synelmis amoureuxi	**SIO-BIC A4721**	Carrie Bow Cay, Belize (16.8032, −88.0778)	10	**PP034430**	**OR123442**
Lacydonia sp.	**SIO-BIC A2650**	Hydrate Ridge, OR, USA (44.6701, −125.0987)	587–610	**PP034431**	**PP035856**
Phyllodoce medipapillata	**SIO-BIC A4340**	La Jolla, CA, USA (32.8145, −117.2740)	1	**PP034432**	**PP035857**

Table 2. *Cont.*

Species	Voucher	Locality	Depth (m)	18S rRNA	Mitochondrial Genome
Struwela camposi	**SIO-BIC A13437**	San Felipe, Mexico (31.0700, −114.8400)	1	**PP033480**	**PP035858**
Hermundura fauveli	USNM1643733	Bremerton, WA, USA (47.5471, −122.6620)	-	**OR159894**	**OR124844**
Microphthalmus listensis	85792 [28]	List, Germany (55.0156, 8.4379)	-	-	MN855111, MN855121, MN855130, MN855139, MN855149, MN855158, MN855175, MN855183, MN855191,
	76292 [28]	List, Germany (55.0232, 8.4401)	-	-	MN855200, MN855210 MN855206
Microphthalmus similis	76290	List, Germany (55.0232, 8.4401)	-	-	MN855112, MN855122, MN855131, MN855140, MN855150, MN855160, MN855168, MN855184, MN855192, MN855201
Chrysopetalum debile	[29]	Mallorca, Spain	1	MZ450125	MZ506670
Arichlidon gathofi	AG01 [28]	-	-	-	OQ732695
	13915 [30]	NC, USA (33.9993, −76.7026)	-	-	MN855107, MN855116, MN855126, MN855135, MN855144, MN855154, MN855164, MN855171, MN855178,
	18126 [30]	Bocas del Toro, Panama (9.3339, −82.2205)	-	-	MN855188, MN855196 MN855127, MN855197, MN855205
Bhawania goodei	27046 [30]	Bocas del Toro, Panama (9.3667, −82.3000)	-	-	MN855118, MN855128, MN855146, MN855156, MN855166, MN855173, MN855180, MN855189, MN855198, MN855208
Nereis pelagica	SIO-BIC A6054 [31]	Trondheim, Norway (63.4410, 10.3482)	0	OR437939	OL782598
Nectoneanthes oxypoda	SIO-BIC A13109 [31]	Osaka Bay, Japan (34.3300, 135.1400)	-	OR437940	OL782599
Oxydromus pugettensis	23185 [30]	Snug Harbor, WA, USA (48.5755, −123.1699)	-	-	MN855113, MN855123, MN855132, MN855141, MN855151, MN855161, MN855176, MN855185, MN855193, MN855202, MN855211
	[26]	-	-	DQ790086	-
Leocrates chinensis	XMU-Pol-2021-354 [32]	Hong Kong, China (22.2360, 114.1852)	9.1	-	NC066969
	SMNH83510 [33]	Lifou, New Caledonia	-	DQ442589	-
Glycinde armigera	FS17 [34]	Bellingham Bay, WA, USA	-	KT989339	KT989325
Goniada japonica	[35]	Hailing Island, China	-	-	KP867019
Hemipodia simplex	FS13 [34]	Bamfield, Canada	-	KT989342	KT989322
Glycera dibranchiata	FS05 [34]	Loagy Bay, MA, USA	-	KT989350	KT989318

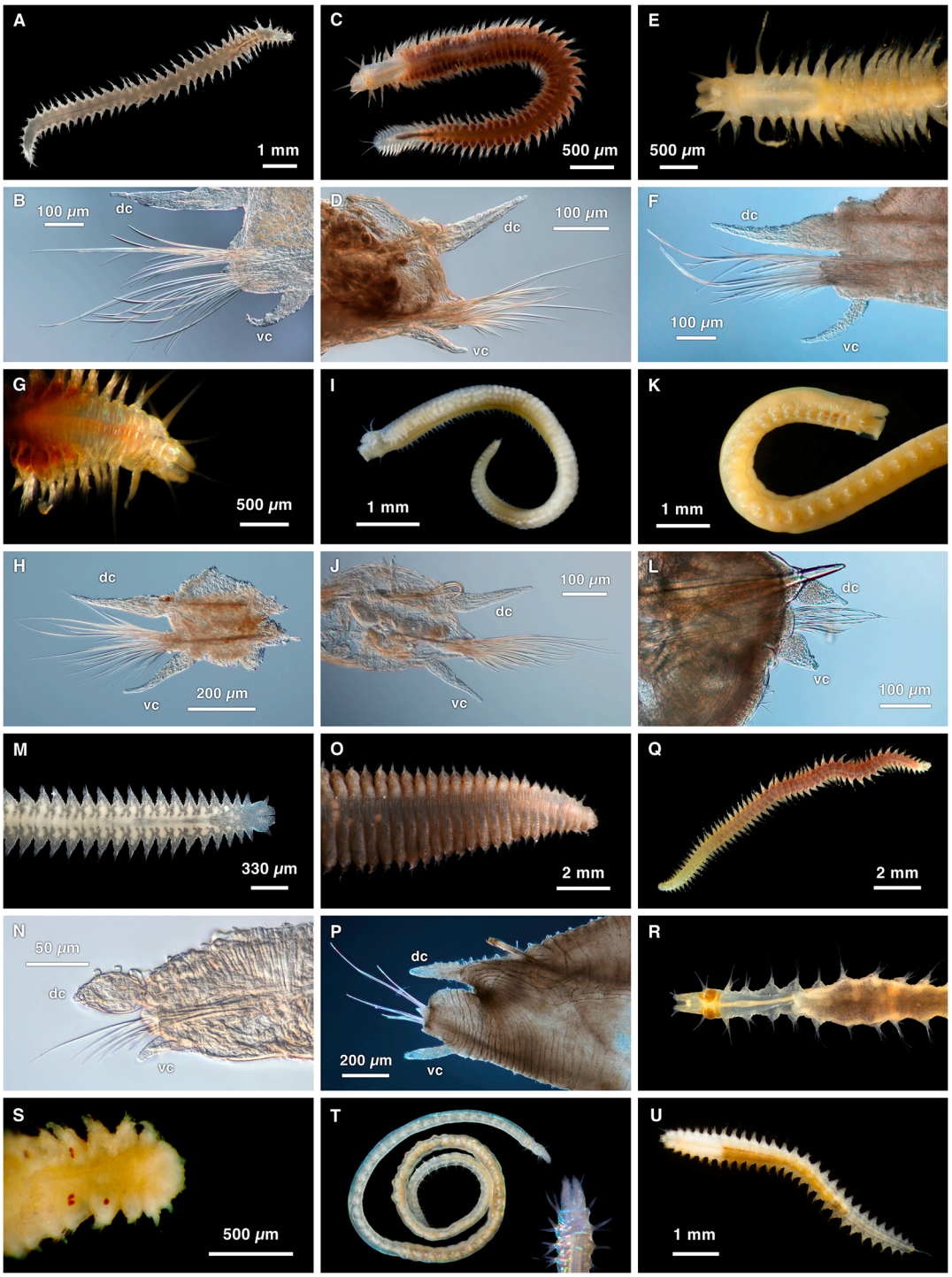

Figure 1. Diversity of newly collected Pilargidae and a nephtyid outgroup. *Otopsis* sp.: (**A**) live dorsal photo, (**B**) preserved parapodium; *Sigambra* sp. 3: (**C**) live dorsal photo, (**D**) preserved parapodium; *Sigambra* sp. 1: (**E**) live anterodorsal photo, (**F**) preserved parapodium; *Sigambra* sp. 2: (**G**) live anterodorsal photo, (**H**) preserved parapodium; *Sigambra hanaokai*: (**I**) live lateral photo, (**J**) preserved parapodium; *Synelmis amoureuxi*: (**K**) preserved lateral anterior photo, (**L**) preserved parapodium; *Pilargis* cf. *cholae*: (**M**) live dorsal anterior photo, (**N**) preserved parapodium; *Ancistrosyllis* sp.: (**O**) live dorsal anterior photo, (**P**) preserved parapodium; (**Q**) *Ancistrosyllis breviceps* live dorsal photo, (**R**) *Glyphohesione klatti* live dorsal anterior photo, (**S**) *Pilargis verrucosa* preserved dorsal anterior photo, (**T**) *Pseudexogone* cf. *backstromi* live photo, (**U**) outgroup *Micronephthys minuta* live dorsal photo. Abbreviations: dc, dorsal cirrus; vc, ventral cirrus. Scales provided when known.

2.2. DNA Extraction, Amplification, Sequencing, and Assembly

DNA was extracted using the Zymo Research Quick-DNA ™ Miniprep (most specimens) or Microprep (SIO-BIC: A2813, A4846, A6066, A6261, A9843, A13955, A16333) Plus Kit (Zymo Research Corporation, Irvine, CA, USA), following the manufacturer-supplied protocol. Regions of the mitochondrial genes cytochrome oxidase subunit I (COI) and 16S rRNA (16S) and the nuclear gene 18S rRNA (18S) were amplified on Eppendorf thermal cyclers using the primers in Table A2. PCR amplification was performed with a mixture of 8.5 µL of ddH_2O, 1 µL of each appropriate forward and reverse primer (Table A2), 2 µL of eluted DNA, and 12.5 µL of Apex 2.0x Taq Red DNA Polymerase Master Mix (Genesee Scientific Corporation, El Cajon, CA, USA) for most amplifications or Conquest ™ PCR 2x Master Mix-1 (Lamda Biotech, Ballwin, MO, USA) for others (Table A3). See Table A4 for PCR protocols. The primer pair AnnF/16Sb was used in PCR reactions for 16S for samples SIO-BIC: A13955, A15537, A15568, A16333, and A16381 and USNM1499416 and USNM1643733, while the primer pair 16SarL/16SbrH was used for all other 16S PCR amplifications. The ExoSAP-IT protocol (Affymetrix, Santa Clara, CA, USA) was used to purify the PCR products, which were then Sanger sequenced by Eurofins Genomics (Louisville, KY, USA). The "De Novo Assembly" option with default settings was used to assemble consensus sequences in Geneious Prime v. 2022.2.2 [36].

The DNA extractions from specimens SIO-BIC: A1516, A2650, A4340, A4721, A6066, A10175, A13437, A13955, A12279, A12326, A15537, A15568, and A15574, USNM1499416, and USNM1643733 were sent to Novogene www.novogene.com/us-en (accessed on 31 January 2024) for library preparation and whole genome skimming using 150 base pair (bp) paired-end reads on the Illumina NovaSeq 6000 platform (Illumina, San Diego, CA, USA); Table A5 shows the number of generated paired-end 150 bp long raw reads per sample. Before this, whole genomic extractions from samples SIO-BIC A13955, USNM1499416, and USNM1643733 were amplified to reach sufficient DNA concentrations using the Illustra Ready-To-Go GenomiPhi V3 DNA Amplification Kit (Cytiva, Marlborough, MA, USA), according to the manufacturer's protocol, except in the amount of DNA added for sample USNM1643733, for which there was only 4.65 ng of total DNA available instead of the recommended minimum of 10 ng. The sequence reads, which were trimmed and cleaned with Trimmomatic v. 0.39 [37], were then assembled using MitoFinder v. 1.4 [38], using The Invertebrate Mitochondrial Code (NCBI; transl_table = 5) to translate the 13 protein-coding genes. The reference file used for MitoFinder contained the complete records for all RefSeq annelid mitogenomes that were publicly available on NCBI GenBank. The integrated MitoFinder pipeline with MEGAHIT v. 1.2.9 [39] and Arwen v.1.2.3 [40] parameters was used to annotate the assembled mitochondrial genomes. Sample USNM1643733 was also assembled and annotated using NOVOPlasty [41] and MitoZ [42]. The MITOS Web Server [43] was used to check annotations, and Geneious Prime v. 2022.2.2 [36] was used to manually modify the annotated mitogenome assemblies if needed, extract the finalized nucleotide genes, and translate the protein-coding genes into amino acids, using The Invertebrate Mitochondrial genetic code. The paired-end reads were also used to obtain mapped 18S sequences for samples SIO-BIC: A1516, A2650, A4340, A4721, A6066, A10175, A12326, A13437, and A15574, using MITObim [44], Minimap2 v. 2.22 [45,46], and SamTools 1.13 [47] to interleave and map the reads to a reference file of publicly available Phyllodocida 18S sequences from NCBI GenBank. Mapped reads were visualized with Geneious Prime v. 2022.2.2 [36], and a consensus 18S sequence was chosen for each specimen.

The complete COI genes obtained through bioinformatically assembled whole mitogenomes of *Antonbruunia milenae* sp. nov. (SIO-BIC A12279) and *Synelmis amoureuxi* (SIO-BIC A4721) contained an apparent intron; thus, three primer pairs (Table A2) were designed within Geneious Prime v. 2022.2.2 [36] using a modified version of Primer3 2.3.7 [48] to either confirm this or show they represented assembly artifacts. For all three primer pairs, a mix of 12.5 µL of Conquest ™ PCR 2x Master Mix-1 (Lamda Biotech), 8.5 µL of ddH_2O, 1 µL of both the forward and reverse primer, and 2 µL of eluted DNA was used. See Table A4 for PCR protocols. The amplified *Antonbruunia milenae* sp. nov. intron

sequence spans the terminal end of the first COI segment, the entire intron, and the initial part of the second COI segment. Because the *Synelmis amoureuxi* intron was so long, the first primer pair was designed to amplify only the terminal end of the first COI segment and the initial part of the intron, while the second primer pair was designed to amplify only the terminal end of the intron and the initial part of the second COI segment. To confirm that the presence of introns was not a bioinformatic artifact, the resulting Sanger sequences were pairwise aligned with the bioinformatically assembled COI sequences in Geneious Prime v. 2022.2.2 [36] with MUSCLE alignment using Muscle v. 3.8.425 [49]. Then, the uncorrected pairwise distance between the introns was calculated using PAUP* v.40a [50].

2.3. Morphological Analyses

Parapodia and isolated chaetae of preserved specimens were permanently mounted on slides with Aquamount ® (Thermo Fisher Scientific, Waltham, MA, USA) and observed on a Leica DMR HC with a compound light microscope with differential interference contrast. A Leica MZ12.5 or MZ9.5 stereomicroscope (Leica Microsystems Inc., Deerfield, IL, USA) was used for observing whole or larger sections of the preserved specimens. A Canon Rebel T6i camera (Canon U.S.A., Inc, Melville, NY, USA) was used for taking light micrographs. Additionally, a Zeiss EVO10 (Carl Zeiss AG, Oberkochen, Germany) was used for scanning electron microscopy (SEM). Samples that were prepared for SEM were first dehydrated in an ethanol series, transferred to hexamethyldisilazane (HMDS), and then air dried in a fume hood overnight. Larger pieces were first rehydrated in distilled water, soaked in 4% osmium tetroxide for 1.5 h, then rinsed with more distilled water for three days, and finally once again dehydrated in an ethanol series. Once dry, samples were mounted on a double-sided adhesive carbon tab and aluminum tape covered aluminum stubs, and then they were sputter coated with gold-palladium (Au-Pd) using a Quorum SC7620 Mini Sputter Coater (Quorum Technologies, East Sussex, UK). SEM stubs with prepared specimen samples were lodged at SIO-BIC.

2.4. Phylogenetic Analyses

All obtained single gene sequence datasets were aligned in the program Mesquite v3.61 [51] using MAFFT v.7.453 [52] under the default G-INSI-I method, with gaps included for all the nucleotide single gene datasets (Table A6) used and MUSCLE v.3.8.31 [53] with the default setting and gaps included for all the amino acid single gene datasets used (Table A6). The concatenated COI, 16S, and 18S phylogeny single gene datasets used Sanger sequences whenever possible, while datasets used in the concatenated 13 protein-coding, 12S rRNA (12S), and 16S mitochondrial and 18S nuclear gene phylogeny used data obtained through genome skimming whenever possible. Based on Tilic et al. [6], Nephtyidae Grube, 1850, is the sister taxon to Pilargidae and so was chosen as the outgroup for pilargids and *Antonbruunia* in the three-gene phylogeny. In the 16-gene phylogeny, Phyllodociformia, Glyceriformia, and Nereidiformia were also included as further outgroups for Pilargidae, *Antonbruunia*, and Nephtyidae. RAxML GUI 2.0 v.2.0.10 [54] was used to concatenate each gene partition for each analysis. The "raxml-ng-ARM64" setting was used for the maximum likelihood + thorough bootstrap + consensus analysis of the three-gene phylogeny with 500 runs, 1000 reps, and a seed of 291395. The substitution model, proportion of invariant sites, and rate heterogeneity were chosen with the integrated "RUN MODELTEST" function for each partition (Table A6). The 16-gene mitochondrial (Table A6) maximum likelihood + thorough bootstrap + consensus phylogeny was analyzed using the "raxml-ng" setting with 100 runs, 1000 reps, and a seed of 897189. The substitution model, proportion of invariant sites, and rate heterogeneity were chosen with the integrated "modeltest-ng" option for each partition (Table A6). FigTree v1.4.4 [55] was used for displaying the trees. PopART [56] was used to create and visualize the *Antonbruunia milenae* sp. nov. haplotype network. Mitochondrial gene orders were analyzed with default settings using TreeREx v.1.85 [57] and CREx [58] to infer ancestral gene order states and the locations and types of changes along the phylogeny, and IQ-TREE v.1.6.12 [59–61] was used to perform the

approximately unbiased (AU) topology test [62] with the same dataset and models used for the 16-gene mitogenome phylogeny (Table A6). A total of 10,000 replicates were used to generate *p*-values and likelihood scores for unconstrained and constrained trees to assess the monophyly of Pilargidae and Microphthalmidae Hartmann-Schröder, 1971.

3. Results

3.1. Phylogenetic Results

The 16-loci maximum likelihood (ML) tree (combining mitochondrial genomes and nuclear 18S rRNA, Figure 2) recovered a strongly supported clade of Pilargidae that included *Antonbruunia milenae* sp. nov. Two major pilargid clades were apparent—a highly supported Pilarginae and less supported Synelminae. Within Pilarginae, the monophyly of *Sigambra* was not recovered, as *Ancistrosyllis* was nested inside, albeit with low support. Within Synelminae, *Antonbruunia milenae* sp. nov. formed a well-supported clade as a sister taxon to *Otopsis* Ditlevsen, 1917, and *Glyphohesione klatti* Friedrich, 1950, with the latter taxon currently considered part of Pilarginae [63]. *Synelmis amoureuxi* Salazar-Vallejo, 2003, was recovered as a sister group to the *Otopsis* + *Glyphohesione* + *Antonbruunia* clade, though with low support. Currently considered part of Synelminae [64,65], *Hermundura fauveli* was not recovered within Pilargidae but as sister to *Microphthalmus* Mecznikow, 1865, though with low support. The AU topology test [62] of the best unconstrained tree (Figure 2) versus a constrained tree, where *Hermundura* was part of Pilargidae, showed that the best tree was significantly better than the constrained topology ($p = 0.00018$). Notably, Microphthalmidae was non-monophyletic (Figure 2) with *Struwela camposi* Salazar-Vallejo, de León-Gonzáles and Carrera-Parra, 2019, as sister to Nereididae Blainville, 1818, and not *Microphthalmus*. However, an AU test with Microphthalmidae constrained as monophyletic was not significantly worse than the best tree topology shown in Figure 2 ($p = 0.187$).

The concatenated mitochondrial COI, 16S rRNA, and nuclear 18S rRNA ML analysis of Pilargidae rooted with nephtyids (Figure 3) was generated to show a greater variety of pilargids and include more genera for which mitogenomes were unavailable (*Cabira* Webster, 1879, *Litocorsa* Pearson, 1970, *Pseudexogone*, Augener 1922). *Hermundura* was excluded based on the results shown in Figure 2 and the AU topology test. Figure A1 shows that if *Hermundura* is included in the three gene concatenated ML analysis, then it appears as a sister taxon to all pilargids; although, this is arguably misleading given the limited taxon selection.

A well-supported Pilarginae, including *Pilargis* Saint-Joseph, 1899, *Cabira*, *Sigambra*, and *Ancistrosyllis* was congruent with the mitogenome tree (Figure 2). *Sigambra* was again non-monophyletic, forming two distinct well-supported clades, one of which was a sister taxon to the *Ancistrosyllis* clade, though with low support. Synelminae was not monophyletic, forming a grade with respect to Pilarginae, and it included *Synelmis* [12], *Pseudexogone* [66], *Litocorsa* [12], *Glyphohesione klatti*, *Otopsis*, and *Antonbruunia* (Figure 2). In contrast to Figure 2, *Antonbruunia* was sister to *Otopsis* sp. with high support, and *Glyphohesione klatti* Friedrich, 1950, formed a highly supported (100) clade with these terminals. This result also supported *Antonbruunia* as nested within Pilargidae.

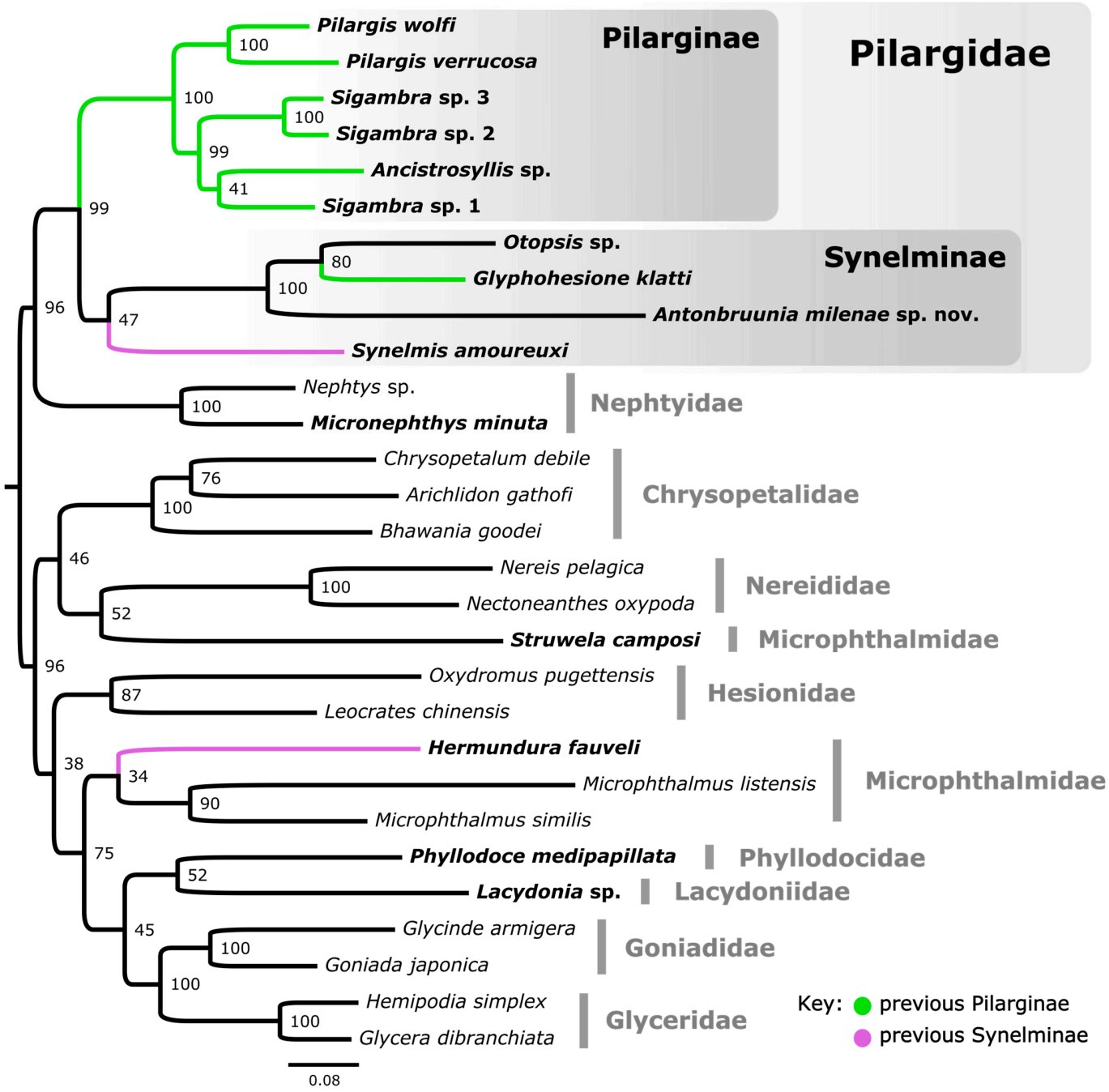

Figure 2. Concatenated maximum likelihood (ML) tree of Pilargidae and Nephtyidae with Chrysopetalidae, Nereididae, Microphthalmidae, Hesionidae, Phyllodocidae, Lacydoniidae, Goniadidae, and Glyceridae as the outgroup using the thirteen protein-coding mitochondrial genes, two non-protein-coding mitochondrial genes 12S rRNA and 16S rRNA, and the nuclear 18S rRNA gene. The protein-coding genes were input as amino acid sequences, while the rRNA genes coded as nucleotides. ML thorough bootstrap values are represented by numbers at the nodes. Species names set in bold indicate new sequences obtained in this study. Purple branches indicate species currently placed within Synelminae, green branches indicate species currently placed within Pilarginae, and black pilargid branches indicate unknown sub-familial placement until this study. Gray rectangles grouped pilargids together based on new family and sub-familial delimitations, while gray vertical lines grouped non-pilargid species into their respective families.

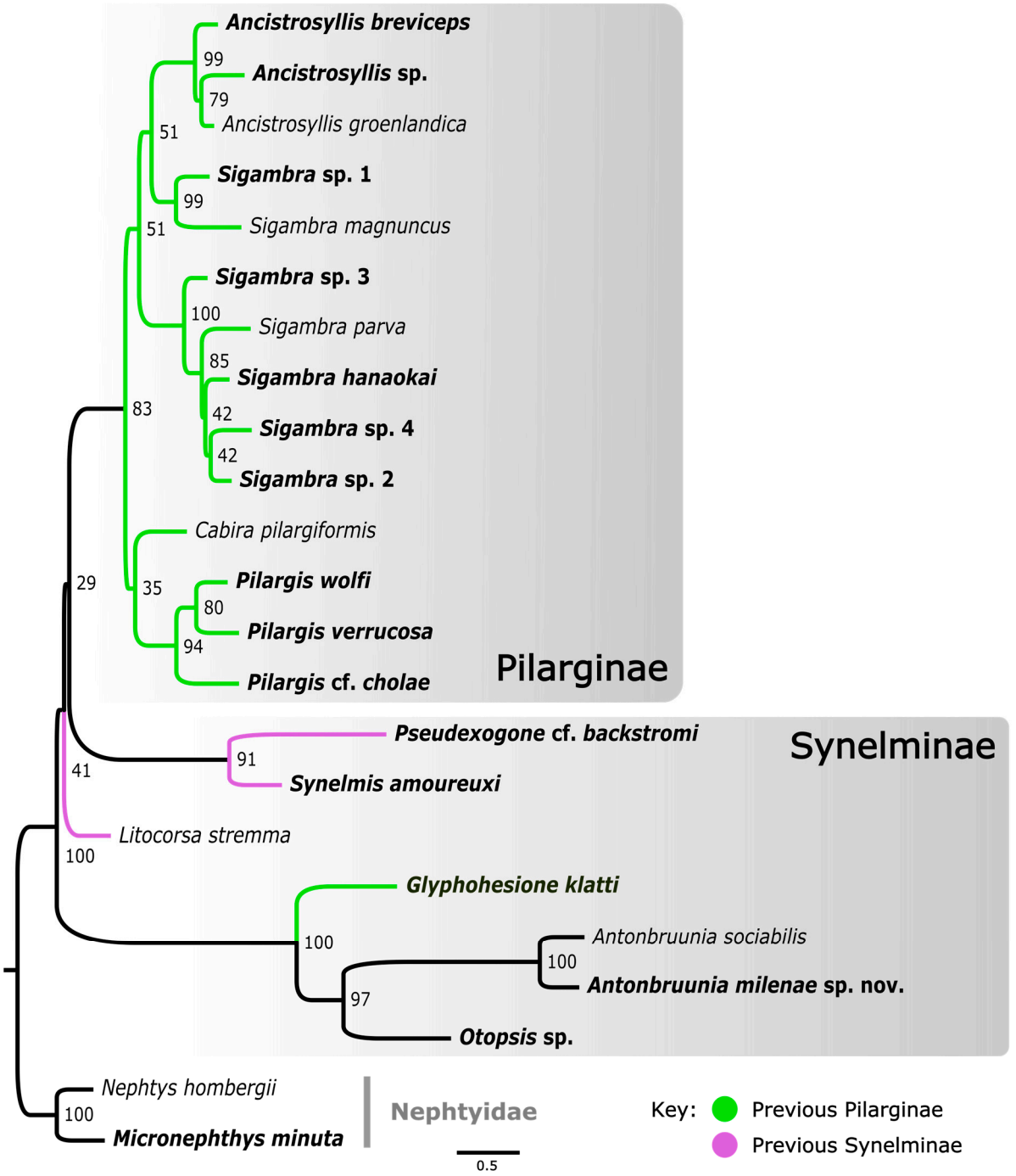

Figure 3. Concatenated nucleotide sequences of mitochondrial COI, 16S rRNA, and nuclear 18S rRNA gene data to generate an ML tree of Pilargidae, excluding *Hermundura*, with two nephtyids as the outgroup. Thorough bootstrap values are represented by numbers at the nodes. Species names set in bold indicate new sequences obtained in this study. Purple branches indicate species currently placed within Synelminae, green branches indicate species currently placed within Pilarginae, and black pilargid branches indicate unknown sub-familial placement until this study. Gray rectangles grouped pilargid species together based on new sub-familial delimitations, see Figure 2.

3.2. Haplotype Network

A COI haplotype network of *Antonbruunia milenae* sp. nov. (Figure 4) shows each of the five sequenced specimens has their own haplotype, even when recovered from within the same clam. Sequences were from one to four base pairs different from each other.

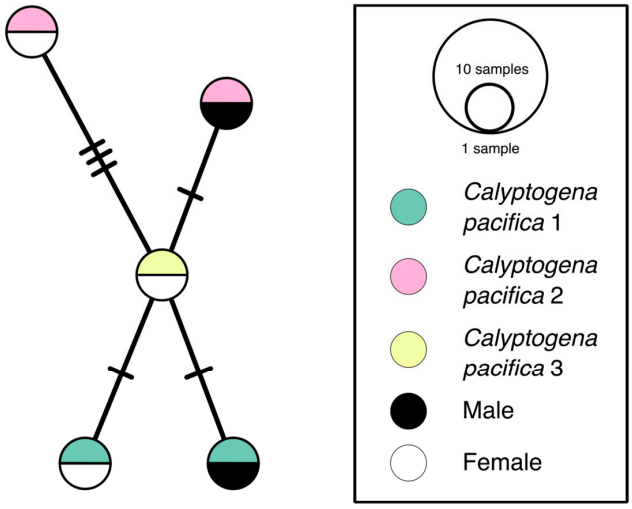

Figure 4. *Antonbruunia milenae* sp. nov. COI haplotype network. Each circle represents one individual; the bottom halves of the circles are white for females or black for males, while the top halves of the circles are sage for specimens found in *Calyptogena pacifica* 1 (SIO-BIC M18180), light pink for specimens found in *Calyptogena pacifica* 2 (SIO-BIC M18183), or light yellow for specimens found in *Calyptogena pacifica* 3 (SIO-BIC M18184). Each mark on the line connecting two circles represents a difference of one nucleotide base pair (bp) between two haplotypes.

3.3. Mitogenome Organization

The complete circularized mitochondrial genomes for ten pilargids *Antonbruunia milenae* sp. nov. (17,540 bp, Figure A2), *Pilargis verrucosa* Saint-Joseph, 1899 (15,131 bp, Figure A3), *Pilargis wolfi* (15,506 bp, Figure A4), *Ancistrosyllis* sp. (15,392 bp, Figure A5), *Glyphohesione klatti* (15,490 bp, Figure A6), *Otopsis* sp. (15,694 bp, Figure A7), *Sigambra* sp. 1 (15,680 bp, Figure A8), *Sigambra* sp. 2 (15,304, Figure A9), *Sigambra* sp. 3 (15,304 bp, Figure A10), and *Synelmis amoureuxi* (18,460 bp, Figure A11) had lengths between 15,131 bp and 18,460 bp. Four other complete circularized mitogenomes of outgroup species were also obtained: *Micronephthys minuta* Théel, 1879, (16,335 bp, Figure A12), *Lacydonia* sp. Marion, 1874 (14,704 bp, Figure A13), *Phyllodoce medipapillata* Moore, 1909 (15,741 bp, Figure A14), and *Struwela camposi* (15,488 bp, Figure A15). An incomplete mitogenome of *Hermundura fauveli* (missing the tRNA-Ala gene, Figure A16) was also obtained. *Antonbruunia milenae* sp. nov. (Figure A2) and *Synelmis amoureuxi* (Figure A11) had an intron in their COI gene, 305 bp and 2459 bp long, respectively. The introns were validated through Sanger sequencing; in the case of *Antonbruunia milenae* sp. nov., the entire intron was sequenced, while only 486 bp of the initial and 664 bp of the terminal ends of the *Synelmis amoureuxi* intron were sequenced. Additionally, unlike the other mitogenomes, the *Micronephthys minuta* COI gene started with the start codon GTG instead of ATG or ATA, which has been observed before in nephtyids [67].

All complete pilargid and nephtyid mitogenomes fell into one of four distinct mitogenome gene order groups, as shown in Figure 5. Group I comprised *Ancistrosyllis* sp., *Sigambra* sp. 1, *Sigambra* sp. 2, *Sigambra* sp. 3, *Pilargis verrucosa*, *Pilargis wolfi*, and the nephtyid *Micronephthys minuta*; Group II included only *Synelmis amoureuxi*; Group III contained *Glyphohesione klatti* and *Otopsis* sp.; while Group IV included only *Antonbruunia milenae* sp. nov. Based on the gene order of the recovered genes (Figure A16), *Hermundura fauveli* is most likely part of Group I because the genes that are present are in the order of Group I with no spaces in between large enough for a tRNA to be. Therefore, it is likely that tRNA-Ala is either before the first gene tRNA-Leu2 or after the last gene tRNA-Ser2, and if this is the case, then the gene order is identical to Group I. The TreeREx analysis excluding *Hermundura fauveli* (per Figure 2) showed that a transposition occurred between Pilarginae and Synelminae (Figures 5A and 6A), a transposition followed either by one of two possible combinations of two transpositions or a transposition and a tandem duplication random

loss (TDRL) occurred at some point on the branch leading to *Synelmis amoureuxi* after it branched off from the rest of the Synelminae (Figures 5B and 6B), and a TDLR occurred at some point along the branch of *Antonbruunia milenae* sp. nov. after the node it shares with *Otopsis* sp. (Figures 5C and 6C). The Group I mitogenome gene order was inferred as the ancestral state for Pilargidae.

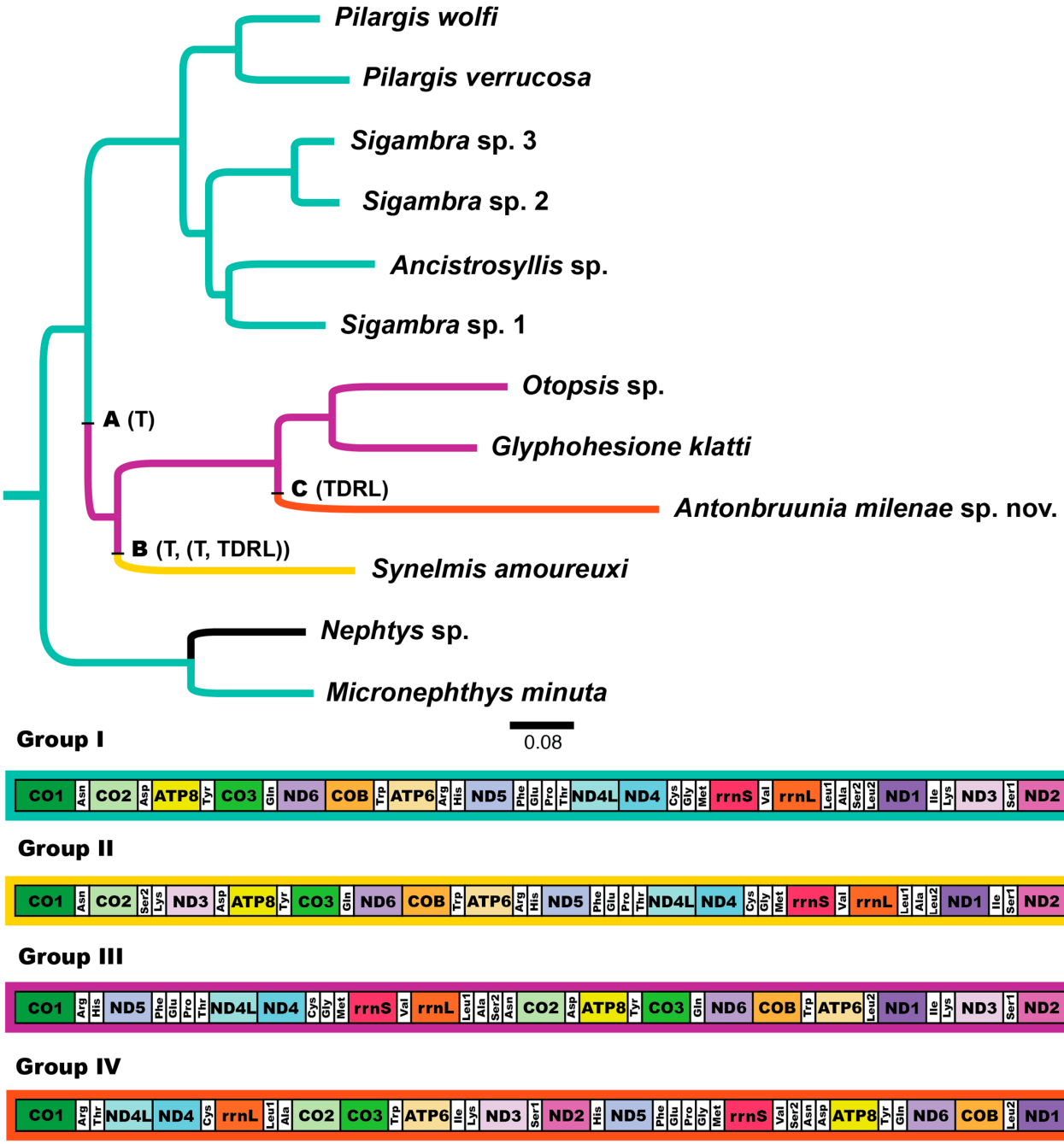

Figure 5. Sixteen-gene phylogeny including only Pilargidae and rooted with Nephtyidae, showing gene orders and changes in gene orders inferred with TreeREx v.1.85 [57] and CREx [58]. Tree branches are color coded for mitogenome gene order group when known (Group I is teal, Group II is yellow, Group III is purple, Group IV is orange). **A** Marks the branch along which the inferred transposition from gene orders I to III occured. **B** Marks the branch along which the inferred transpositions and a tandem duplication random loss (TDRL) from gene orders III to II occured. **C** Marks the branch along which the inferred gene order changes of a TDRL from gene orders III to IV occured. The gene order for *Nephtys* sp. could not be inferred, as it was incomplete.

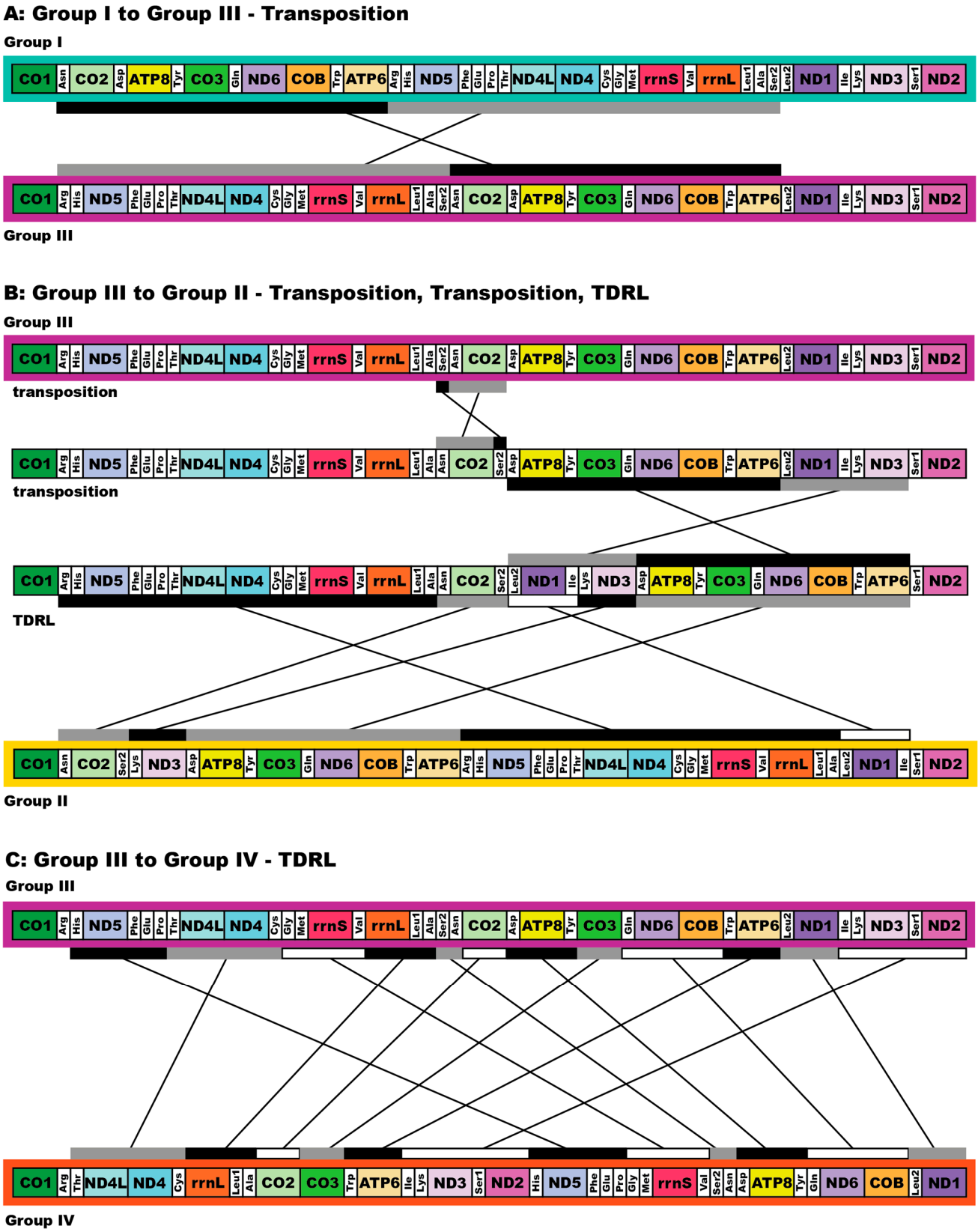

Figure 6. Visualized changes in the mitogenome gene orders based on TreeREx v.1.85 [57] and CREx [58]. (**A**) Transposition from Group I (teal) to Group III (purple); (**B**) transposition, transposition, TDRL from Group III (purple) to Group II (yellow) showing the intermediate stages; (**C**) TDRL from Group III (purple) to Group IV (orange). Black, gray, and white rectangles are used to show groups of genes that moved at once; black lines show where which group of genes moved to in the subsequent gene order.

3.4. Taxonomy

Pilargidae Saint-Joseph, 1899 [68]
[8,68–77]
Type genus. *Pilargis* Saint-Joseph, 1899 [68]
Diagnosis (emended).

Phyllodocida with cylindrical to ribbonlike bodies; integument smooth or papillose to verrucose. Prostomium bearing paired dorsolateral antennae and a single posteromedial one (may be absent), or antennae entirely absent; anteroventral palps biarticulated or simple, variably fused to each other, rarely absent; usually with an accessory palpal papilla. Brain may extend into several chaetigers. First segment achaetous with two pairs of cirri. Dorsal and ventral cirri variable, short, cirriform, or lobulated. Subbiramous parapodia lateral but may appear ventrally displaced in cylindrical forms, notopodia reduced to dorsal cirri, neuropodia distinct. Chaetae always simple. Notochaetae include often-emergent hooks or spines, usually positioned above the dorsal cirri, rarely with capillary chaetae, or without chaetae (one genus with emergent notaciculae below the dorsal cirri). Neurochaetae include limbate capillaries, hirsute or distally bifid falcate spines, distally smooth spines, and delicate furcate chaetae. Alimentary canal includes tubular, muscular pharynx lacking true jaws, and gut diverticula (caeca) variably developed throughout most of body.

Included genera: *Ancistrosyllis* McIntosh, 1878, *Antonbruunia* Hartman and Boss, 1965, *Cabira* Webster, 1879, *Glyphohesione* Friedrich, 1970, *Litocorsa* Pearson, 1970, *Otopsis* Ditlevsen, 1917, *Pilargis* Saint-Joseph, 1899, *Pseudexogone* Augener, 1922, *Sigambra* Müller, 1858, *Sigatargis* Misra, 1999, *Synelmis* Chamberlin, 1919.

Remarks.

Emended from Glasby and Salazar-Vallejo [13] to exclude less than two pairs of cirri (often referred to as tentacular cirri) on the first achaetous segment because of the exclusion of *Hermundura* (Figure 2), exclude uniramous parapodia since all pilargid parapodia are subbiramous, and explicitly include non-emergent notopodial hooks or spines. The large brain noted by Fitzhugh and Wolf [15] in many Pilargidae was also included. Additionally, it was reiterated that Pilargidae uniformly lack jaws because Fauvel (1932) [78] made an incorrect evaluation that *Hermundura* had denticulate band-resembling pharyngeal structures [65,79]. *Sigatargis* is the only genus not placed in a pilargid subfamily due to a lack of genetic data.

Pilarginae Saint-Joseph, 1899 [68]
[68–70,74]
Type genus. Pilargis Saint-Joseph, 1899 [68]
Diagnosis (emended).

Pilargidae with tapered body, rarely cylindrical, integument papillated or verrucose, never entirely smooth. Prostomium with paired biarticulated palps, 2–3 antennae. Brain may extend into several chaetigers. First segment achaetous, with two pairs of cirri. Parapodia with or without emergent notopodial hooks. Proboscis often with terminal papillae; proximal papillae (rarely denticles) also present.

Included genera: *Ancistrosyllis*, *Cabira*, *Pilargis*, *Sigambra*.

Remarks.

Emended from Salazar-Vallejo [12], who included the genera *Ancistargis* Jones, 1961, *Ancistrosyllis*, *Antonbruunia*, *Cabira*, *Otopsis*, *Paracabira* Britaev and Saphronova, 1981, *Pilargis*, and *Sigambra*. *Ancistargis* was synonymized with *Ancistrosyllis* [80], *Paracabira* with *Cabira* [81], and this study shows that *Otopsis* and *Antonbruunia* fall within Synelminae (Figure 2). With these changes, all genera within Pilarginae must have at least some papillae or verrucae on their integument [11,80,82]. When Pilarginae was erected, *Paracabira*, now *Cabira*, was thought to lack lateral antennae; however, they are just small [82]; this brings the antennae count from 0–3 to 2–3. Emergent neuropodial hooks are absent from all pilargids [7,13], but the presence (*Ancistrosyllis*, *Cabira*, *Sigambra*) or absence (*Pilargis*) of emergent notopodial hooks or spines remains. *Sigambra* and some *Ancistrosyllis* have termi-

nal papillae on the proboscis [13]. Proximally, *Cabira* and *Sigambra* (unknown in *Pilargis*) have soft pharyngeal papillae, some of which are hardened denticules in *Sigambra*. *Cabira incerta* Webster, 1879, *C. saithipae* Plathong, Dean and Plathong, 2021, and *Ancistrosyllis matlaensis* Mandal and Deb, 2018, proximally have only hardened denticles [13,69,82].

Synelminae Salazar-Vallejo 1987 [12]

[10,12,66,72,73,75–77,83–85]

Type genus. *Synelmis* Chamberlin, 1919 [77]

Diagnosis (emended).

Pilargidae with body cylindrical or dorsoventrally flattened, integument smooth. Prostomium with paired palps, fused or biarticulate, or lacking palps; up to three antennae. Brain may extend into several chaetigers. First segment achaetous, with two pairs of cirri. Notopodia with or without emerging straight or curved spines. Free-living or symbiotic.

Included genera: *Antonbruunia*, *Glyphohesione*, *Litocorsa*, *Otopsis*, *Pseudexogone*, *Synelmis*.

Remarks.

Synelminae is emended from Salazar-Vallejo's description [12] based on the mitogenome and 18S phylogenetic results in this study (Figure 2) to newly include *Glyphohesione* (previously in Pilarginae Saint-Joseph, 1899), *Antonbruunia* (previously in Antonbruunidae), and *Otopsis* (previously unassigned subfamily level) by allowing for a dorsoventrally flattened body shape and iridescence to be absent or present. It was reiterated that notopodial spines may (*Synelmis*, *Glyphohesione*, *Pseudexogone*, *Litocorsa*) or may not (*Antonbruunia*, *Otopsis*) be present. The spines may be straight or curved, as in *Pseudexogone* [66], which was described after the original diagnosis of Synelminae. *Hermundura*, now excluded from Pilargidae based on molecular data (Figure 2), lacks cirri on the first segment. There is some variation in prostomial appendages; Glasby and Salazar-Vallejo [13] interpreted *Pseudexogone*, *Synelmis*, and *Otopsis* as having both palpostyles and palpal papillae. They also interpreted *Litocorsa* as having both, though palpostyles are sometimes absent, and *Glyphohesione* and *Antonbruunia* as having only palpostyles, though the appendages in the latter two genera could instead be considered palpal papillae. We agree with Aguado [86] and Glasby and Salazar-Vallejo [13], and we consider *Glyphohesione* and *Antonbruunia* to have palpostyles. Given their phylogenetic position (Figures 2 and 3), they are likely homologous structures. Additionally, the new *Otopsis* species we used in this study does not have palpal papillae, nor do two of the other three *Otopsis* species, *O. longipes* Ditlevsen, 1917 [72], and *O. chardyi* Katzmann, 1974 [87]. Palpal papillae are only potentially present based on the original drawings in *O. kurilensis* Uschakov, 1971 [88], but they may be an artifact or misinterpretation, which could mean the lack of palpal papillae is homologous between all three closely related genera (Figures 2 and 3). Further histological study of these appendages is needed to be sure.

***Antonbruunia* Hartman and Boss, 1965** [8]

Antonbruunia milenae sp. nov.

Figures 7–11

Antonbruunia sp. n. Rouse et al. 2022: 59–60 [2]

Material examined.

Holotype: SIO-BIC A12281* (prepared for SEM), female of pair found in *Calyptogena pacifica* clam SIO-BIC M18183 [GenBank accession number OR126013 for COI], Rosebud whale fall, San Diego, CA, USA, 32.7769° N 117.4881° W, ~845 m depth, 9 February 2020, ROV *Doc Ricketts*, R/V *Western Flyer*, dive #DR1253.

Paratypes: SIO-BIC: A12280* (prepared for SEM) male of pair found in clam M18183, A12278* male and A12279* female of pair found in clam M18180, A12282 male and A12283* female of pair found in clam M18184, Rosebud whale fall, San Diego, CA, USA, 32.7769° N 117.4881° W, ~845 m depth, 9 February 2020, ROV *Doc Ricketts*, R/V *Western Flyer*, dive #DR1253. For GenBank accession number details, see Tables 1 and 2; * indicates sequenced specimens.

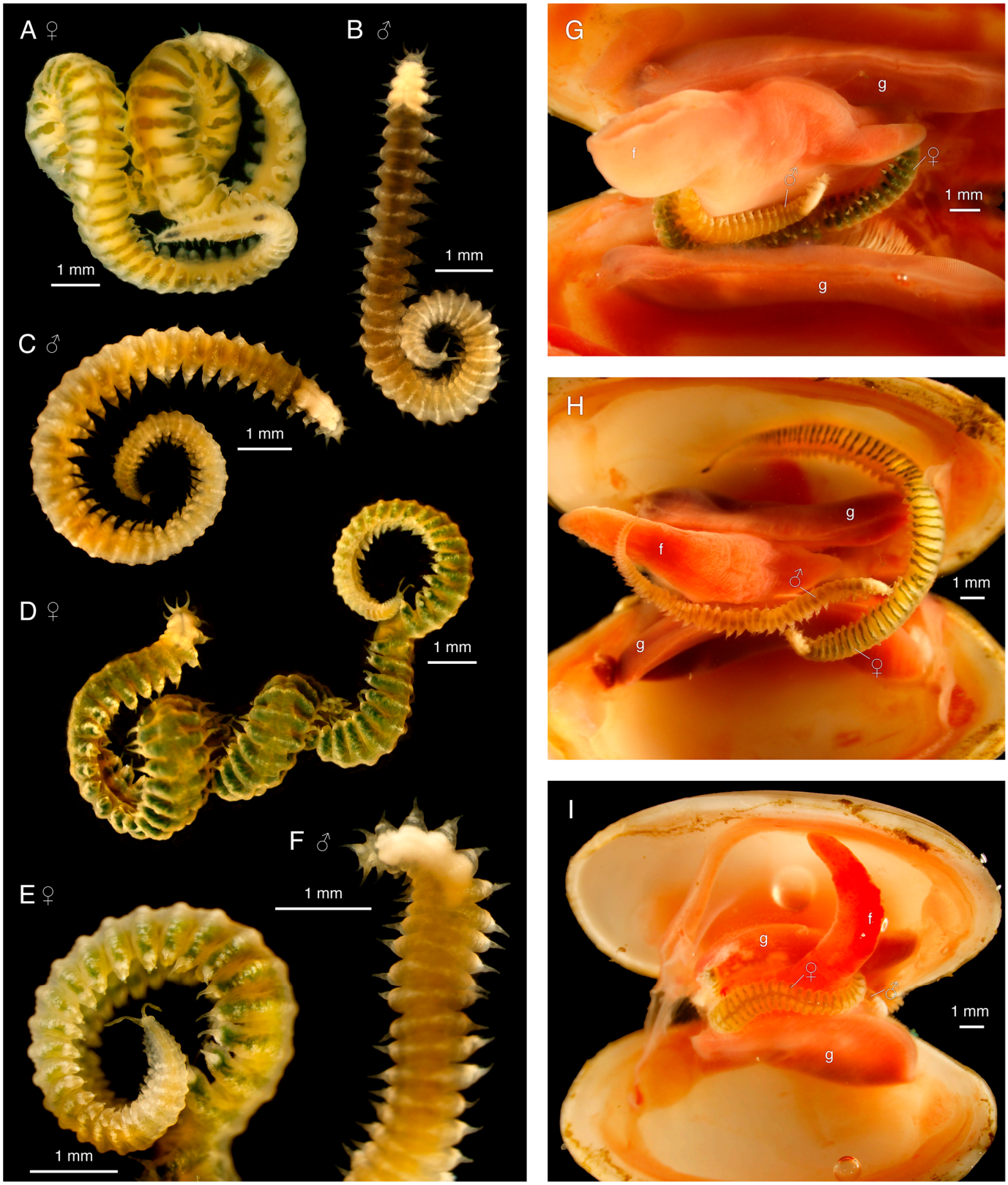

Figure 7. *Antonbruunia milenae* sp. nov. live photos. (**A**) Female holotype SIO-BIC A12281; (**B**) male paratype SIO-BIC A12282; (**C**) male paratype SIO-BIC A12280; (**D**) female paratype SIO-BIC A12279; (**E**) pygidial cirri of female paratype SIO-BIC A12279; (**F**) anterior of male paratype SIO-BIC A12278; (**G**) paratypes SIO-BIC: A12278 and A12279 in *Calyptogena pacifica* M18180; (**H**) holotype SIO-BIC A12281 and paratype SIO-BIC A12280 in *Calyptogena pacifica* M18183; (**I**) paratypes SIO-BIC: A12282 and A12283 in *Calyptogena pacifica* M18184. Abbreviations: f, foot; g, gills.

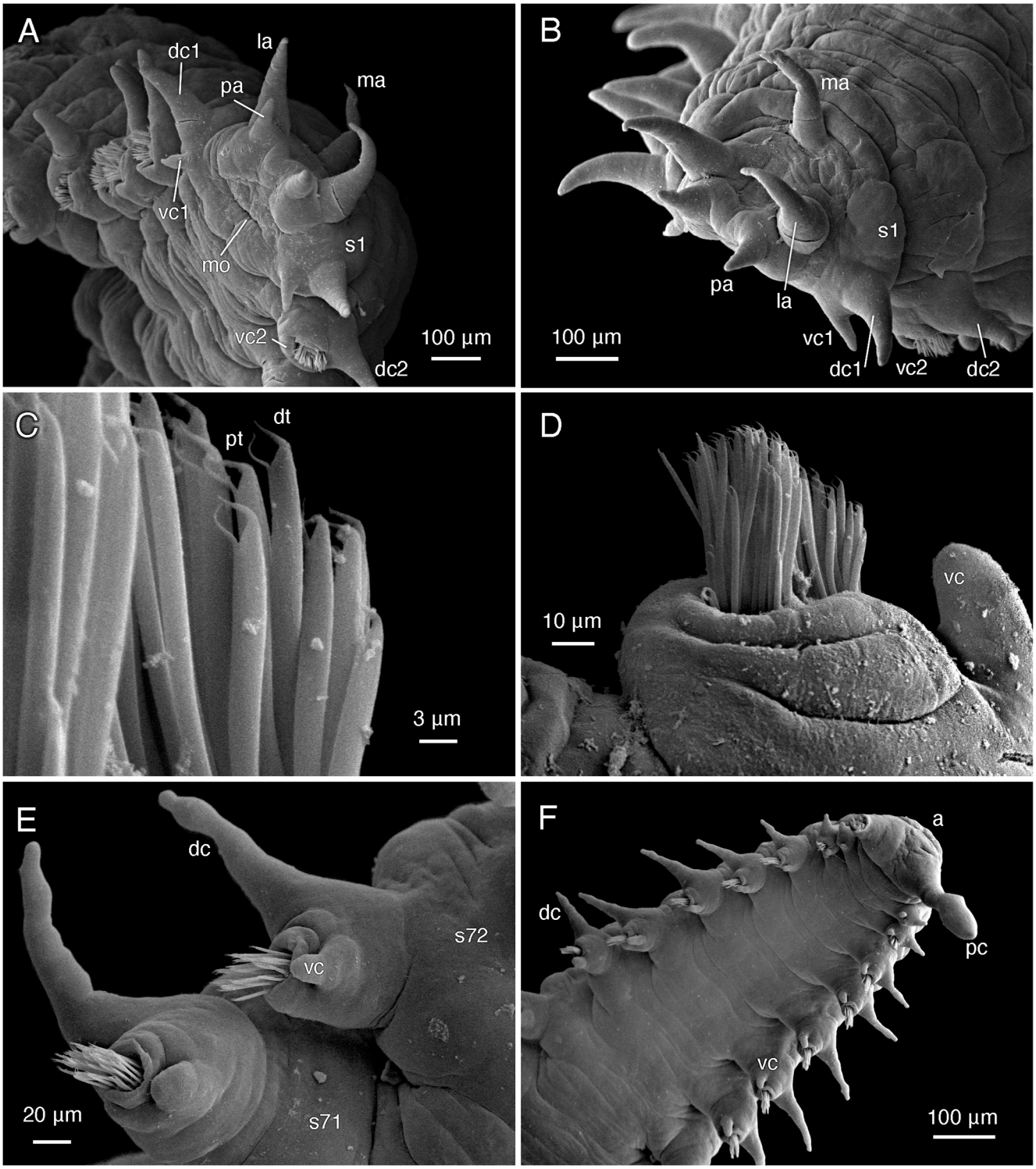

Figure 8. SEM images of *Antonbruunia milenae* sp. nov. holotype SIO-BIC A12281: (**A**) anteroventral view of anterior, (**B**) laterodorsal view of anterior, (**C**) detail of chaetae from anterior neuropodium, (**D**) anterior neuropodium, (**E**) posterior neuropodia, (**F**) ventral view of posterior. Abbreviations: a, anus; dc, dorsal cirrus; dc1, dorsal cirrus of first segment; dc2, dorsal cirrus of second segment; dt, distal tooth of chaeta; la, lateral antenna; ma, median antenna; mo, mouth; np71, neuropodium of segment 71; np72, neuropodium of segment 72; pa, palp; pc, pygidial cirrus; pt, proximal tooth of chaeta; s1, segment 1; s71, segment 71; s72, segment 72; vc, ventral cirrus; vc1, ventral cirrus of first segment; vc2, ventral cirrus of second segment.

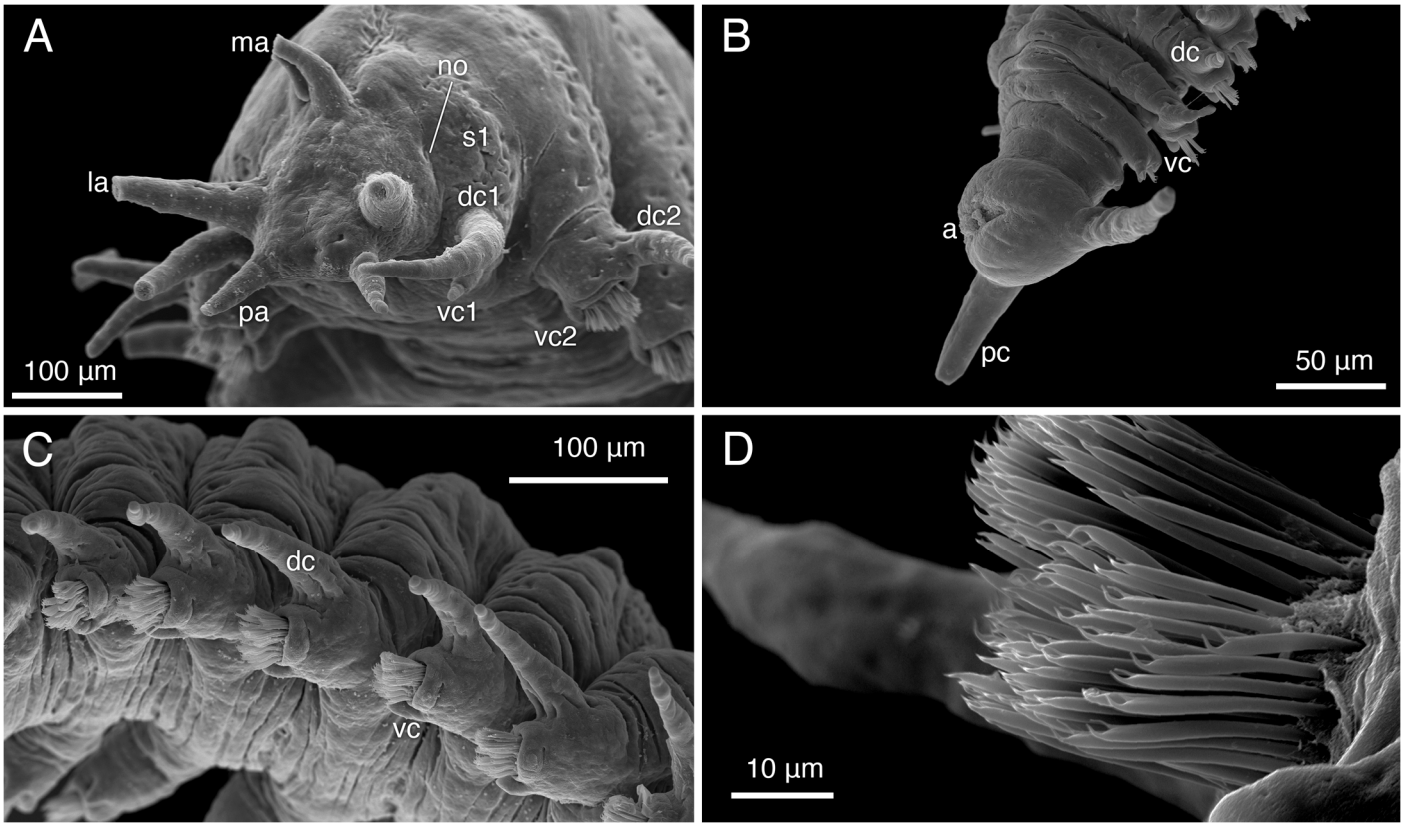

Figure 9. SEM images of *Antonbruunia milenae* sp. nov. paratype SIO-BIC A12280: (**A**) anterolateral view of anterior, (**B**) dorsolateral view of pygidium, (**C**) lateral view of midsection, (**D**) chaetae closeup. Abbreviations: a, anus; dc, dorsal cirrus; dc1, dorsal cirrus of first segment; dc2, dorsal cirrus of second segment; la, lateral antenna; ma, median antenna; no, nuchal organ; pa, palp; pc, pygidial cirrus; vc, ventral cirrus; vc1, ventral cirrus of first segment; vc2, ventral cirrus of second segment.

Figure 10. *Cont*.

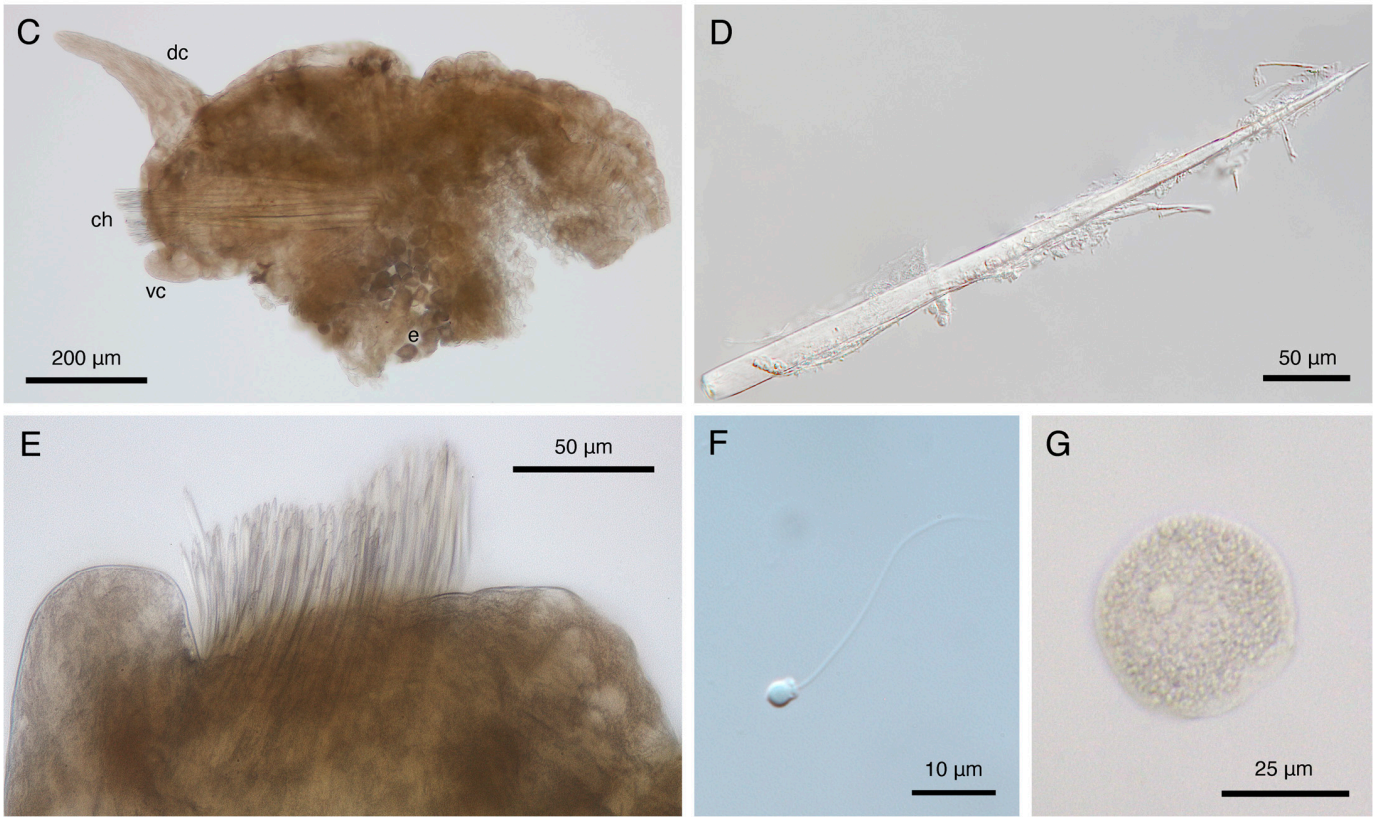

Figure 10. *Antonbruunia milenae* sp. nov. DIC microscopy images: (**A**) mid-anterior region cross-section of male paratype SIO-BIC A12278, (**B**) single chaeta of female paratype SIO-BIC A12283, (**C**) anterior parapodium of holotype SIO-BIC A12281, (**D**) acicula of female paratype SIO-BIC A12283, (**E**) detail of anterior neuropodium of holotype SIO-BIC A12281, (**F**) sperm of male paratype SIO-BIC A12280, (**G**) egg of holotype SIO-BIC A12281. Abbreviations: ch, chaetae; dc, dorsal cirrus; dt, distal tooth of chaeta; e, egg; gu, gut; pt, proximal tooth of chaeta; vc, ventral cirrus.

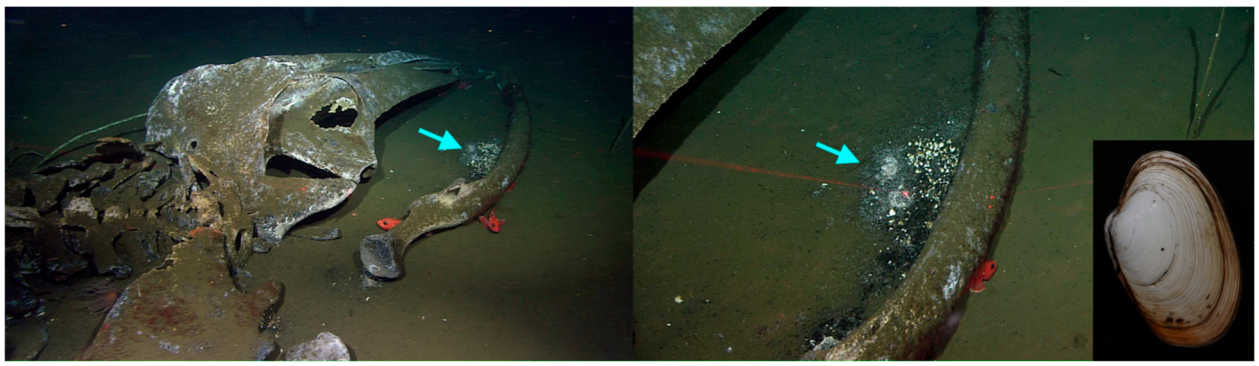

Figure 11. Rosebud whale fall (whale carcass on the sea floor) in February 2020 with *Calyptogena pacifica* clams in a cluster by the whale jawbone, in anoxic black sediments. Closeup of clam. Turquoise arrows point to the clam bed. Scale: red lasers are 29 cm apart. Whale fall images used with permission from S. Goffredi, expedition chief scientist, Occidental College, copyright 2020 Monterey Bay Aquarium Research Institute (MBARI).

3.4.1. Description

Holotype, female, ~18.5 mm long, width up to ~1 mm including parapodia, ~80 segments. Segment width rapidly increases in anterior tenth (~10 segments), remains evenly wide ~40 segments, gradually decreases in posterior fourth (Figure 7A,H). Body vermiform, arched dorsally, ventrally flattened (Figure 7A,H), with ventral groove (Figure 8A,F).

Translucent yellowish white body color in life, dark greenish dorsal median longitudinal stripe and one horizontal medio-dorsal stripe per segment, except on first four bright, opaque white segments, possibly representing the brain. Green coloration width decreases, fades to partial or complete absence in posterior eighth (Figure 7A,H). Color entirely yellowish white after preservation (formalin/ethanol).

Prostomium shape trapezoidal, lacking eyes, with pair of conical 0.1 mm palps on anterior margin, pair of tapered conical 0.2 mm anterior dorso-lateral antennae, single posterior dorsal 0.2 mm median antenna similar to paired antennae, but obviously narrower base (Figure 8A,B). Nuchal organs not clearly observed, may be present at posterior margin of prostomium, as seen in male paratype SIO-BIC A12280 (Figure 9A). Peristomium present as ventral transverse slit-like mouth, no visible margins (Figure 8A). Jawless pharynx. First segment achaetous, with two pairs of tapered conical cirri; dorsal cirrus 130 µm, base almost 2× width of 70 µm long ventral cirrus (Figure 8A,B). First segment dorsal cirri not obviously longer than following parapodial dorsal cirri, ventral cirrus longer, much more conical than parapodial ventral cirri (Figure 8A,B).

Subbiramous parapodia appear to have a single acicula (Figure 10A,C). Parapodia with conical, distally tapered dorsal cirri with single embedded distally pointed notoacicula; much smaller, bluntly rounded ventral cirri, with base ~two thirds width of dorsal cirri (Figures 8A,E,F and 10A,C). Ventral cirri much shorter, blunter on anterior parapodia (Figures 8A,B and 9A), lengthening, tapering towards posterior (Figures 8E,F and 9C). Parapodia with multiple thickly arranged chaetae (Figures 8D and 10C,E), with embedded, distally pointed neuroaciculae (Figure 10C,D). Anterior, posterior parapodia have at least 27 chaetae, largest middle parapodia up to 135 chaetae. Chaetae simple, slightly curved, distally thickened, bifid with angled straight distal tooth, inwardly curved proximal tooth (Figures 8C, 9D and 10B). Pygidium with two ~0.1 mm pygidial cirri, inflated in distal fourth (Figures 7A and 8F). Anus dorsal (Figures 8F and 9B).

3.4.2. Variation

Sexual dimorphism present. Males smaller, ~50% body length of females (Figure 7); female paratype SIO-BIC A12279 ~18.5 mm long like holotype, ~85 segments; three male paratypes ~8.5–10.5 mm, ~42–57 segments. Color variation between sexes: all males uniformly different from females; in life, dull yellowish white (some with slight dark green tinge in anterior two thirds) with opaque bright white patchy horizontal mediodorsal line on most segments (Figure 7B,C,F). Color variation within females: in life, paratype SIO-BIC A12279 anteriorly, instead of stripes, more general green coloration than holotype, paratype SIO-BIC A12283 (Figure 7D,G). Male dorsal cirri of first segment obviously longer than parapodial dorsal cirri (Figure 9A), unlike females. Pygidial cirri of males (Figure 9B) and paratype SIO-BIC A12283 conical and uniformly tapering, no inflation. Paratype SIO-BIC A12279 inflation in distal fifth (Figure 7E). Male pygidial cirri length ~ 50 µm, female up to 0.2 mm (Figures 7E and 9B). Putative nuchal organs found in male paratype SIO-BIC A12280 between posterior prostomium and first segment (Figure 9A).

3.4.3. Habitat

Antonbruunia milenae sp. nov. has only been found in the mantle cavity of the chemosynthetic vesicomyid clam *Calyptogena pacifica* at ~845 m off the coast of San Diego, California. Inside each collected clam, two individuals were found wrapped around the foot: one smaller male and one larger female (Figure 7G–I). The clams were collected from the blackened sulphidic sediments surrounding the jaw bones of the Rosebud whale fall (Figure 11). Therefore, this is the first *Antonbruunia* species associated with whale falls.

3.4.4. Reproduction

A male and female pair of non-closely related individuals lives in each clam; females have eggs 40 µm wide in their preserved state (Figure 10G), and males have sperm with 5 µm head and midpiece regions and 40 µm long tails in unpreserved states (Figure 10F).

3.4.5. Remarks

Antonbruunia milenae sp. nov. is morphologically most similar to *A. sociabilis* from the North-East Atlantic Ocean, with notably similar pygidial regions. According to Mackie et al. [7], *A. sociabilis* has only 32–52 segments, while *A. milenae* sp. nov. females have ~80–85 segments and males have ~42–57. *Antonbruunia sociabilis* has no ventral groove. The number of chaetae is lower in *A. sociabilis*; parapodia of the largest segments have 40–45 chaetae, and posterior segment parapodia have less than 5–6 chaetae, while *A. milenae* has 27–135 chaetae. *Antonbruunia sociabilis'* bifid chaetae have a less curved proximal and more curved distal tooth than *A. milenae* sp. nov. Additionally, *A. sociabilis* differs in the collection locality, depth of 1187–1200 m, and host bivalve *Thyasira scotiae*. Genetically, they are clearly different (Figure 3); though, unfortunately, there is no COI data for *A. sociabilis*, the uncorrected pairwise distance based on 16S is 7.56%.

Antonbruunia viridis, from near Madagascar, is also similar to *A. milenae* sp. nov., but there are no DNA sequences available to compare the two species. However, according to Hartman and Boss (1965) [8], the female holotype of *A. viridis* is 14 mm long and has only 52 segments and 26–30 chaetae per parapodium compared to *A. milenae* sp. nov., with ~18.5 mm length, ~80–85 segments, and up to 135 chaetae. Visible in SEM images, *A. viridis* has proportionately distally wider chaetae than *A. milenae* sp. nov., with a wider distal tooth relative to the proximal tooth [86]. *Antonbruunia milenae* sp. nov. has notopodial cirri with a wider base, and the neuropodial cirri are more blunt and shorter relative to the dorsal cirri than in *A. viridis*, especially anteriorly. Additionally, the *A. viridis* collection locality of the Indian Ocean off the SW coast of Madagascar, depth of 70–80 m, and host clam species *Opalocina fosteri* sets the species apart.

Antonbruunia milenae sp. nov. differs most from *A. gerdesi*. According to Quiroga and Sellanes (2009) [9], *A. gerdesi* males are 5.86 mm long with 33 segments, and females are 16.4 mm long with 53 segments, both of which are shorter than *A. milenae* sp. nov. However, *A. gerdesi* is about twice as wide as *A. milenae* sp. nov. *Antonbruunia gerdesi* lacks a ventral groove, has wider and shorter antennae and palps in proportion to the head, has bifid chaetae teeth that are straight and similar in length instead of the proximal tooth being curved, and has clearly different pygidial cirri (Quiroga and Sellanes [9] refer to them as anal cirri) that are proportionately shorter and thicker than those in *A. milenae* sp. nov. While both species are found in the Pacific Ocean at similar depths, *A. gerdesi* is found much further south off the coast of Concepción, Chile, and inside the host clam species *Calyptogena gallardoi*.

The whitish pigmented patch that extends for several segments posterior to the prostomium in both sexes of *A. milenae* sp. nov. (Figure 7A–D,F) is proposed here to represent the enlarged brain that is commonly seen in Pilargidae [15]. No report of such a region has been made for other *Antonbruunia*, and its presence will need to be confirmed with a histological study.

3.4.6. Etymology

Antonbruunia milenae sp. nov. is named after the first author's maternal great-grandmother, (Mama) Milena Trontelj, for being the first to spark the first author's love of marine invertebrates.

4. Discussion

This study represents the broadest phylogenetic study of Pilargidae to date. Having access to genetic samples of *Antonbruunia milenae* sp. nov. and to all accepted pilargid genera except for *Sigatargis* Misra, 1999, has allowed for a thorough reevaluation of the phylogenetic position of *Antonbruunia*, as well as clarity regarding sub-familial classifications of other genera. In both the three-gene nucleotide and sixteen-gene amino acid and nucleotide phylogenies (Figures 2 and 3), *Antonbruunia* is nested within Pilargidae, forming a well-supported clade (bootstrap support = 100) with *Glyphohesione klatti* and *Otopsis* sp.

Therefore, Antonbruunidae is regarded as a junior synonym of Pilargidae, as previously proposed [2,11–13].

The relationships between pilargid genera were not congruent in the two phylogenies (Figures 2 and 3), notably regarding the position of *Synelmis amoureuxi*. In the three-gene phylogeny (Figure 3), *Synelmis amoureuxi* and its well supported sister taxon *Pseudexogone* cf. *backstromi* Augener, 1922, formed one of four major pilargid clades, but its position suffers from very poor support. In the sixteen-gene phylogeny (Figure 2), *Synelmis amoureuxi* was instead recovered as a member of the clade that further includes *Glyphohesione klatti*, *Otopsis* sp., and *Antonbruunia milenae* sp. nov. We here favor the second topology, given the broader sampling of loci, though the support was still low. With this evidence, the genus *Antonbruunia* is considered to belong to Synelminae, along with *Otopsis*, which had previously not been given a sub-familial affiliation. *Glyphohesione* is transferred here from Pilarginae [63] to Synelminae to reflect its phylogenetic position (Figures 2 and 3). Additionally, the synelmin *Litocorsa stremma* Pearson, 1970, is arguably excluded from the well-supported (83) Pilarginae clade (and branches off between the *Antonbruunia* clade and *Synelmis* clade) in the three-gene phylogeny (Figure 3), indicating that it may belong in Synelminae. Consequently, Pilarginae includes only *Pilargis*, *Sigambra*, *Ancistrosyllis*, and *Cabira*.

Interestingly, *Hermundura fauveli* (the identification of which was confirmed using the physical voucher specimen borrowed from the Florida Museum of Natural History, which corresponds to the DNA extraction borrowed from the USNM, and by comparing sequences with those of *Hermundura americana* Hartman, 1947) grouped with Microphthalmidae rather than Pilargidae in the 16-gene phylogeny (Figure 2) and branched off first from the rest of the pilargids if included in the three-gene phylogeny (Figure A1). The conducted AU topology test [62] result also placed *Hermundura* as sister to Microphthalmidae. Hartman [64] had previously hypothesized that *Loandalia* Monro, 1936, and *Talehsapia* Fauvel, 1932, both now known as *Hermundura* [65], could potentially be their own family because of their morphological differences compared to the other pilargids. Besides the lack of enlarged cirri on the first segment, she also cited the lack of antennae on the prostomium; however, that trait is also present in *Litocorsa* [10,75] and is not unique to *Hermundura*. The "ovate to rounded, spoon-like with dorsal concavity" [65] pygidium found in *Hermundura* could be considered homologous to the anal membrane, typical of Microphthalmidae [89] however, once again, some *Litocorsa* also have rounded pygidia [90]. While it seems clear that *Hermundura* is not a pilargid, it is also not necessarily part of Microphthalmidae. *Hermundura* features, such as a relatively long body length (most species of *Hermundura* are longer than 5 mm) [12,64,65,74,78,91–100], usual absence of antennae and enlarged anterior cirri on achaetous anterior segments, small biarticulated palps, terminal pharyngeal papillae, and the absence of dorsal cirri (a feature of all *Hermundura* species besides *H. aberrans* (Monro, 1936) [65]), are not seen not in microphthalmids [89]. Further anatomical and molecular studies are needed before *Hermundura* can with certainty be considered within Microphthalmidae or as a sister taxon to it. Therefore, we consider *Hermundura* as Phyllodocida *incertae sedis*. The total number of genera in Pilargidae remains unchanged at eleven because of the addition here of *Antonbruunia*.

Further adding uncertainty to the monophyly of Microphthalmidae (and inclusion or exclusion of *Hermundura*) was the position of *Struwela camposi*, as it formed a poorly supported (bootstrap support = 52) clade with Nereididae. This indicates the need for additional sampling and larger scale data, such as transcriptomes or genomes. Additionally, if *Struwela camposi* is not a microphthalmid, then there could be implications for the interfamilial relationships within Phyllodocida, since it was used to represent Microphthalmidae in the transcriptomic phylogenies of the clade [6].

Pilarginae was congruent in topology across both phylogenies (Figures 2 and 3). *Pilargis* is a well-supported clade, but *Sigambra* is non-monophyletic. There is not currently enough evidence to either split *Sigambra* into two genera or to consider *Ancistrosyllis* as a junior synonym of *Sigambra*. Further sampling or additional data of more species from

both genera would be needed, particularly the type species *Sigambra grubii* Müller, 1859, and *Ancistrosyllis groenlandica* McIntosh, 1878. Though COI and 18S of the latter were used in this study, obtaining at least mitogenomes is likely needed for further clarification of the phylogenetic relationships within Pilarginae.

This study also presents ten pilargid, a nephtyid, phyllodocid, lacydoniid, and two microphthalmid (accepting *Hermundura*) mitochondrial genomes, for a total of fifteen. *Antonbruunia milenae* sp. nov. and *Synelmis amoureuxi*, which have an intron in their COI gene, had mitogenome sizes of 17,540 bp and 18,460 bp, respectively, while the rest of the pilargids had mitogenome sizes between 15,131 bp and 15,694 bp. Based on the taxa location on the phylogenies (Figures 2 and 3), it is possible that the introns occurred independently. Additionally, both species had unique mitogenome gene orders (Figure 5). *Pilargis*, *Sigambra*, and *Ancistrosyllis* sp. had the Group I gene order, *Glyphohesione klatti* and *Otopsis* sp. had the Group III gene order, while *Synelmis amoureuxi* was the only species in this study with the Group II gene order, and *Antonbruunia milenae* sp. nov. was the only species with the Group IV gene order. Based on the recovered genes, it is possible to infer that *Hermundura fauveli* most likely also has the Group I gene order. The Group I gene order is widespread across Annelida [101] and is inferred here as the plesiomorphic condition for Pilargidae and was shared with the nephtyid outgroup. In Figure 5, a transposition (Figures 5A and 6A) is shown before the most recent common ancestor of *Synelmis*, *Glyphohesione*, *Otopsis*, and *Antonbruunia*, indicating that the ancestral state of Synelminae is the gene order of Group III. However, the ancestral node was colored red in the original TreeREx output (Appendix B Figure A17), indicating that this gene order was computed using the fallback algorithm for this node [57]. This means it was determined through maximum parsimony based on the other nodes in the tree, since the algorithm could not reliably decide using its bottom-up approach, which of the three possible change scenarios (Group I to II, III, or IV) occurred from the ancestral synelmin node to *Synelmis amoureuxi*, but it infers fewer individual changes if we assume that Group II comes from Group III rather than from Group I (Figures 5B and 6B). With further sampling of Synelminae, the changes in gene order along this branch will likely become clearer. Along the branch leading to *Antonbruunia milenae* sp. nov., a tandem duplication random loss (TDRL) event occurred (Figures 5C and 6C), leading to gene order Group IV, which seems most different from other pilargids. This could possibly be a result of large genetic changes necessary for its inquiline lifestyle, which are also reflected in its relatively long branch (Figures 2 and 3).

Antonbruunia milenae sp. nov. is the fourth described within the genus [7–9]. Based on the haplotype network (Figure 4), it appears the male and female individuals in a pair inside a single clam are not siblings, since they each have their own individual haplotype. It is interesting that there was an isolated heterosexual pair of worms in each clam, as this is not a common occurrence among commensal polychaetes [102]. Besides *Antonbruunia viridis* and *A. milenae* sp. nov., this has been observed in the sea star associated *Bathynoe cascadiensis* Ruff, 1991 [103], the deep-sea sponge dwelling *Harmothoe hyalonemae* Martin, Rossel and Uriz, 1992 [104], and *Veneriserva pygoclava* Rossi, 1984, which inhabits aphroditid scaleworms [105]. It is likely that antagonistic intraspecific interactions are to blame for the exclusivity of the pair [106]; for instance, either the annelids killing or repelling additional individuals from their host. Nothing else is known about the reproductive habits of the species, but based on their deep-sea inquiline lifestyle and restricted locality, it is unlikely that the larvae are planktotrophic, which the small egg size [107,108], also observed in *Antonbruunia sociabilis* [7], indicates [2]. Therefore, they have unusually small eggs for potentially lecithotrophic larvae. Because each species has been found only once, it is unclear how much dispersal *Antonbruunia* is capable of, but we do know that the *Calyptogena pacifica* clam bed at the Rosebud whale fall appeared some years after the whale was sunk [109]. Even though San Diego is the only known locality of *Antonbruunia milenae* sp. nov., its host species *Calyptogena pacifica* is found across the Pacific Ocean [110,111]. If it should be observed that the new species of worm is present within its host species throughout the clam's entire distribution, then perhaps the larvae of *A. milenae* sp. nov. are

in fact planktotrophic, like in other deep-sea annelids with a wide distribution, such as some scale worms [112]. However, it might be exactly the inquiline, potentially parasitic lifestyle that accounts for the small egg size. While non-planktotrophic eggs are usually larger [2], a decrease in egg size has been seen in some non-planktotrophic annelid clades, such as in the symbiotic/parasitic annelids in Myzostomida von Graff, 1877 [113,114]. In the case of *Antonbruunia*, this could be because they live within clams, which can form densely populated clam beds (Figure 11), meaning larvae would not need to travel far before settling at a food source. Additionally, lower yolk levels may allow the potentially lecithotrophic larvae to remain smaller longer than annelids with higher yolk levels, allowing for easier entry into a clam through filtration, which would mean easier access to the host organism.

During this study, thirteen other pilargid species were morphologically examined. Six of them, which will be described in a future publication, were shown to be new species: *Ancistrosyllis* sp., *Otopsis* sp., *Sigambra* sp. 1, *Sigambra* sp. 2, *Sigambra* sp. 3, and *Sigambra* sp. 4. This study also provides the first DNA sequences of the genera *Otopsis*, *Pseudexogone*, and *Synelmis*, and it documents a range extension of ~250 km for *Pilargis cholae* Salazar-Vallejo and Harris, 2006 [115].

In conclusion, the present investigation has molecularly confirmed the phylogenetic placement of *Antonbruunia* within Pilargidae, facilitated by the collection and description of the new species *Antonbruunia milenae*, sp. nov., described herein. Fifteen new mitogenomes are presented, showing the ancestral state mitogenome gene order for Pilargidae, Pilarginae, and Synelminae and the proposed changes between generic gene orders. While Synelminae was emended to include *Antonbruunia*, *Glyphohesione*, and *Otopsis* and exclude *Hermundura*, which is now part of Phyllodocida *incertae sedis*, and Pilarginae was emended to include only *Ancistrosyllis*, *Cabira*, *Pilargis*, and *Sigambra*, more work must be conducted to fully elucidate the intergeneric relationships within Pilargidae. The eleventh pilargid genus *Sigatargis* cannot yet be placed within a subfamily without any genetic samples. This study was unable to obtain mitochondrial genomes of the genera *Cabira*, *Litocorsa*, and *Pseudexogone*, and additional morphological and phylogenetic samples are needed to resolve the current non-monophyly of *Sigambra*.

Author Contributions: Conceptualization, G.W.R. and S.H.; methodology, S.H., A.S.H. and M.F.M.; validation, G.W.R., S.H., A.S.H. and M.F.M.; formal analysis, S.H., A.S.H. and M.F.M.; investigation, G.W.R., S.H., A.S.H. and M.F.M.; resources, G.W.R., A.S.H. and M.F.M.; data curation, G.W.R., S.H. and A.S.H.; writing—original draft preparation, S.H.; writing—review and editing, G.W.R. and A.S.H.; visualization, S.H. and G.W.R.; supervision, G.W.R.; project administration, G.W.R. and S.H.; funding acquisition, G.W.R. All authors have read and agreed to the published version of the manuscript.

Funding: This research was funded by the US National Science Foundation (NSF-OCE 0939557) for the collection of Costa Rican specimens (*Sigambra* sp. 1) under the following permits issued by CONAGEBIO (Comisión Nacional para la Gestión de la Biodiversidad) and SINAC (Sistema Nacional de Áreas de Conservación) under MINAE (Ministerio de Ambiente y Energía), Government of Costa Rica: SINAC- CUSBSE-PI-R-032-2018 and the Contract for the Grant of Prior Informed Consent between MINAE-SINAC-ACMC and Jorge Cortés Nuñez for the Basic Research Project "Cuantificación de los vínculos biológicos, químicos y físicos entre las comunidades quimiosintéticas con el mar profundo circundante.' Specimens from California (*Ancistrosyllis, Antonbruunia, Otopsis*) were collected thanks to the Monterey Bay Aquarium Research Institute (Packard Foundation) and University of California Ship Funds.

Institutional Review Board Statement: Not applicable.

Data Availability Statement: Publicly available datasets on NCBI GenBank or BOLD were analyzed in this study. See Tables 1 and 2 for accession numbers. Additionally, raw reads used to assemble the mitogenomes were deposited in the NCBI GenBank SRA database under the BioProject ID PRJNA1075478 and BioSample accession numbers SAMN39918025-SAMN39918039.

Acknowledgments: Thank you to the captains and crews of R/V *Western Flyer*, R/V *Atlantis*, R/V *Falkor*, R/V *Nereus*, R/V *Melville*, and R/V *Burin* and the pilots of ROVs *Doc Ricketts*, *Jason II*, and *SuBastian* and the HOV (human operated vehicle) *Alvin* who made sample collection possible throughout the years, and thank you to expedition chief scientist S. Goffredi and MBARI for in situ photos and Fredrik Pleijel and Ernesto Campos for collecting annelid specimens. Thanks also to Damhnait McHugh for sending us *Hermundura americana* specimens. Special thanks to Charlotte Seid for her able assistance with sample organization and draft review. Thanks also to Nicolás Mongiardino Koch for draft review, The Smithsonian Institution (NMNH) and Florida Museum of Natural History for loaned valuable specimens needed to complete this study, and Chris Glasby and an anonymous reviewer for their valuable comments on the initial manuscript.

Conflicts of Interest: The authors declare no conflicts of interest.

Appendix A

Table A1. Overview of *Antonbruunia* species.

Species	Locality	Depth (m)	Host	Worms per Host	Habitat	Reference
A. viridis	Madagascar	70	*Lucina fosteri*	Usually 2 (male + female)	Hypoxic sediment	Hartman and Boss 1965 [8]
A. gerdesi	Central Chile	800	*Calyptogena gallardoi*	Usually 1	Gas hydrate environment	Quiroga and Sellanes, 2009 [9]
A. sociabilis	Scotland	1200	*Thyasira scotiae*	2–9	Sulfide seep	Mackie, Oliver, and Nygren, 2015 [7]
A. milenae sp. nov.	CA, USA	845	*Calyptogena pacifica*	2 (male + female)	Whale fall	This study

Table A2. Forward (F) and reverse (R) primers used for each gene and references.

Gene	Primer Name	Primer Sequence	Reference
COI	polyLCO (F)	5′-GAYTATWTTCAACAAATCATAAAGATATTGG-3′	[116]
COI	polyHCO (R)	5′-TAMACTTCWGGGTGACCAAARAA TCA-3′	[116]
16S	16S-AnnF (F)	5′-GCGGTATCCTGACCGTRCWAAGGTA-3′	[117]
16S	16Sb (R)	5′-CTCCGGTTTGAACTCAGATCA -3′	[118]
16S	16SarL (F)	5′-CGCCTGTTTATCAAAAACAT-3′	[119]
16S	16SbrH (R)	5′-CCGGTCTGAACTCAGATCACGT-3′	[119]
18S	18S-1F (F)	5′-TACCTGGTTGATCCTGCCAGTAG-3′	[120]
18S	18S-5R (R)	5′-CTTGGCAAATGCTTTCGC-3′	[120]
18S	18S-3F (F)	5′-GTTCGATTCCGGAGAGGGA-3′	[120]
18S	18S-bi (R)	5′-GAGTCTCGTTCGTTATCGGA-3′	[121]
18S	18S-a2.0 (F)	5′-ATGGTTGCAAAGCTGAAAC-3′	[121]
18S	18S-9R (R)	5′-GATCCTTCCGCAGGTTCACCTAC-3′	[120]
COI intron	AntonbruuniaCOIintron-205F	5′-GGGGGTTTAACAGGGATTGTC-3′	This Study
COI intron	AntonbruuniaCOIintron-683R	5′-TTGTTTATGGAGTGTTAACCCTCT-3′	This Study
COI intron	Synelmis-Intron3,011F	5′-GGTTAGAACGAGTGCCGCTA-3′	This Study
COI intron	Synelmis-Intron3,714R	5′-CTCCTGCTCCGTATCACACC-3′	This Study
COI intron	Synelmis-Intron4,990F	5′-AGTAACCCTCGCTCCAAAGC-3′	This Study
COI intron	Synelmis-Intron5,755R	5′-CCAAGTGTGCCGAATGGTTC-3′	This Study

Table A3. Primer pairs and voucher numbers of PCR reactions where Conquest ^{TM} PCR 2x Master Mix-1 (Lamda Biotech) was used.

Voucher	COI	16S rRNA	18S rRNA
A12280	PolyLCO/PolyHCO	-	-
A12283	PolyLCO/PolyHCO	-	-
A13955	PolyLCO/PolyHCO	AnnF/16Sb	18S-1F/18S-5R, 18S-3F/18S-bi, 18S-a2.0/18S-9R

Table A3. *Cont.*

Voucher	COI	16S rRNA	18S rRNA
A15568	PolyLCO/PolyHCO	-	-
A16333	PolyLCO/PolyHCO	AnnF/16Sb	-
A16381	PolyLCO/PolyHCO	AnnF/16Sb	18S-1F/18S-5R, 18S-3F/18S-bi, 18S-a2.0/18S-9R
A16382	PolyLCO/PolyHCO	-	18S-3F/18S-bi, 18S-a2.0/18S-9R
USNM1499416	PolyLCO/PolyHCO	AnnF/16Sb	18S-1F/18S-5R, 18S-3F/18S-bi, 18S-a2.0/18S-9R
USNM1643733	-	AnnF/16Sb	18S-1F/18S-5R, 18S-3F/18S-bi, 18S-a2.0/18S-9R
A6261	-	16SarL/16SbrH	-
A5771	-	16SarL/16SbrH	18S-1F/18S-5R
A5926	-	16SarL/16SbrH	18S-1F/18S-5R, 18S-3F/18S-bi
A4846	-	-	18S-1F/18S-5R

Table A4. PCR reaction protocols for corresponding primers.

Primer Pair	Initial Denaturation	Cycles of Denaturation (Denaturation, Annealing, Elongation)	Final Extension	Max Amplified Base Pairs
polyLCO/polyHCO	95 °C for 3 min	40 (95 °C for 40 s, 42 °C for 45 s, 72 °C for 50 s)	72 °C for 5 min	684
16S-AnnF/16Sb	94 °C for 2 min	35 (94 °C for 40 s, 60 °C for 40 s, 70 °C for 45 s)	72 °C for 7 min	442
16SarL/16SbrH	95 °C for 3 min	35 (95 °C for 40 s, 50 °C for 40 s, 72 °C for 50 s)	72 °C for 5 min	530
18S-1F/18S-5R and 18S-a2.0/18S-9R	95 °C for 3 min	40 (95 °C for 30 s, 50 °C for 30 s, 72 °C for 90 s)	72 °C for 8 min	1792
18S-3F/18S-bi	95 °C for 3 min	40 (95 °C for 30 s, 52 °C for 30 s, 72 °C for 90 s)	72 °C for 8 min	
AntonbruuniaCOIintron-205F/ AntonbruuniaCOIintron-683R	95 °C for 3 min	40 (95 °C for 40 s, 48 °C for 40 s, 72 °C for 50 s)	72 °C for 5 min	451
Synelmis-Intron3,011F/ Synelmis-Intron3,714R	95 °C for 3 min	40 (95 °C for 40 s, 51 °C for 40 s, 72 °C for 50 s)	72 °C for 5 min	673
Synelmis-Intron4,990F/ Synelmis-Intron5,755R	95 °C for 3 min	40 (95 °C for 40 s, 51 °C for 40 s, 72 °C for 50 s)	72 °C for 5 min	730

Table A5. Number, total length, and individual length of Novogene genome skimming raw reads for the specified species and the number of reads retained after using Trimmomatic [37].

Species	Total Number of Raw Reads (Paired-End)	Total Length of Raw Reads (Paired-End)	Individual Length of Raw Reads	Number of Reads Post-Trimmomatic (Paired-End)
Antonbruunia milenae sp. nov.	3,702,263	555,339,450	150	3,662,081 (98.91%)
Ancistrosyllis sp.	4,226,103	633,915,450	150	4,160,625 (98.45%)
Otopsis sp.	10,035,386	1,505,307,900	150	9,912,137 (98.77%)

Table A5. *Cont.*

Species	Total Number of Raw Reads (Paired-End)	Total Length of Raw Reads (Paired-End)	Individual Length of Raw Reads	Number of Reads Post-Trimmomatic (Paired-End)
Sigambra sp. 1	8,748,561	1,312,284,150	150	8,609,906 (98.42%)
Sigambra sp. 2	9,106,118	1,505,307,900	150	8,996,276 (98.79%)
Sigambra sp. 3	6,241,943	936,291,450	150	6,134,740 (98.28%)
Glyphohesione klatti	9,850,116	1,477,517,400	150	9,682,419 (98.30%)
Synelmis amoureuxi	10,165,381	1,524,807,150	150	10,023,655 (98.61%)
Pilargis verrucosa	8,696,621	1,304,493,150	150	8,479,066 (97.50%)
Pilargis wolfi	7,213,725	1,082,058,750	150	7,062,447 (97.90%)
Hermundura fauveli	7,387,747	1,108,162,050	150	7,253,809 (98.19%)
Micronephthys minuta	6,284,087	942,613,050	150	6,159,575 (98.02%)
Struwela camposi	8,715,828	1,307,374,200	150	8,631,491 (99.03%)
Lacydonia sp.	8,319,473	1,247,920,950	150	8,213,908 (98.73%)
Phyllodoce medipapillata	9,488,143	1,423,221,450	150	9,378,425 (98.84%)

Table A6. Data type (either nucleotide (NT) or amino acid (AA)) and RAxML model test results of single gene datasets, grouped by concatenated 16-gene and concatenated three-gene phylogenies.

Mitochondrial Genome Phylogeny Dataset					
Gene	**Data Type**	**Substitution Model**	**Stationary Frequencies**	**Proportion of Invariant Sites**	**Rate Heterogeneity**
ATP6	AA	MTZOA	+F (empirical)	-	+GAMMA (mean)
ATP8	AA	MTART	-	-	+GAMMA (mean)
COI	AA	MTZOA	-	+I (ML estimate)	+GAMMA (mean)
COII	AA	MTZOA	-	-	+GAMMA (mean)
COIII	AA	MTZOA	-	+I (ML estimate)	+GAMMA (mean)
CYTB	AA	MTZOA	-	+I (ML estimate)	+GAMMA (mean)
ND1	AA	MTART	-	+I (ML estimate)	+GAMMA (mean)
ND2	AA	MTMAM	+F (empirical)	-	+GAMMA (mean)
ND3	AA	MTART	-	+I (ML estimate)	+GAMMA (mean)
ND4	AA	MTZOA	+F (empirical)	-	+GAMMA (mean)
ND4L	AA	MTMAM	-	-	+GAMMA (mean)
ND5	AA	MTART	+F (empirical)	+I (ML estimate)	+GAMMA (mean)
ND6	AA	MTART	-	+I (ML estimate)	+GAMMA (mean)
12S	NT	TIM2	-	-	+GAMMA (mean)
16S	NT	TN93	-	+I (ML estimate)	+GAMMA (mean)
18S	NT	TN93	-	+I (ML estimate)	+GAMMA (mean)
Concatenated COI, 16S rRNA, and 18S rRNA Phylogeny Dataset					
Gene	**Data Type**	**Substitution Model**	**Stationary Frequencies**	**Proportion of Invariant Sites**	**Rate Heterogeneity**
COI	NT	GTR	-	+I (ML estimate)	+GAMMA (mean)
16S	NT	TIM3	-	+I (ML estimate)	+GAMMA (mean)
18S	NT	TIM3	-	+I (ML estimate)	+GAMMA (mean)

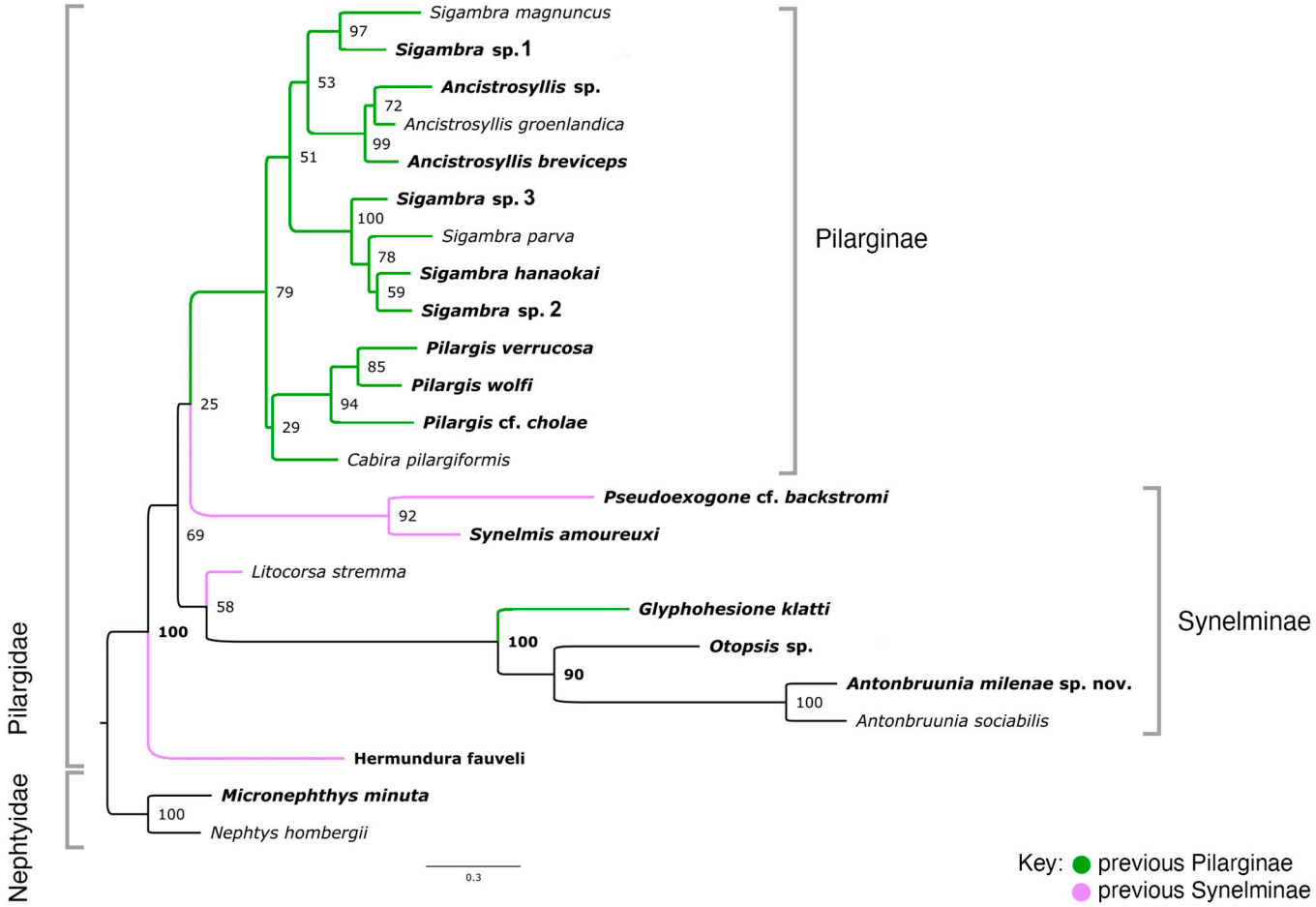

Figure A1. Concatenated nucleotide sequences of mitochondrial COI, 16S rRNA, and nuclear 18S rRNA gene data to generate an ML tree of Pilargidae, including *Hermundura*, with two nephtyids as the outgroup. A total of 20 runs and 500 reps were executed; the seed was 552840. *Sigambra* sp. 4 is excluded. Thorough bootstrap values are represented by numbers at the nodes. Species names set in bold indicate new sequences obtained in this study. Purple branches indicate species currently placed within Synelminae, green branches are species currently placed within Pilarginae, and black pilargid branches indicate unknown sub-familial placement until this study. Gray brackets group species together based on family and new sub-familial delimitations, see Figure 2.

Appendix B

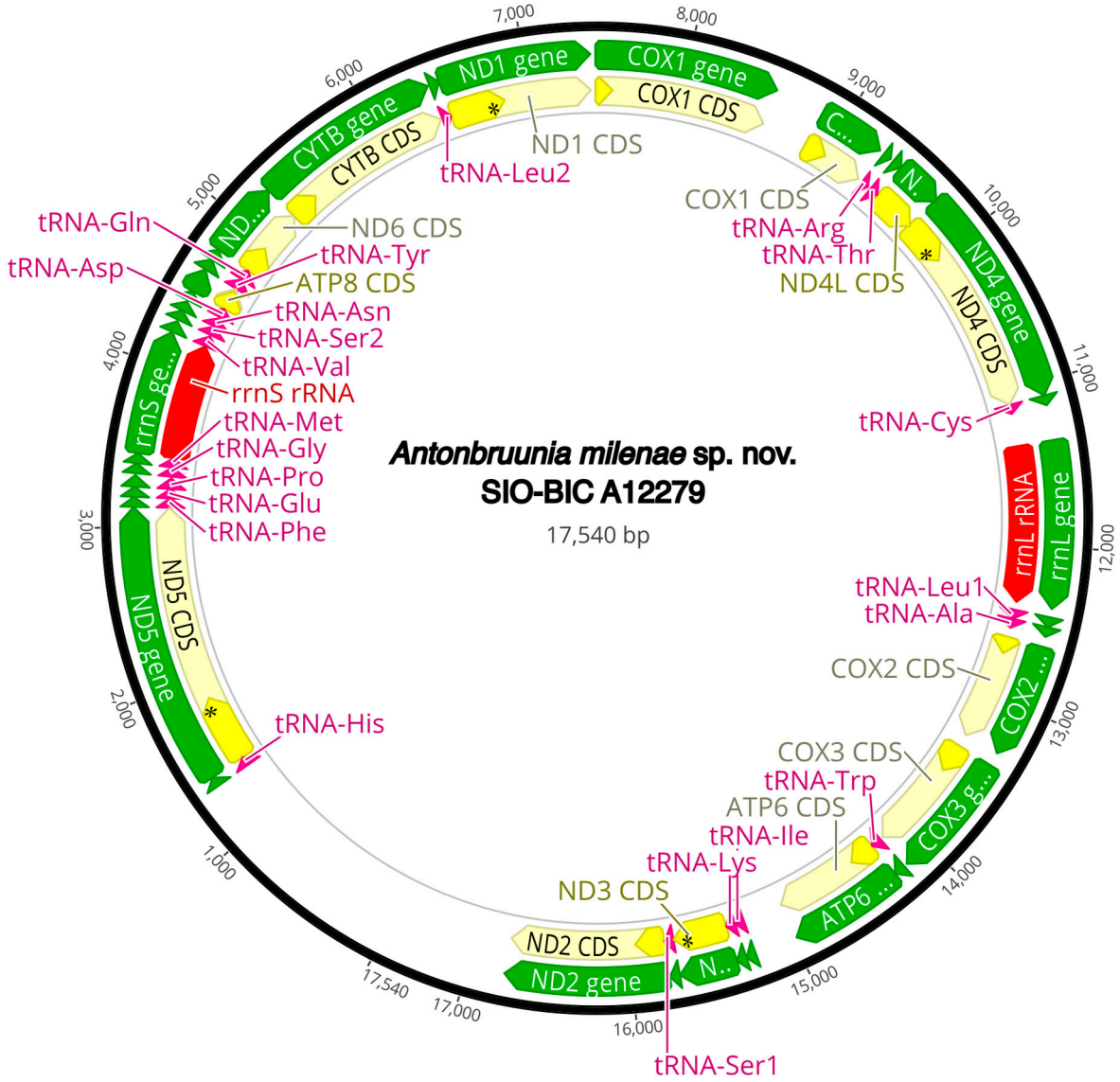

Figure A2. *Antonbruunia milenae* sp. nov. complete mitogenome. The thick black circle shows the circularized sequence, numbers mark base pairs. Green arrows represent genes, yellow arrows represent protein coding sequences (CDS), pink arrows represent tRNAs, red arrows represent rRNAs. The direction of the arrow represents the direction of the gene. Where genes are long enough, their name is written on the arrow, otherwise their names and whether they are a CDS, tRNA, or rRNA is written next to the gene and connected to it via yellow (CDS), pink (tRNA), or red (rRNA) line. Geneious version 2022.2 created by Biomatters was used to generate this figure. Available from https://www.geneious.com (accessed on 31 January 2024) [36].

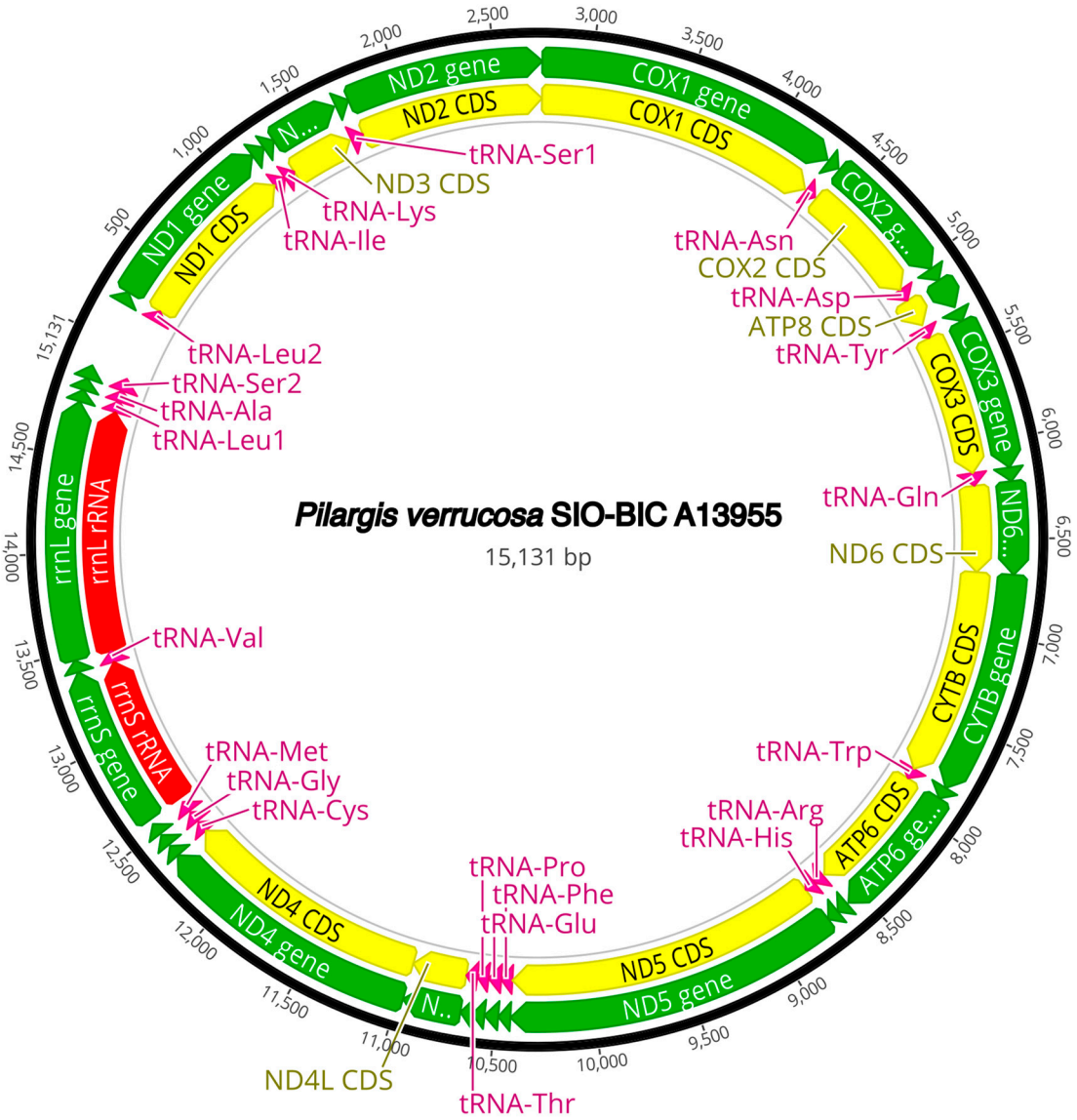

Figure A3. *Pilargis verrucosa* complete mitogenome. The thick black circle shows the circularized sequence, numbers mark base pairs. Green arrows represent genes, yellow arrows represent protein coding sequences (CDS), pink arrows represent tRNAs, red arrows represent rRNAs. The direction of the arrow represents the direction of the gene. Where genes are long enough, their name is written on the arrow, otherwise their names and whether they are a CDS, tRNA, or rRNA is written next to the gene and connected to it via yellow (CDS), pink (tRNA), or red (rRNA) line. Geneious version 2022.2 created by Biomatters was used to generate this figure. Available from https://www.geneious.com (accessed on 31 January 2024) [36].

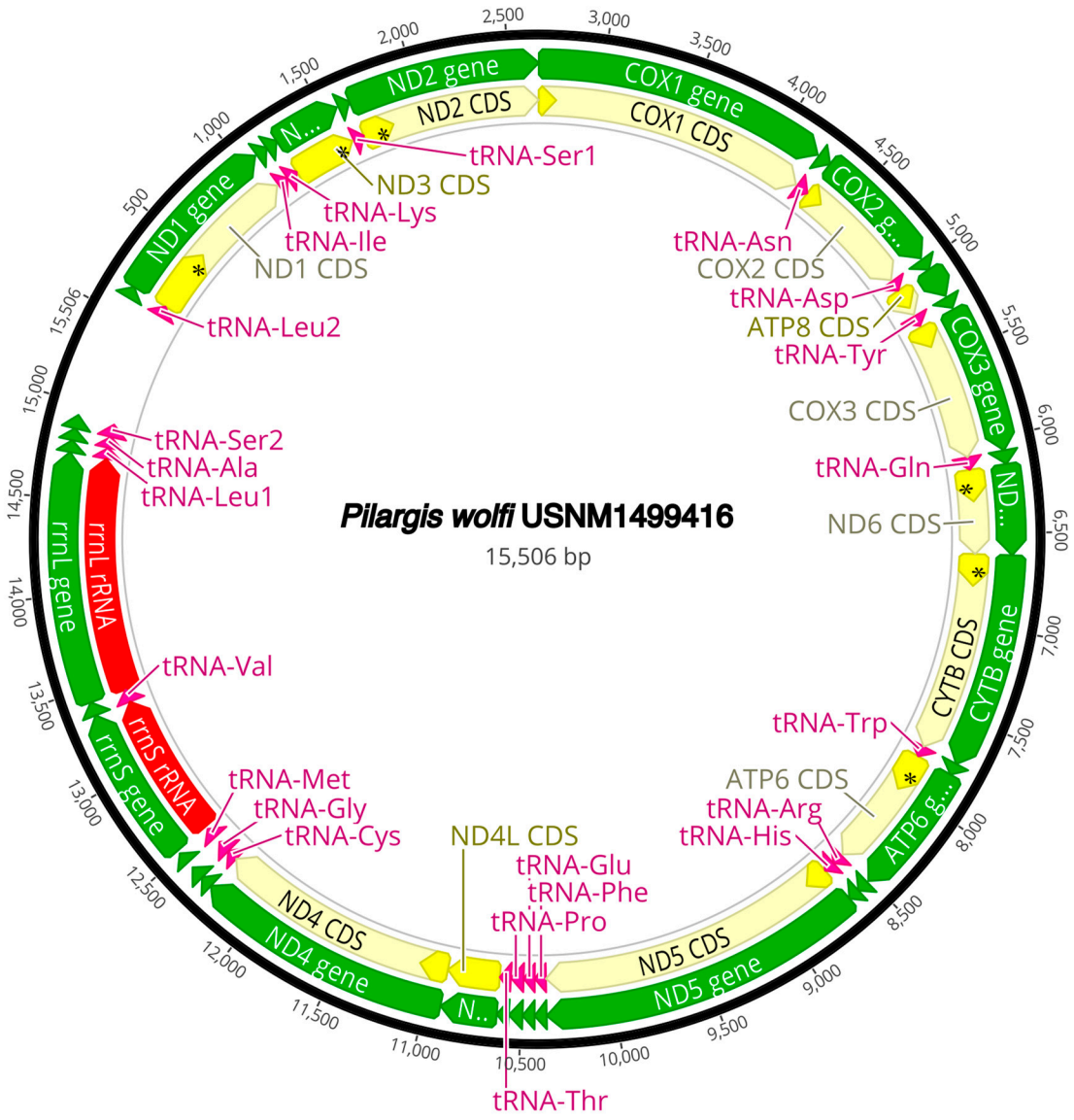

Figure A4. *Pilargis wolfi* complete mitogenome. The thick black circle shows the circularized sequence, numbers mark base pairs. Green arrows represent genes, yellow arrows represent protein coding sequences (CDS), pink arrows represent tRNAs, red arrows represent rRNAs. The direction of the arrow represents the direction of the gene. Where genes are long enough, their name is written on the arrow, otherwise their names and whether they are a CDS, tRNA, or rRNA is written next to the gene and connected to it via yellow (CDS), pink (tRNA), or red (rRNA) line. Geneious version 2022.2 created by Biomatters was used to generate this figure. Available from https://www.geneious.com (accessed on 31 January 2024) [36].

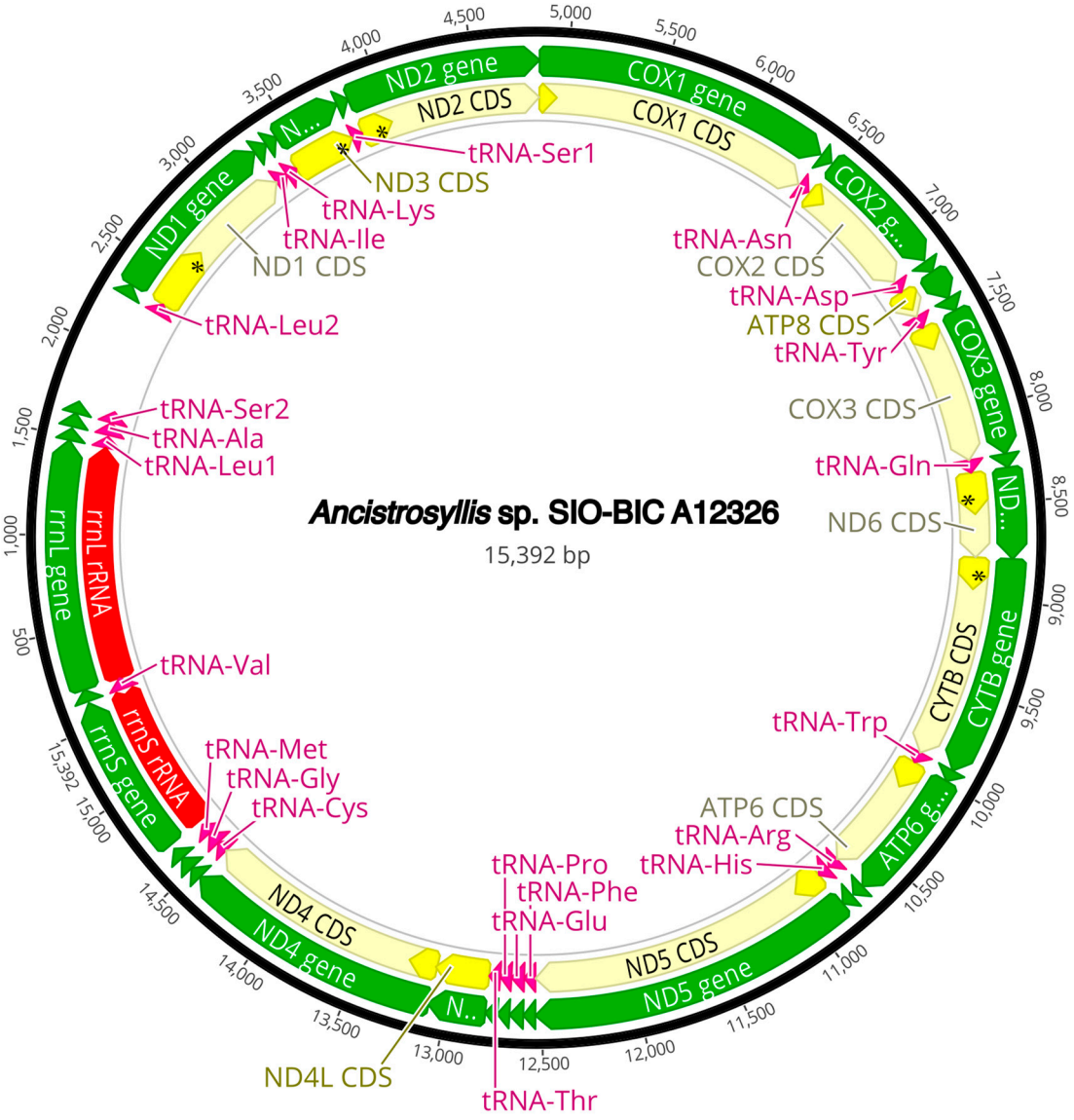

Figure A5. *Ancistrosyllis* sp. complete mitogenome. The thick black circle shows the circularized sequence, numbers mark base pairs. Green arrows represent genes, yellow arrows represent protein coding sequences (CDS), pink arrows represent tRNAs, red arrows represent rRNAs. The direction of the arrow represents the direction of the gene. Where genes are long enough, their name is written on the arrow, otherwise their names and whether they are a CDS, tRNA, or rRNA is written next to the gene and connected to it via yellow (CDS), pink (tRNA), or red (rRNA) line. Geneious version 2022.2 created by Biomatters was used to generate this figure. Available from https://www.geneious.com (accessed on 31 January 2024) [36].

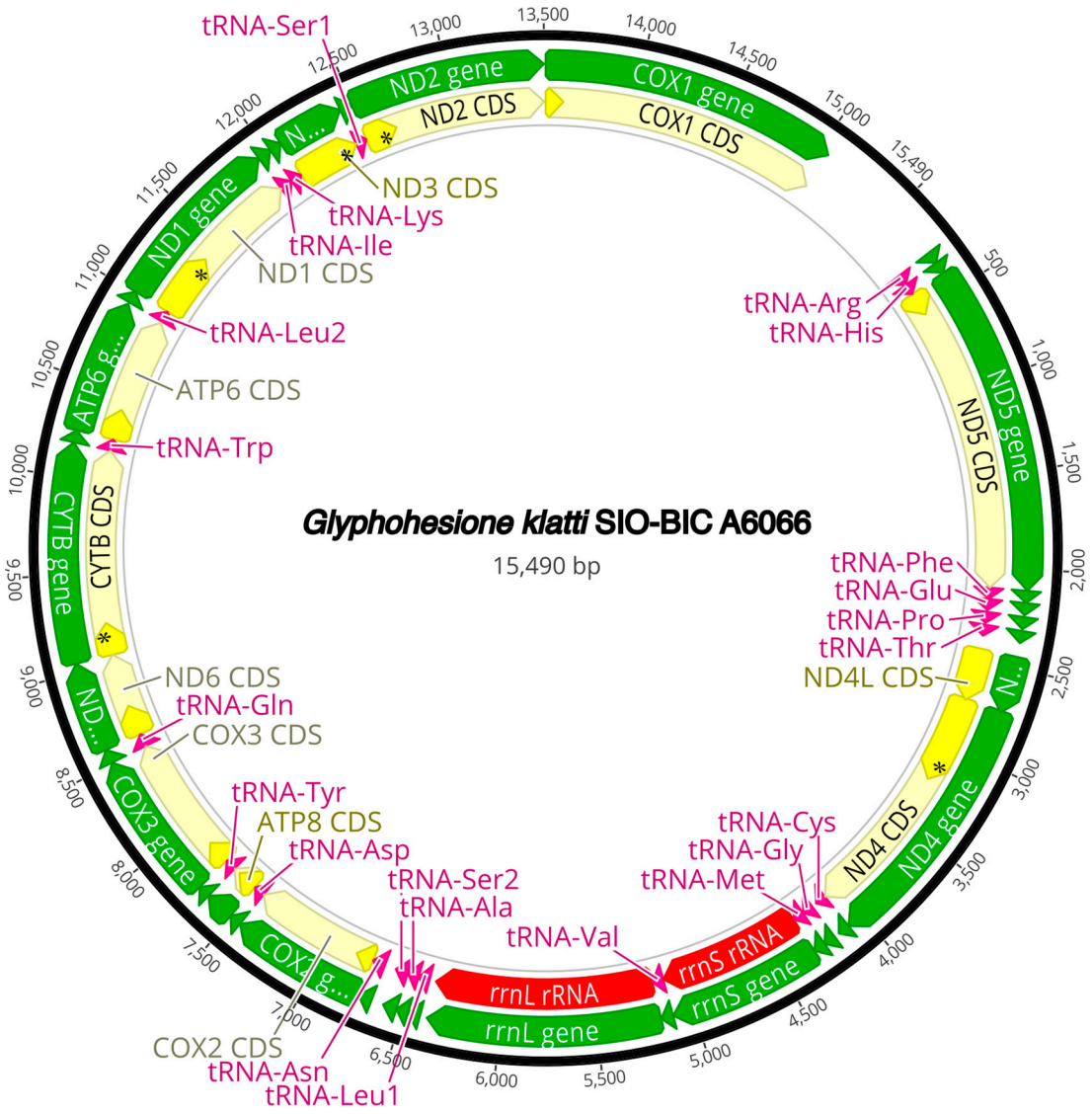

Figure A6. *Glyphohesione klatti* complete mitogenome. The thick black circle shows the circularized sequence, numbers mark base pairs. Green arrows represent genes, yellow arrows represent protein coding sequences (CDS), pink arrows represent tRNAs, red arrows represent rRNAs. The direction of the arrow represents the direction of the gene. Where genes are long enough, their name is written on the arrow, otherwise their names and whether they are a CDS, tRNA, or rRNA is written next to the gene and connected to it via yellow (CDS), pink (tRNA), or red (rRNA) line. Geneious version 2022.2 created by Biomatters was used to generate this figure. Available from https://www.geneious.com (accessed on 31 January 2024) [36].

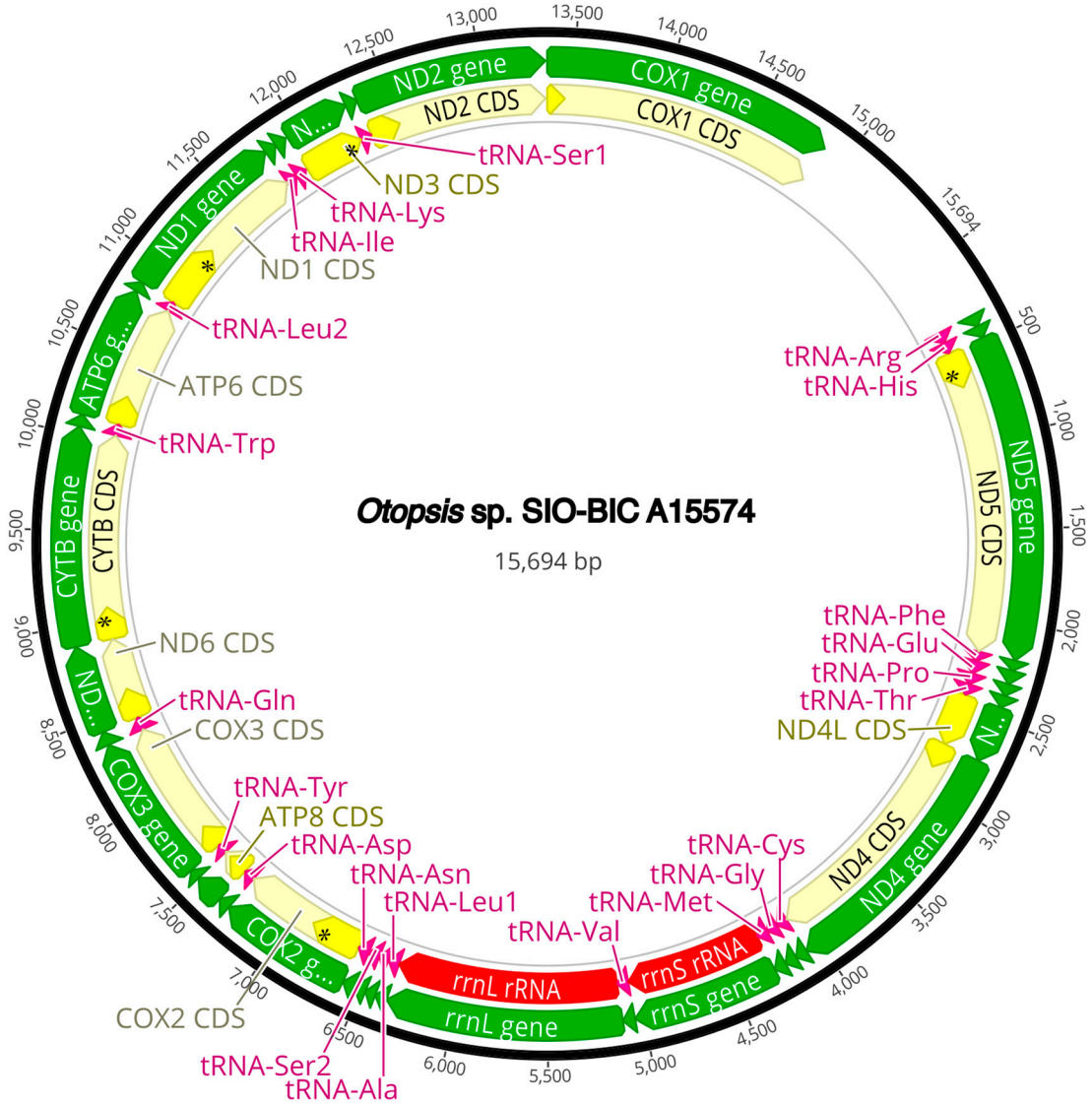

Figure A7. *Otopsis* sp. complete mitogenome. The thick black circle shows the circularized sequence, numbers mark base pairs. Green arrows represent genes, yellow arrows represent protein coding sequences (CDS), pink arrows represent tRNAs, red arrows represent rRNAs. The direction of the arrow represents the direction of the gene. Where genes are long enough, their name is written on the arrow, otherwise their names and whether they are a CDS, tRNA, or rRNA is written next to the gene and connected to it via yellow (CDS), pink (tRNA), or red (rRNA) line. Geneious version 2022.2 created by Biomatters was used to generate this figure. Available from https://www.geneious.com (accessed on 31 January 2024) [36].

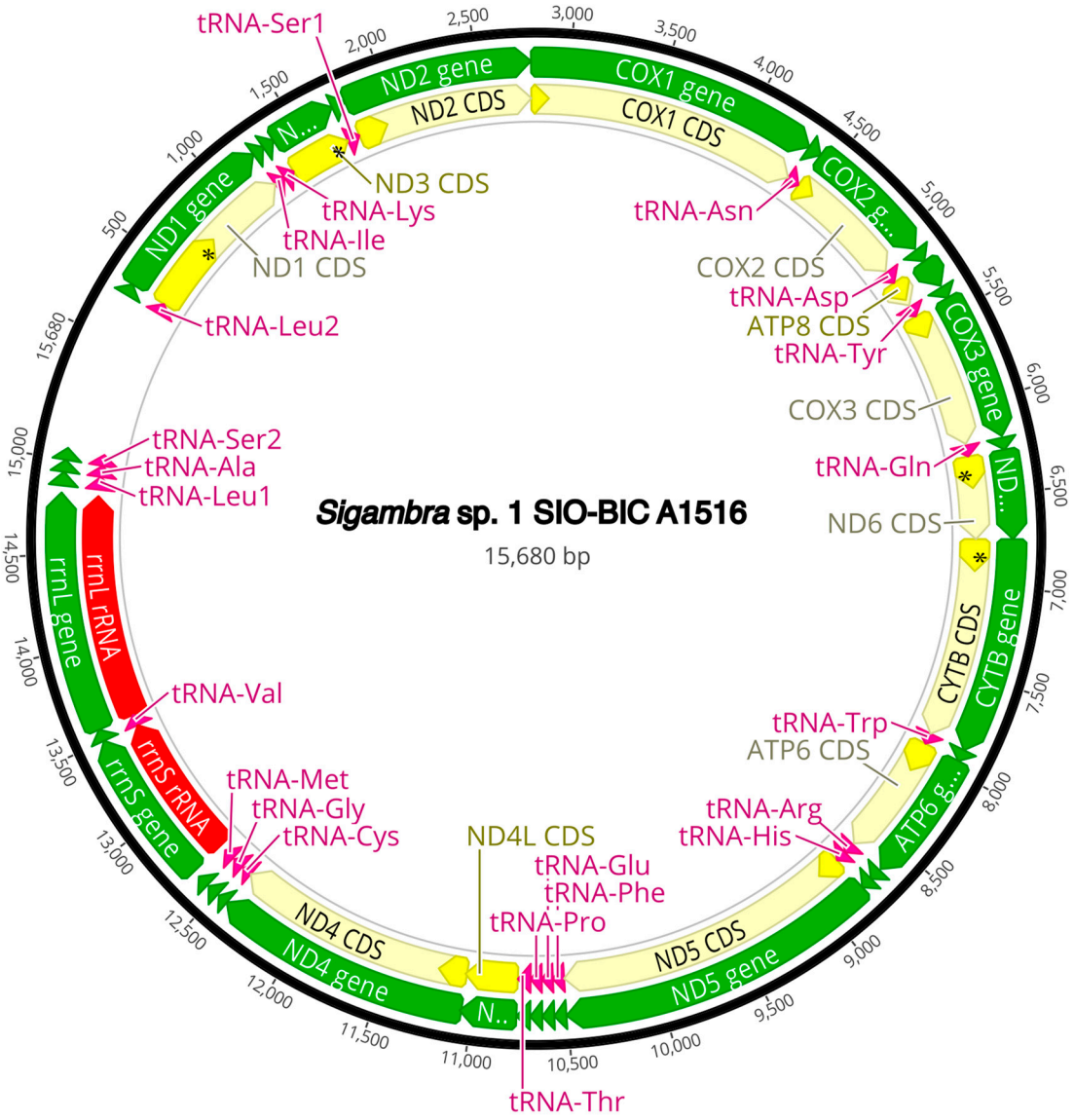

Figure A8. *Sigambra* sp. 1 complete mitogenome. The thick black circle shows the circularized sequence, numbers mark base pairs. Green arrows represent genes, yellow arrows represent protein coding sequences (CDS), pink arrows represent tRNAs, red arrows represent rRNAs. The direction of the arrow represents the direction of the gene. Where genes are long enough, their name is written on the arrow, otherwise their names and whether they are a CDS, tRNA, or rRNA is written next to the gene and connected to it via yellow (CDS), pink (tRNA), or red (rRNA) line. Geneious version 2022.2 created by Biomatters was used to generate this figure. Available from https://www.geneious.com (accessed on 31 January 2024) [36].

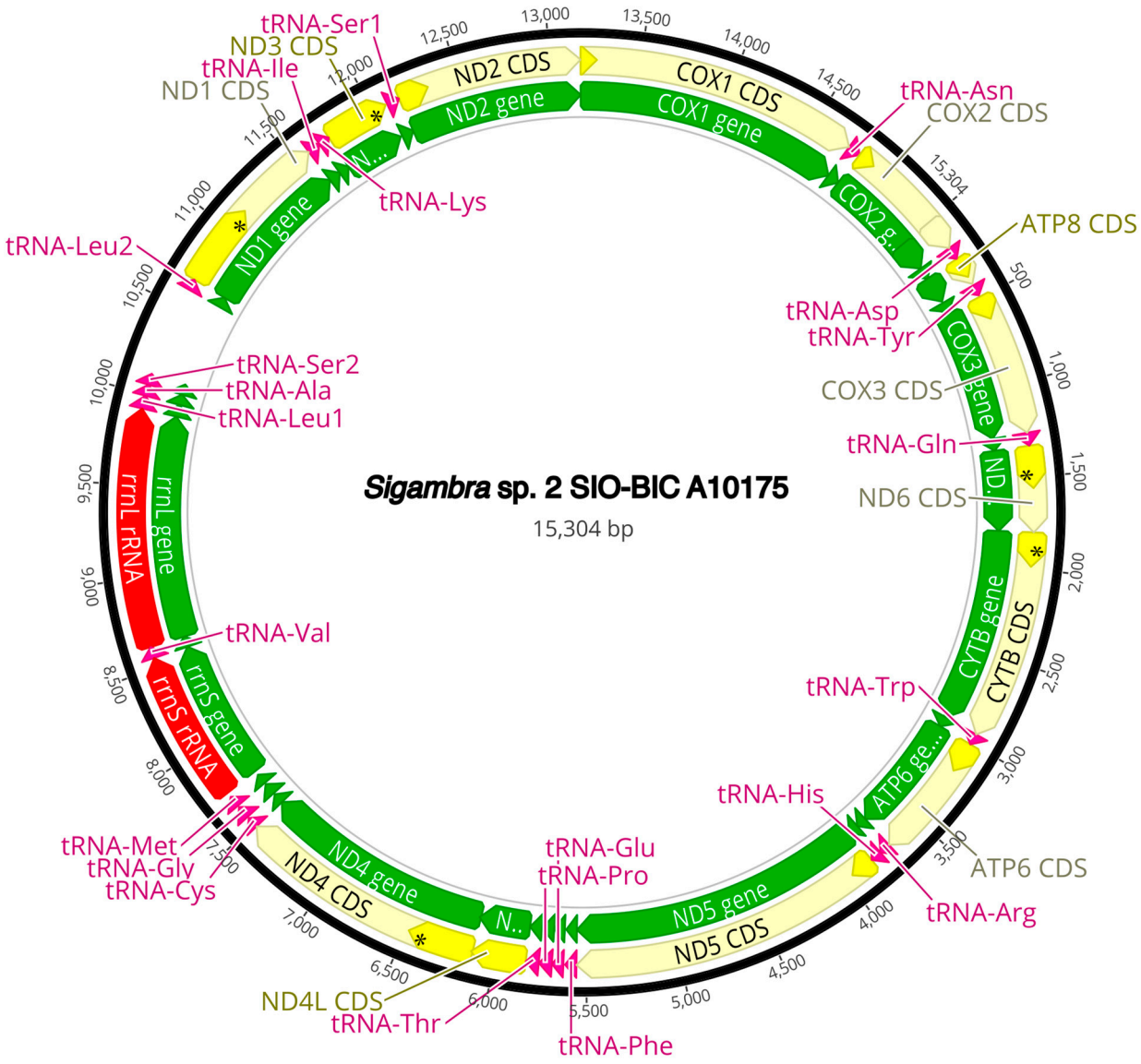

Figure A9. *Sigambra* sp. 2 complete mitogenome. The thick black circle shows the circularized sequence, numbers mark base pairs. Green arrows represent genes, yellow arrows represent protein coding sequences (CDS), pink arrows represent tRNAs, red arrows represent rRNAs. The direction of the arrow represents the direction of the gene. Where genes are long enough, their name is written on the arrow, otherwise their names and whether they are a CDS, tRNA, or rRNA is written next to the gene and connected to it via yellow (CDS), pink (tRNA), or red (rRNA) line. Geneious version 2022.2 created by Biomatters was used to generate this figure. Available from https://www.geneious.com (accessed on 31 January 2024) [36].

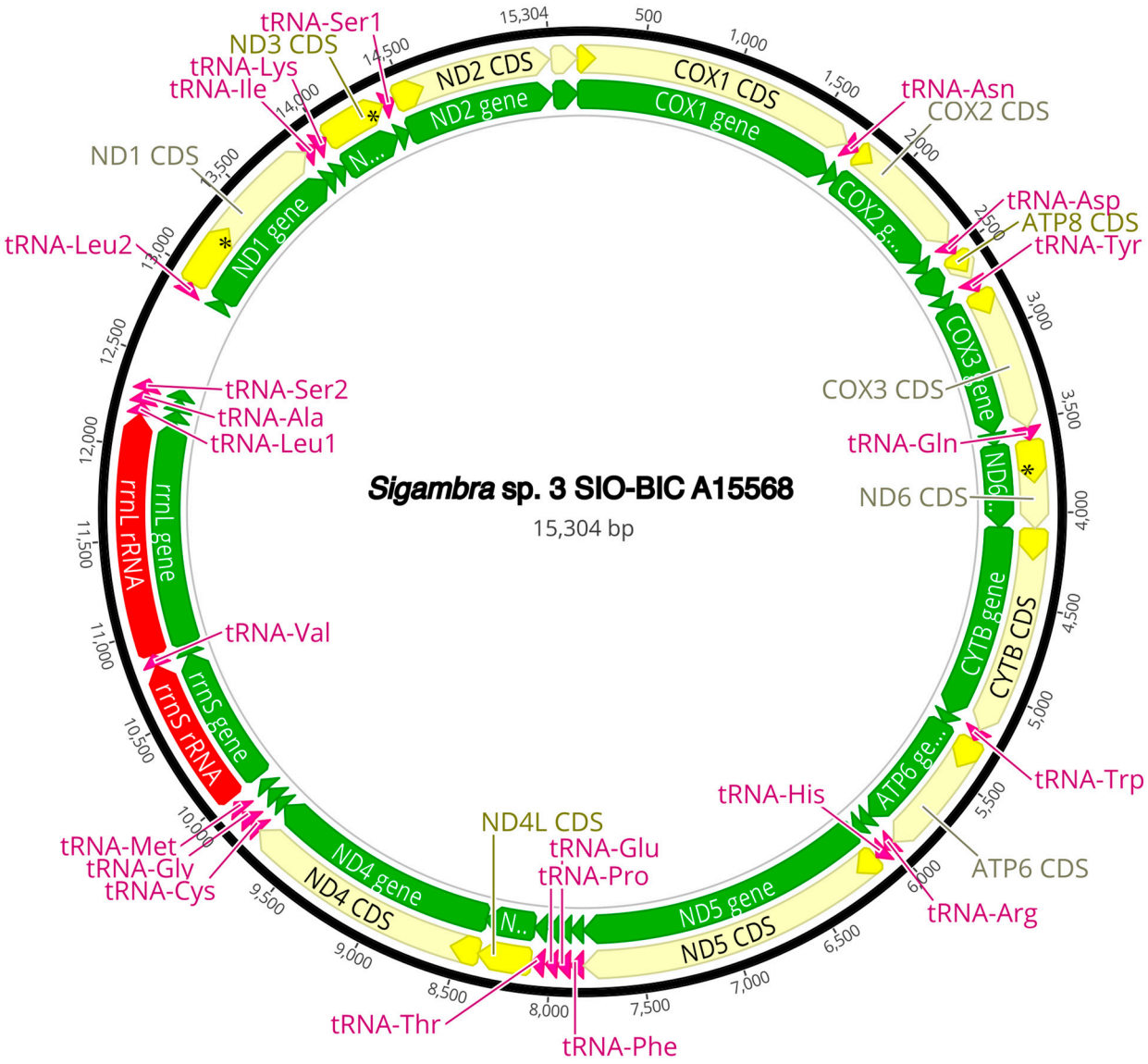

Figure A10. *Sigambra* sp. 3 complete mitogenome. The thick black circle shows the circularized sequence, numbers mark base pairs. Green arrows represent genes, yellow arrows represent protein coding sequences (CDS), pink arrows represent tRNAs, red arrows represent rRNAs. The direction of the arrow represents the direction of the gene. Where genes are long enough, their name is written on the arrow, otherwise their names and whether they are a CDS, tRNA, or rRNA is written next to the gene and connected to it via yellow (CDS), pink (tRNA), or red (rRNA) line. Geneious version 2022.2 created by Biomatters was used to generate this figure. Available from https://www.geneious.com (accessed on 31 January 2024) [36].

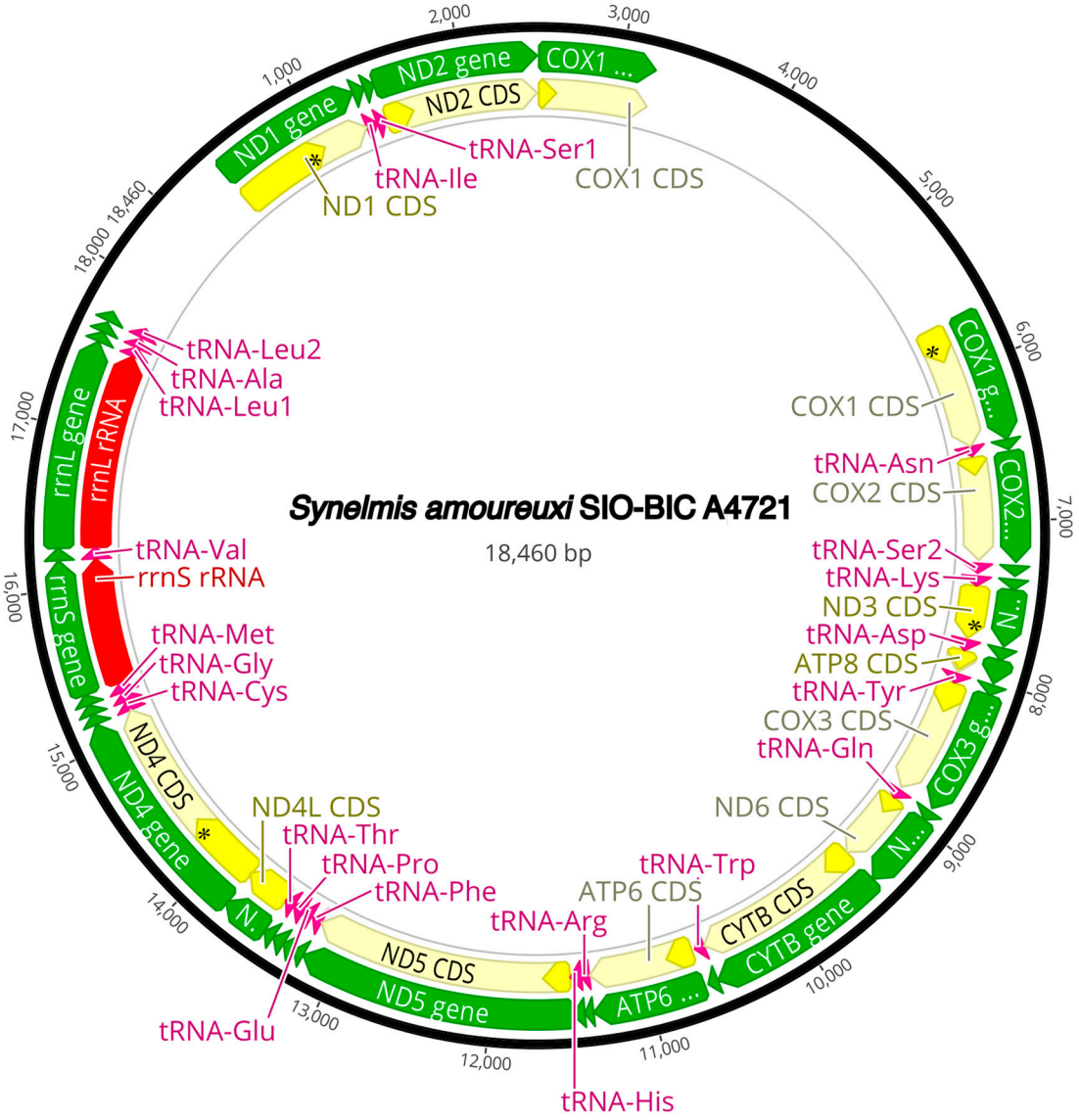

Figure A11. *Synelmis amoureuxi* complete mitogenome. The thick black circle shows the circularized sequence, numbers mark base pairs. Green arrows represent genes, yellow arrows represent protein coding sequences (CDS), pink arrows represent tRNAs, red arrows represent rRNAs. The direction of the arrow represents the direction of the gene. Where genes are long enough, their name is written on the arrow, otherwise their names and whether they are a CDS, tRNA, or rRNA is written next to the gene and connected to it via yellow (CDS), pink (tRNA), or red (rRNA) line. Geneious version 2022.2 created by Biomatters was used to generate this figure. Available from https://www.geneious.com (accessed on 31 January 2024) [36].

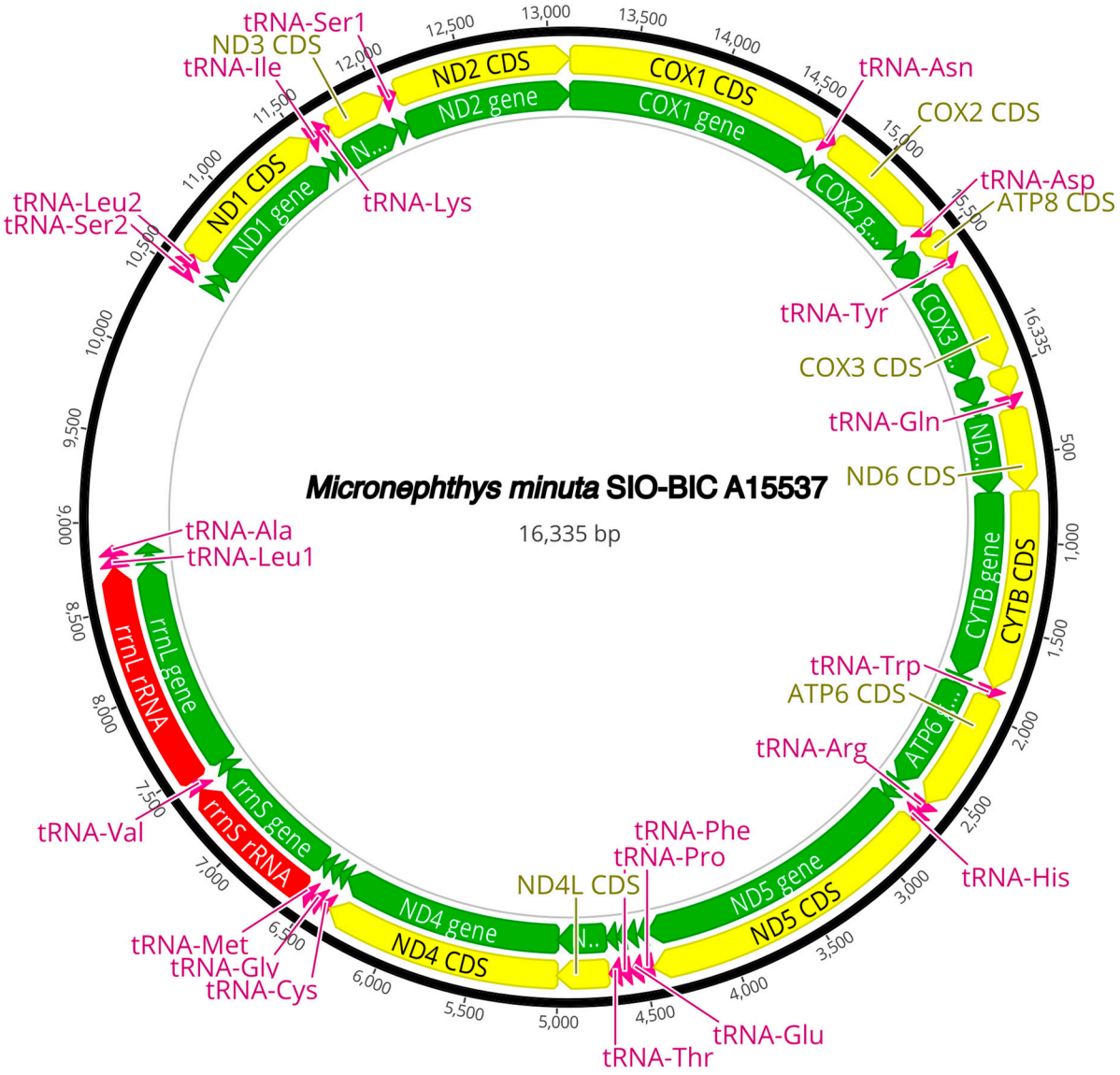

Figure A12. *Micronephthys minuta* (Nephtyidae) complete mitogenome. The thick black circle shows the circularized sequence, numbers mark base pairs. Green arrows represent genes, yellow arrows represent protein coding sequences (CDS), pink arrows represent tRNAs, red arrows represent rRNAs. The direction of the arrow represents the direction of the gene. Where genes are long enough, their name is written on the arrow, otherwise their names and whether they are a CDS, tRNA, or rRNA is written next to the gene and connected to it via yellow (CDS), pink (tRNA), or red (rRNA) line. Geneious version 2022.2 created by Biomatters was used to generate this figure. Available from https://www.geneious.com (accessed on 31 January 2024) [36].

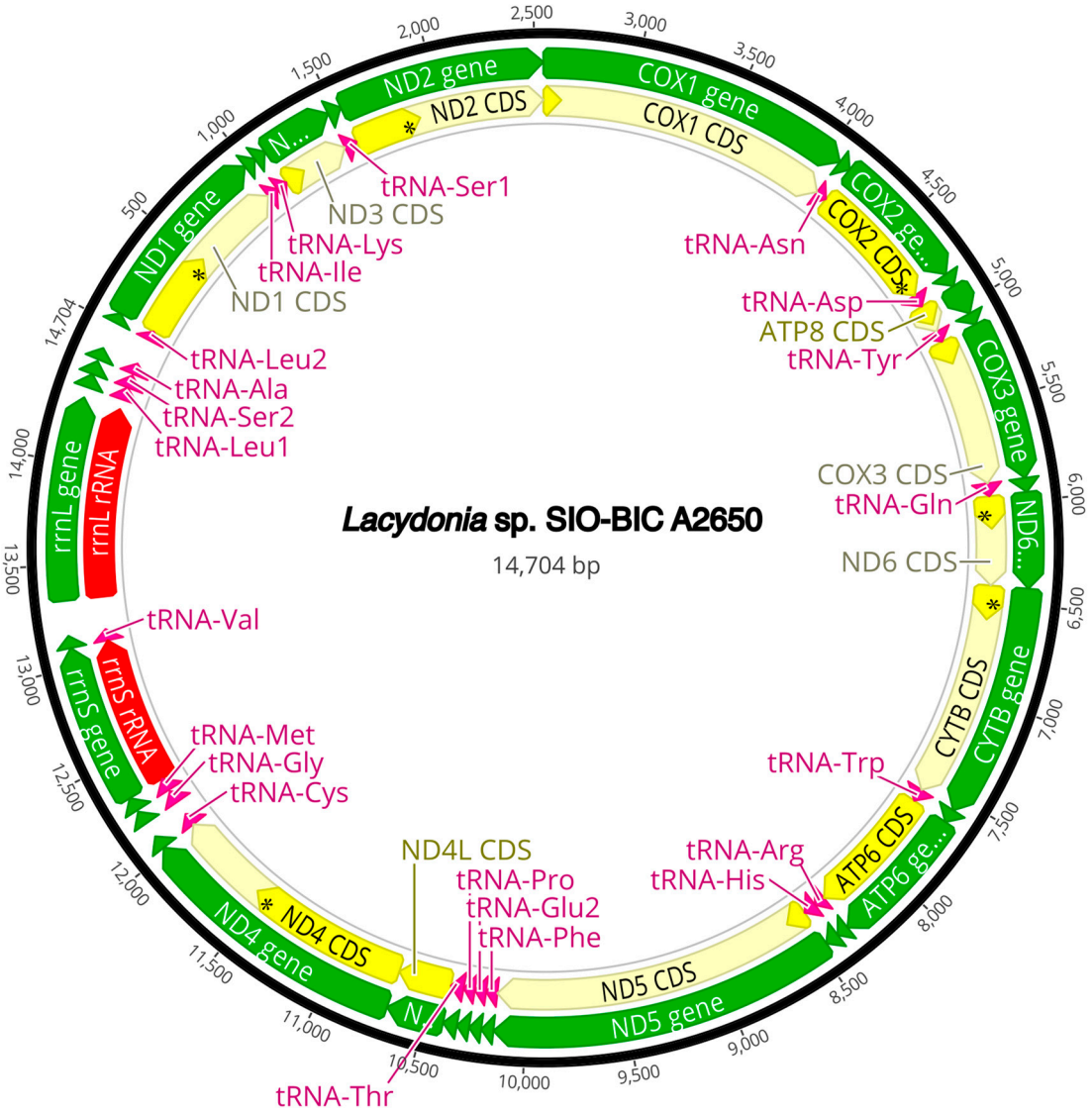

Figure A13. *Lacydonia* sp. (Lacydoniidae) complete mitogenome. The thick black circle shows the circularized sequence, numbers mark base pairs. Green arrows represent genes, yellow arrows represent protein coding sequences (CDS), pink arrows represent tRNAs, red arrows represent rRNAs. The direction of the arrow represents the direction of the gene. Where genes are long enough, their name is written on the arrow, otherwise their names and whether they are a CDS, tRNA, or rRNA is written next to the gene and connected to it via yellow (CDS), pink (tRNA), or red (rRNA) line. Geneious version 2022.2 created by Biomatters was used to generate this figure. Available from https://www.geneious.com (accessed on 31 January 2024) [36].

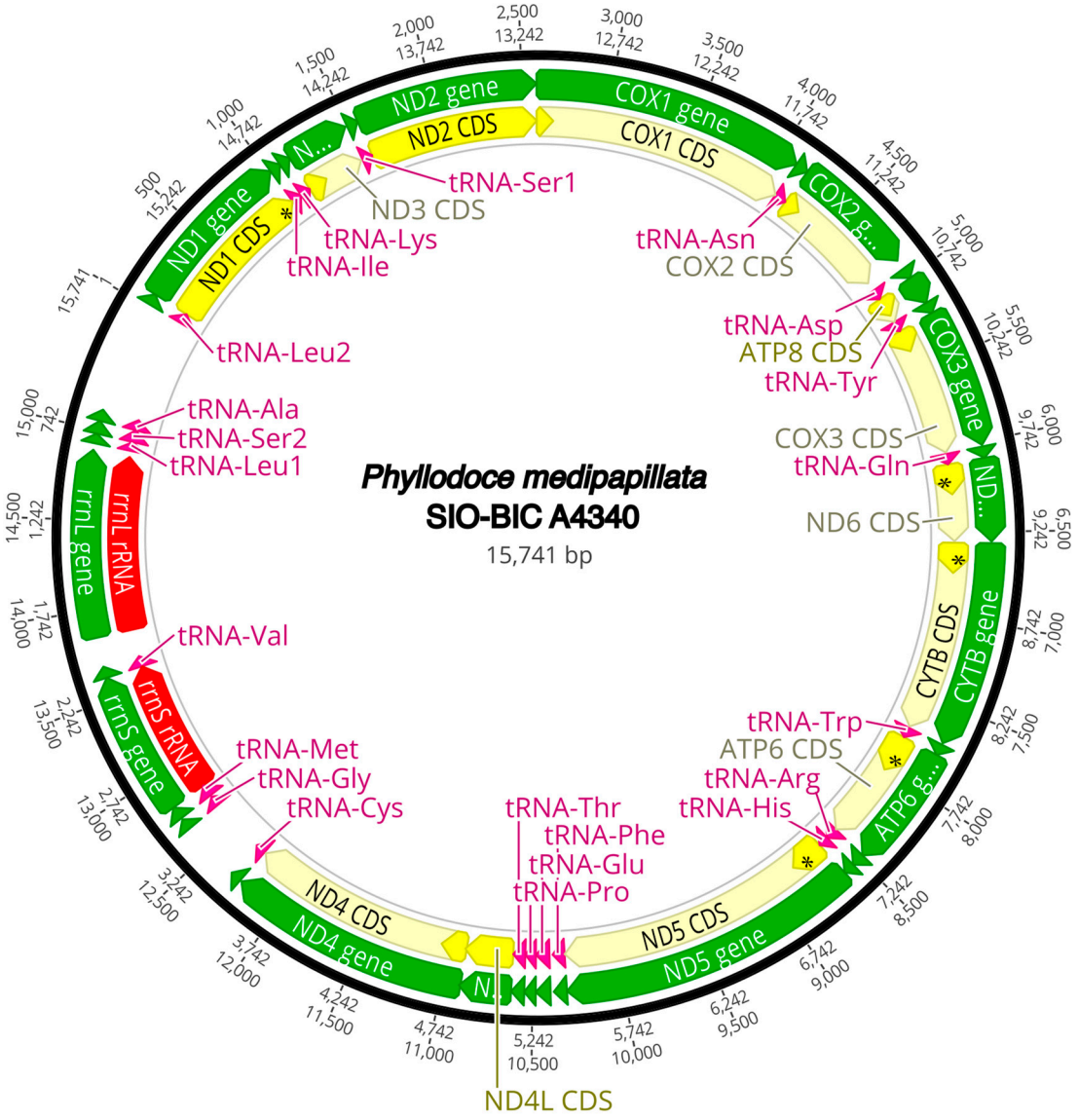

Figure A14. *Phyllodoce medipapillata* (Phyllodocidae) complete mitogenome. The thick black circle shows the circularized sequence, numbers mark base pairs. Green arrows represent genes, yellow arrows represent protein coding sequences (CDS), pink arrows represent tRNAs, red arrows represent rRNAs. The direction of the arrow represents the direction of the gene. Where genes are long enough, their name is written on the arrow, otherwise their names and whether they are a CDS, tRNA, or rRNA is written next to the gene and connected to it via yellow (CDS), pink (tRNA), or red (rRNA) line. Geneious version 2022.2 created by Biomatters was used to generate this figure. Available from https://www.geneious.com (accessed on 31 January 2024) [36].

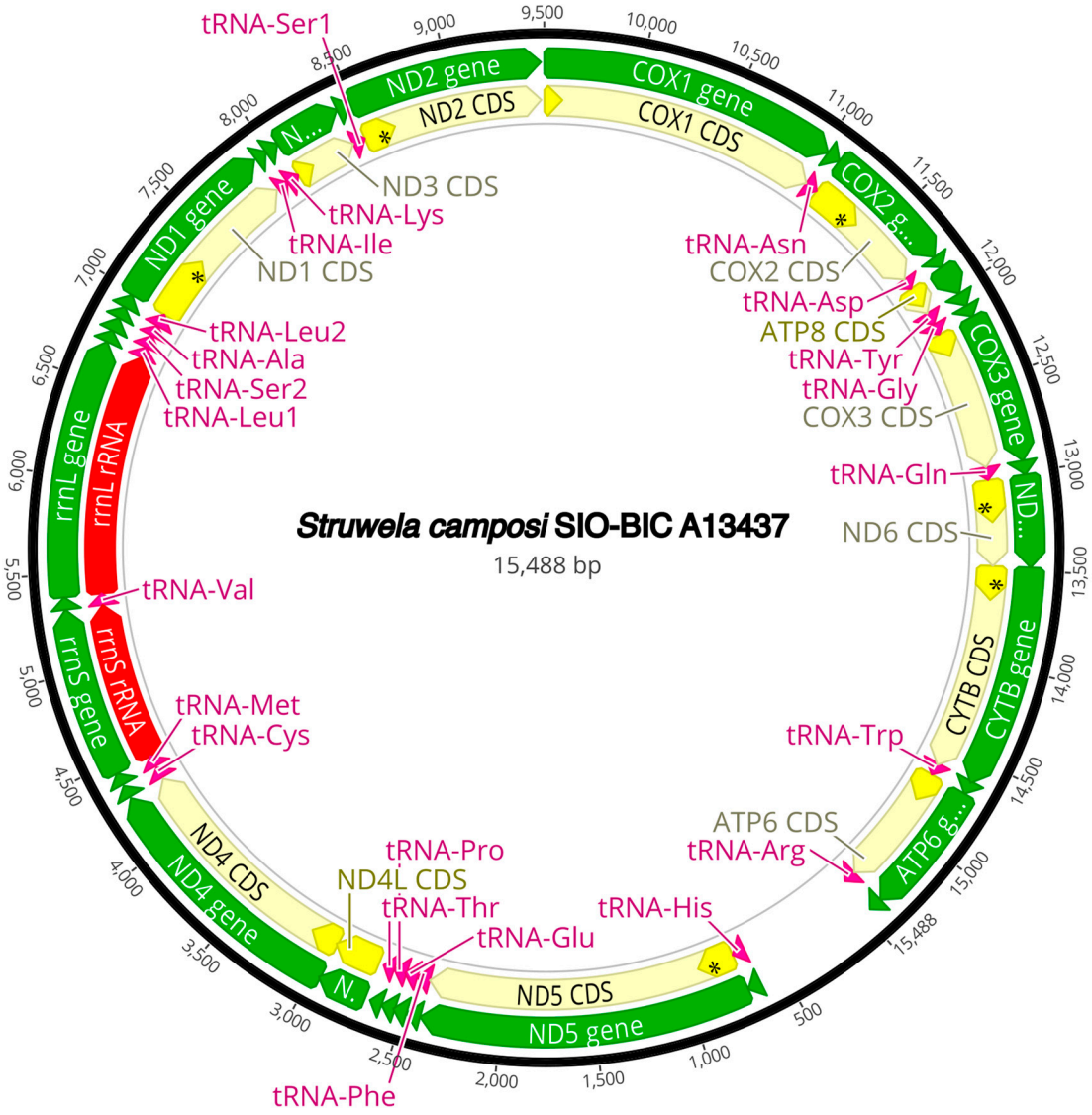

Figure A15. *Struwela camposi* (Microphthalmidae) complete mitogenome. The thick black circle shows the circularized sequence, numbers mark base pairs. Green arrows represent genes, yellow arrows represent protein coding sequences (CDS), pink arrows represent tRNAs, red arrows represent rRNAs. The direction of the arrow represents the direction of the gene. Where genes are long enough, their name is written on the arrow, otherwise their names and whether they are a CDS, tRNA, or rRNA is written next to the gene and connected to it via yellow (CDS), pink (tRNA), or red (rRNA) line. Geneious version 2022.2 created by Biomatters was used to generate this figure. Available from https://www.geneious.com (accessed on 31 January 2024) [36].

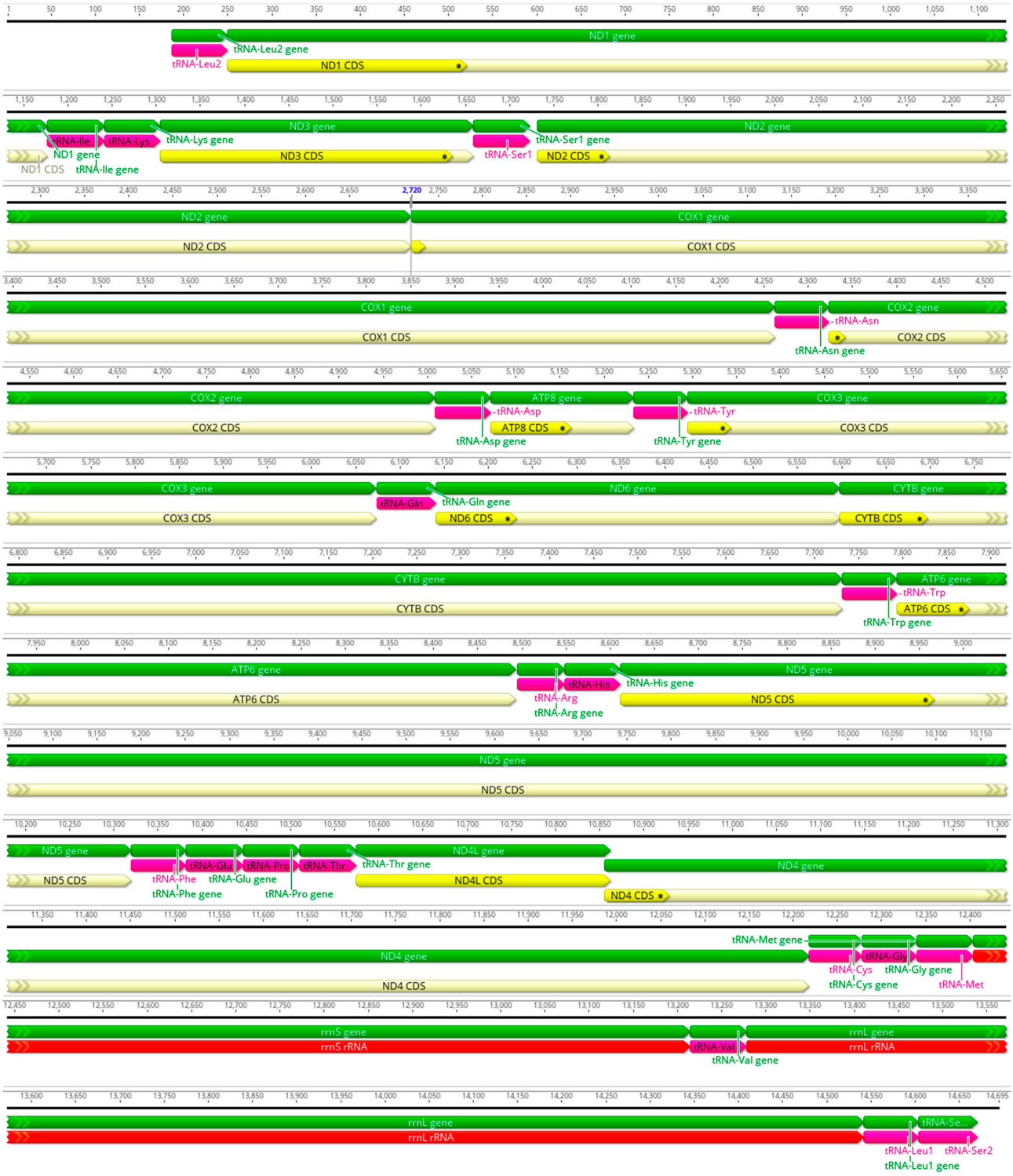

Figure A16. *Hermundura fauveli* (Microphthalmidae) incomplete mitogenome. The thick black line shows the sequence, numbers mark base pairs. Green arrows represent genes, yellow arrows represent protein coding sequences (CDS), pink arrows represent tRNAs, red arrows represent rRNAs. The direction of the arrow represents the direction of the gene. Where genes are long enough, their name is written on the arrow, otherwise their names and whether they are a CDS, tRNA, or rRNA is written next to the gene and connected to it via yellow (CDS), pink (tRNA), or red (rRNA) line. Geneious version 2022.2 created by Biomatters was used to generate this figure. Available from https://www.geneious.com (accessed on 31 January 2024) [36].

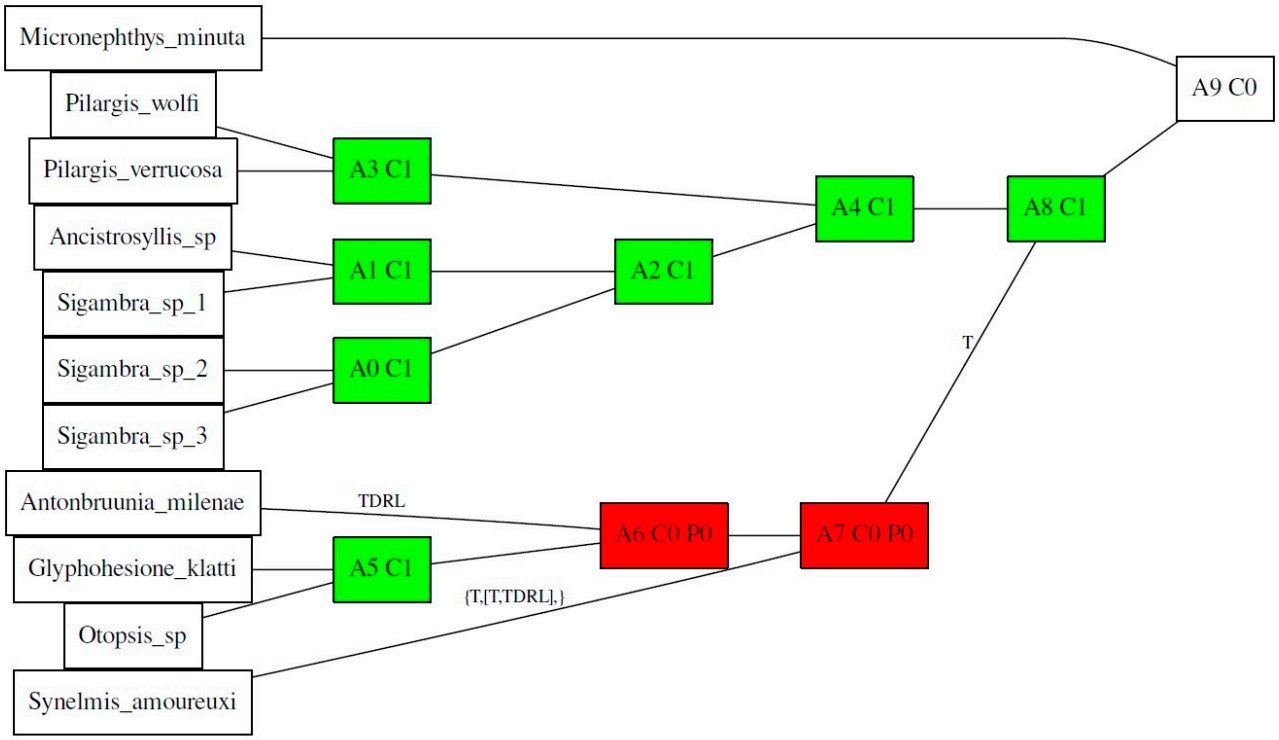

Figure A17. Original TreeREx output of mitogenome gene orders and changes along the phylogeny. Each rectangle to the right of the taxa indicates a node. Abbreviations: T, transposition; TDRL, tandem duplication random loss.

References

1. Capa, M.; Hutchings, P. Annelid Diversity: Historical Overview and Future Perspectives. *Diversity* **2021**, *13*, 129. [CrossRef]
2. Rouse, G.; Pleijel, F.; Tilic, E. *Annelida*; Oxford University Press: Oxford, UK, 2022; ISBN 0192591622.
3. Watson, C.; Tilic, E.; Rouse, G.W. Revision of *Hyalopale* (Chrysopetalidae; Phyllodocida; Annelida): An Amphi-Atlantic *Hyalopale bispinosa* Species Complex and Five New Species from Reefs of the Caribbean Sea and Indo-Pacific Oceans. *Zootaxa* **2019**, *4671*, 339–368. [CrossRef]
4. Pearson, K.A.M.; Rouse, G.W. Vampire Worms; A Revision of *Galapagomystides* (Phyllodocidae, Annelida), with the Description of Three New Species. *Zootaxa* **2022**, *5128*, 451–485. [CrossRef] [PubMed]
5. Summers, M.M.; Rouse, G.W. Phylogeny of Myzostomida (Annelida) and Their Relationships with Echinoderm Hosts. *BMC Evol. Biol.* **2014**, *14*, 1–15. [CrossRef] [PubMed]
6. Tilic, E.; Stiller, J.; Campos, E.; Pleijel, F.; Rouse, G.W. Phylogenomics Resolves Ambiguous Relationships within Aciculata (Errantia, Annelida). *Mol. Phylogenetics Evol.* **2022**, *166*, 107339. [CrossRef] [PubMed]
7. Mackie, A.S.Y.; Oliver, P.G.; Nygren, A. *Antonbruunia sociabilis* sp. nov. (Annelida: Antonbruunidae) Associated with the Chemosynthetic Deep-Sea Bivalve *Thyasira scotiae* Oliver & Drewery, 2014, and a Re-Examination of the Systematic Affinities of Antonbruunidae. *Zootaxa* **2015**, *3995*, 20–36. [CrossRef] [PubMed]
8. Hartman, O.; Boss, K.J. *Antonbruunia viridis*, a New Inquiline Annelid with Dwarf Males, Inhabiting a New Species of Pelecypod, *Lucina fosteri*, in the Mozambique Channel. *Ann. Mag. Nat. Hist.* **1965**, *8*, 177–186. [CrossRef]
9. Quiroga, E.; Sellanes, J. Two New Polychaete Species Living in the Mantle Cavity of *Calyptogena gallardoi* (Bivalvia: Vesicomyidae) at a Methane Seep Site off Central Chile (∼36° S). *Sci. Mar.* **2009**, *73*, 399–407. [CrossRef]
10. Fauchald, K. *The Polychaete Worms, Definitions and Keys to the Orders, Families and Genera*; Science Series; Natural History Museum of Los Angeles County: Los Angeles, CA, USA, 1977; Volume 28, pp. 1–188.
11. Glasby, C.J. Family Revision and Cladistic Analysis of the Nereidoidea (Polychaeta: Phyllodocida). *Invertebr. Syst.* **1993**, *7*, 1551–1573. [CrossRef]
12. Salazar-Vallejo, S.I. Pilargidae (Annelida: Polychaeta) de Mexico: Lista de Especies, Nueva Especie y Biografia. *Cah. Biol. Mar.* **1986**, *27*, 192–210.
13. Glasby, C.J.; Salazar-Vallejo, S.I. Pilargidae Saint-Joseph, 1899. In *Handbook of Zoology. Annelida. Pleistoannelida, Errantia II, Phyllodocida*; Purschke, G., Westheide, W., Böggemann, M., Eds.; De Gruyter: Berlin, Germany, 2022; pp. 308–320.
14. Miura, T.; Laubier, L. Nautiliniellid Polychaetes Collected from the Hatsushima Cold-Seep Site in Sagami Bay, with Descriptions of New Genera and Species. *Zool. Sci.* **1990**, *7*, 319–325.

15. Fitzhugh, K.; Wolf, P.S. Gross Morphology of the Brain of Pilargid Polychaetes: Taxonomic and Systematic Implications. *Am. Mus. Novit.* **1990**, *2992*, 16–23.
16. Beesley, P.L.; Ross, G.J.B.; Glasby, C.J. (Eds.) *Polychaetes & Allies: The Southern Synthesis*; CSIRO Publishing: Clayton, VIC, Australia, 2000; Volume 4.
17. Pleijel, F.; Dahlgren, T. Position and Delineation of Chrysopetalidae and Hesionidae (Annelida, Polychaeta, Phyllodocida). *Cladistics* **1998**, *14*, 129–150. [CrossRef] [PubMed]
18. Rouse, G.W.; Pleijel, F. *Polychaetes*; Oxford University Press: Oxford, UK, 2001; ISBN 0198506082.
19. Kükenthal, W. *Annelida: Volume 1. Annelida Basal Groups and Pleistoannelida, Sedentaria I*; Purschke, G., Westheide, W., Böggemann, M., Eds.; Walter de Gruyter GmbH & Co.: Berlin, Germany, 2019; ISBN 3110291460.
20. Ravara, A.; Wiklund, H.; Cunha, M.R.; Pleijel, F. Phylogenetic Relationships within Nephtyidae (Polychaeta, Annelida). *Zool. Scr.* **2010**, *39*, 394–405. [CrossRef]
21. Bernardino, A.F.; Li, Y.; Smith, C.R.; Halanych, K.M. Multiple Introns in a Deep-Sea Annelid (*Decemunciger*: Ampharetidae) Mitochondrial Genome. *Sci. Rep.* **2017**, *7*, 4295. [CrossRef] [PubMed]
22. Zhou, H.; Liu, X. HZPLY558-13.COI-5P. Available online: http://www.boldsystems.org/index.php/Public_RecordView?processid=HZPLY558-13 (accessed on 20 December 2023).
23. Böggemann, M. Polychaetes (Annelida) of the Abyssal SE Atlantic. *Org. Divers. Evol.* **2009**, *9*, 251–428. [CrossRef]
24. Vijapure, T.; Sukumaran, S.; Manohar, C.S. Molecular Characterization and Phylogenetics of Indian Polychaete Fauna: Scope for Implementation in Ecological Monitoring. *Aquat. Ecol.* **2019**, *53*, 665–677. [CrossRef]
25. Aylagas, E.; Borja, Á.; Irigoien, X.; Rodríguez-Ezpeleta, N. Benchmarking DNA Metabarcoding for Biodiversity-Based Monitoring and Assessment. *Front. Mar. Sci.* **2016**, *3*, 96. [CrossRef]
26. Struck, T.H.; Schult, N.; Kusen, T.; Hickman, E.; Bleidorn, C.; McHugh, D.; Halanych, K.M. Annelid Phylogeny and the Status of Sipuncula and Echiura. *BMC Evol. Biol.* **2007**, *7*, 57. [CrossRef]
27. Paulay, G.; O'Mahoney, M.J.V. BBPS179-19.COI-5P. Available online: http://www.boldsystems.org/index.php/Public_RecordView?processid=BBPS179-19 (accessed on 20 December 2023).
28. Alves, P.R.; Halanych, K.M.; Silva, E.P.; Santos, C.S.G. Nereididae (Annelida) Phylogeny Based on Molecular Data. *Org. Divers. Evol.* **2023**, *23*, 529–541. [CrossRef]
29. Cejp, B.; Ravara, A.; Aguado, M.T. First Mitochondrial Genomes of Chrysopetalidae (Annelida) from Shallow-Water and Deep-Sea Chemosynthetic Environments. *Gene* **2022**, *815*, 146159. [CrossRef] [PubMed]
30. Alves, P.R.; Halanych, K.M.; Santos, C.S.G. The Phylogeny of Nereididae (Annelida) Based on Mitochondrial Genomes. *Zool. Scr.* **2020**, *49*, 366–378. [CrossRef]
31. Villalobos-Guerrero, T.F.; Huč, S.; Tilic, E.; Hiley, A.S.; Rouse, G.W. A Remarkable New Deep-Sea Nereidid (Annelida: Nereididae) with Gills. *PLoS ONE* **2024**, *in press*.
32. Li, X.; Yang, D.; Qiu, J.-W.; Liu, P.; Meng, D.; Zhu, H.; Guo, L.; Luo, S.; Wang, Z.; Ke, C. Mitochondrial Genome of *Leocrates chinensis* Kinberg, 1866 (Annelida: Hesionidae). *Mitochondrial DNA Part B* **2023**, *8*, 172–176. [CrossRef] [PubMed]
33. Ruta, C.; Nygren, A.; Rousset, V.; Sundberg, P.; Tillier, A.; Wiklund, H.; Pleijel, F. Phylogeny of Hesionidae (Aciculata, Polychaeta), Assessed from Morphology, 18S RDNA, 28S RDNA, 16S RDNA and COI. *Zool. Scr.* **2007**, *36*, 99–107. [CrossRef]
34. Richter, S.; Schwarz, F.; Hering, L.; Böggemann, M.; Bleidorn, C. The Utility of Genome Skimming for Phylogenomic Analyses as Demonstrated for Glycerid Relationships (Annelida, Glyceridae). *Genome Biol. Evol.* **2015**, *7*, 3443–3462. [CrossRef] [PubMed]
35. Chen, X.; Li, M.; Liu, H.; Li, B.; Guo, L.; Meng, Z.; Lin, H. The Complete Mitochondrial Genome of the Polychaete, *Goniada japonica* (Phyllodocida, Goniadidae). *Mitochondrial DNA Part A* **2016**, *27*, 2850–2851. [CrossRef]
36. Kearse, M.; Moir, R.; Wilson, A.; Stones-Havas, S.; Cheung, M.; Sturrock, S.; Buxton, S.; Cooper, A.; Markowitz, S.; Duran, C.; et al. Geneious Basic: An Integrated and Extendable Desktop Software Platform for the Organization and Analysis of Sequence Data. *Bioinformatics* **2012**, *28*, 1647–1649. [CrossRef]
37. Bolger, A.M.; Lohse, M.; Usadel, B. Trimmomatic: A Flexible Trimmer for Illumina Sequence Data. *Bioinformatics* **2014**, *30*, 2114–2120. [CrossRef]
38. Allio, R.; Schomaker-Bastos, A.; Romiguier, J.; Prosdocimi, F.; Nabholz, B.; Delsuc, F. MitoFinder: Efficient Automated Large-Scale Extraction of Mitogenomic Data in Target Enrichment Phylogenomics. *Mol. Ecol. Resour.* **2020**, *20*, 892–905. [CrossRef]
39. Li, D.; Luo, R.; Liu, C.M.; Leung, C.M.; Ting, H.F.; Sadakane, K.; Yamashita, H.; Lam, T.W. MEGAHIT v1.0: A Fast and Scalable Metagenome Assembler Driven by Advanced Methodologies and Community Practices. *Methods* **2016**, *102*, 3–11. [CrossRef] [PubMed]
40. Laslett, D.; Canbäck, B. ARWEN: A Program to Detect TRNA Genes in Metazoan Mitochondrial Nucleotide Sequences. *Bioinformatics* **2008**, *24*, 172–175. [CrossRef]
41. Dierckxsens, N.; Mardulyn, P.; Smits, G. NOVOPlasty: De Novo Assembly of Organelle Genomes from Whole Genome Data. *Nucleic Acids Res.* **2017**, *45*, e18. [CrossRef] [PubMed]
42. Meng, G.; Li, Y.; Yang, C.; Liu, S. MitoZ: A Toolkit for Animal Mitochondrial Genome Assembly, Annotation and Visualization. *Nucleic Acids Res.* **2019**, *47*, e63. [CrossRef]
43. Bernt, M.; Donath, A.; Jühling, F.; Externbrink, F.; Florentz, C.; Fritzsch, G.; Pütz, J.; Middendorf, M.; Stadler, P.F. MITOS: Improved de Novo Metazoan Mitochondrial Genome Annotation. *Mol. Phylogenetics Evol.* **2013**, *69*, 313–319. [CrossRef]

44. Hahn, C.; Bachmann, L.; Chevreux, B. Reconstructing Mitochondrial Genomes Directly from Genomic Next-Generation Sequencing Reads—A Baiting and Iterative Mapping Approach. *Nucleic Acids Res.* **2013**, *41*, e129. [CrossRef]
45. Li, H. Minimap2: Pairwise Alignment for Nucleotide Sequences. *Bioinformatics* **2018**, *34*, 3094–3100. [CrossRef]
46. Li, H. New Strategies to Improve Minimap2 Alignment Accuracy. *Bioinformatics* **2021**, *37*, 4572–4574. [CrossRef]
47. Danecek, P.; Bonfield, J.K.; Liddle, J.; Marshall, J.; Ohan, V.; Pollard, M.O.; Whitwham, A.; Keane, T.; McCarthy, S.A.; Davies, R.M.; et al. Twelve Years of SAMtools and BCFtools. *Gigascience* **2021**, *10*, giab008. [CrossRef]
48. Untergasser, A.; Cutcutache, I.; Koressaar, T.; Ye, J.; Faircloth, B.C.; Remm, M.; Rozen, S.G. Primer3—New Capabilities and Interfaces. *Nucleic Acids Res.* **2012**, *40*, e115. [CrossRef]
49. Edgar, R.C. MUSCLE: Multiple Sequence Alignment with High Accuracy and High Throughput. *Nucleic Acids Res.* **2004**, *32*, 1792–1797. [CrossRef]
50. Swofford, D. *PAUP**; Version 4.0b10; Phylogenetic Analysis Using Parsimony (*and Other Methods); Oxford University Press: Oxford, UK, 2002.
51. Maddison, W.P.; Maddison, D.R. Mesquite: A Modular System for Evolutionary Analysis. Version 3.61. Available online: http://www.mesquiteproject.org (accessed on 26 December 2023).
52. Katoh, K.; Misawa, K.; Kuma, K.I.; Miyata, T. MAFFT: A Novel Method for Rapid Multiple Sequence Alignment Based on Fast Fourier Transform. *Nucleic Acids Res.* **2002**, *30*, 3059–3066. [CrossRef]
53. Edgar, R.C. Quality Measures for Protein Alignment Benchmarks. *Nucleic Acids Res.* **2010**, *38*, 2145–2153. [CrossRef]
54. Edler, D.; Klein, J.; Antonelli, A.; Silvestro, D. RaxmlGUI 2.0: A Graphical Interface and Toolkit for Phylogenetic Analyses Using RAxML. *Methods Ecol. Evol.* **2020**, *12*, 373–377. [CrossRef]
55. Rambaut, A. FigTree. Available online: http://tree.bio.ed.ac.uk/software/figtree/ (accessed on 11 March 2021).
56. Leigh, J.W.; Bryant, D. POPART: Full-Feature Software for Haplotype Network Construction. *Methods Ecol. Evol.* **2015**, *6*, 1110–1116. [CrossRef]
57. Bernt, M.; Merkle, D.; Middendorf, M. An Algorithm for Inferring Mitogenome Rearrangements in a Phylogenetic Tree. In *RECOMB International Workshop on Comparative Genomics, Proceedings of the Comparative Genomics, Paris, France, 13–15 October 2008*; Nelson, C.E., Vialette, S., Eds.; Springer: Berlin/Heidelberg, Germany, 2008; pp. 143–157.
58. Bernt, M.; Merkle, D.; Ramsch, K.; Fritzsch, G.; Perseke, M.; Bernhard, D.; Schlegel, M.; Stadler, P.F.; Middendorf, M. CREx: Inferring Genomic Rearrangements Based on Common Intervals. *Bioinformatics* **2007**, *23*, 2957–2958. [CrossRef]
59. von Haeseler, A.; Schmidt, H.A.; Bui, M.Q.; Nguyen, L.T. IQ-TREE: A Fast and Effective Stochastic Algorithm for Estimating Maximum-Likelihood Phylogenies. *Mol. Biol. Evol.* **2014**, *32*, 268–274.
60. Chernomor, O.; von Haeseler, A.; Minh, B.Q. Terrace Aware Data Structure for Phylogenomic Inference from Supermatrices. *Syst. Biol.* **2016**, *65*, 997–1008. [CrossRef] [PubMed]
61. Kalyaanamoorthy, S.; Minh, B.Q.; Wong, T.K.F.; Von Haeseler, A.; Jermiin, L.S. ModelFinder: Fast Model Selection for Accurate Phylogenetic Estimates. *Nat. Methods* **2017**, *14*, 587–589. [CrossRef]
62. Shimodaira, H. An Approximately Unbiased Test of Phylogenetic Tree Selection. *Syst. Biol.* **2002**, *51*, 492–508. [CrossRef] [PubMed]
63. Ribeiro, R.P.; Barbosa, A.D.C.; Freitas, R.; Zanol, J.; Glasby, C.J.; Ruta, C. Pilargidae (Annelida: Phyllodocida) from Coastal and Deep Waters of the Southwestern Atlantic, with Descriptions of Two New Species. *Zootaxa* **2020**, *4878*, 056–076. [CrossRef]
64. Hartman, O. Polychaetous Annelids, Part VIII: Pilargiidae. In *Allan Hancock Pacific Expeditions*; University of Southern California Press: Los Angeles, CA, USA, 1947; Volume 10, pp. 483–523.
65. Glasby, C.J.; Hocknull, S.A. New Records and a New Species of *Hermundura* Müller, 1858, the Senior Synonym of *Loandalia* Monro, 1936 (Annelida: Phyllodocida: Pilargidae) from Northern Australia and New Guinea. *Beagle Rec. Mus. Art Gall. N. Territ.* **2010**, *26*, 57–67.
66. Salazar-Vallejo, S.; Bailey Brock, J.H.; Dreyer, J.C. Revision of *Pseudexogone* Augener, 1922 (Annelida, Polychaeta, Syllidae), and Its Transfer to Pilargidae. *Zoosystema* **2007**, *29*, 535–553.
67. Vallès, Y.; Halanych, K.M.; Boore, J.L. Group II Introns Break New Boundaries: Presence in a Bilaterian's Genome. *PLoS ONE* **2008**, *3*, e1488. [CrossRef] [PubMed]
68. Saint-Joseph, A. d'Anthoine de Note Sur Une Nouvelle Famille d'Annélides Polychètes. *Bull. Muséum D'histoire Nat. Paris* **1899**, *5*, 41–42.
69. Webster, H.E. The Annelida Chaetopoda of the Virginian Coast. *Trans. Albany Inst.* **1879**, *9*, 202–269.
70. McIntosh, W.C. On the Annelida Obtained during the Cruise of H.M.S. 'Valorous' to Davis Strait in 1875. *Trans. Linn. Soc. London. Second. Ser. Zool.* **1878**, *1*, 499–511. [CrossRef]
71. Misra, A. Polychaete Fauna of West Bengal. In *Zoological Survey of India*; Gosh, A.K., Ed.; Director: Calcutta, India, 1999; Volume 10, pp. 125–225.
72. Ditlevsen, H.; Annelids, I. *The Danish Ingolf Expedition*; Nature Publishing Group: Copenhagen, Denmark, 1917; Volume 4, pp. 1–71.
73. Friedrich, H. Zwei Neue Bestandteile in Der Fauna Der Nordsee. *Zool. Anz.* **1950**, *145*, 171–177.
74. Müller, F. Einiges Über Die Annelidenfauna Der Insel Santa Catharina an Der Brasilianischen Küste. *Arch. Naturgeschichte* **1858**, *24*, 211–220.

75. Pearson, T.H. *Litocorsa stremma* a New Genus and Species of Pilargid (Polychaeta: Annelida) from the West Coast of Scotland, with Notes on Two Other Pilargid Species. *J. Nat. Hist.* **1970**, *4*, 69–77. [CrossRef]
76. Augener, H. Litorale Polychaeten von Juan Fernandez. In *The Natural History of Juan Fernandez and Easter Island*; Creative Media Partners, LLC: Sheridan, WY, USA, 1922; Volume 3.2, pp. 161–218.
77. Chamberlin, R.V. *The Annelida Polychaeta*; The Museum of Comparative Zoology at Harvard College: Cambridge, MA, USA, 1919; Volume 48.
78. Fauvel, P. Annelida Polychaeta of the Indian Museum, Calcutta. In *Memoirs of the Indian Museum*; Manager of Publications: Calcutta, India, 1932; Volume 12, pp. 1–261.
79. Salazar-Vallejo, S.I.; Nishi, E.; Anguspanich, S. Rediscovery of *Talehsapia annandalei* (Polychaeta: Pilargidae) in Songkhla Lagoon, Thailand. *Pac. Sci.* **2001**, *55*, 267–273. [CrossRef]
80. Pettibone, M.H. Revision of the Pilargidae (Annelida: Polychaeta), Including Descriptions of New Species, and Redescriptions of the Pelagic Podarmus ploa Chamberlain (Polynoidae). In *Proceedings of the United States National Museum*; Smithsonian Institution Press: Washington, DC, USA, 1966; Volume 118, pp. 155–207.
81. Mandal, S.; Harkantra, S.N.; Salazar-Vallejo, S.I. *Cabira rangarajani* n. sp. (Polychaeta: Pilargidae) from the Goa Coast, Central West Coast of India. *Zootaxa* **2007**, *1446*, 21–29. [CrossRef]
82. Plathong, J.; Dean, H.K.; Plathong, S. Four New Species of Pilargidae (Annelida: Pilarginae) from the Gulf of Thailand. *Zootaxa* **2021**, *5071*, 537–562. [CrossRef]
83. Licher, F. Resurrection of *Glyphohesione* Friedrich, 1950, with Redescription of *G. klatti* Friedrich, 1950 and Description of *G. longocirrata* (Polychaeta: Hesionidae). *Proc. Biol. Soc. Wash.* **1994**, *107*, 600–608.
84. Salazar-Vallejo, S.I. Revision of *Synelmis* Chamberlin, 1919 (Annelida, Polychaeta, Pilargidae). *Zoosystema* **2003**, *25*, 17–42.
85. Ehlers, E. Polychaeten von Java Und Amboina. Ein Beitrag Zur Kenntnis Der Malaiischen Strandfauna. In *Abhandlungen der koeniglichen Gesellschaft der Wissenschaften zu Goettingen, Ser. neue folge*; Forgotten Books: London, UK, 1920; Volume 10, pp. 1–73.
86. Aguado, M.T. Antonbruunidae Fauchald, 1977. In *Handbook of Zoology. Annelida Vol. 4: Pleistoannelida, Errantia II, Phyllodocida*; Purschke, G., Boggemann, M., Westheide, W., Eds.; De Gruyter: Berlin, Germany, 2022; pp. 394–399.
87. Katzmann, W.; Laubier, L.; Ramos, J. Pilargidae (Annélides Polychètes Errantes) de Méditerranée. *Bull. L'institute Océanographique* **1974**, *71*, 1–40.
88. Uschakov, P. V A New Deep-Water Species of *Otopsis* (Polychaeta, Pilargidae) from the Kurile-Kamtchatka Trench. *Zool. Zhurnal* **1971**, *50*, 279–281.
89. Salazar-Vallejo, S.I.; De León-González, J.A.; Carrera-Parra, L.F. Phylogeny of Microphthalminae Hartmann-Schröder, 1971, and Revision of *Hesionella* Hartman, 1939, and *Struwela* Hartmann-Schröder, 1959 (Annelida, Errantia). *PeerJ* **2019**, *7*, e7723. [CrossRef]
90. Darbyshire, T.; Mackie, A.S.Y. Species of *Litocorsa* (Polychaeta: Pilargidae) from the Indian Ocean and South China Sea. *Hydrobiologia* **2003**, *496*, 63–73. [CrossRef]
91. Monro, C.C.A. *Polychaete Worms II*; Discovery Reports; Cambridge University Press: Cambridge, UK, 1936; Volume 12, pp. 59–197.
92. Marks, S.; Hocknull, S. New Species of *Loandalia* (Polychaeta: Pilargidae) from Queensland, Australia. *Zootaxa* **2006**, *1119*, 59–68. [CrossRef]
93. Hartmann-Schröder, G. Zur Ökologie Der Polychaeten Des Mangrove-Estero-Gebietes von El Salvador. *Beitr. Neotropischen Fauna* **1959**, *1*, 69–183. [CrossRef]
94. Emerson, R.R.; Fauchald, K. A Revision of the Genus *Loandalia* Monro with Description of a New Genus and Species of Pilargiid Polychaete. *Bull. South. Calif. Acad. Sci.* **1971**, *70*, 18–22.
95. Solis-Weiss, V. *Parandalia bennei* (Pilargidae) and *Spiophanes lowai* (Spionidae), New Species of Polychaetous Annelids from Mazatlan Bay, Pacific Coast of Mexico. *Proc. Biol. Soc. Wash.* **1983**, *96*, 370–378.
96. Berkeley, E.; Berkeley, C. On a Collection of Polychaeta from Southern California. *Bull. South. Calif. Acad. Sci.* **1941**, *40*, 16–60.
97. Thomas, P.J. Polychaetous Worms from the Arabian Sea, 1: A New Species of the Genus *Loandalia* Monro. *Bull. Dep. Mar. Biol. Oceanogr.* **1963**, *1*, 29–34.
98. Intes, A.; Le Loeuff, P. Les Annélides Polychètes de Côte d'Ivoire. I. Polychètes Errantes—Compte Rendu Systématique. *Cah. ORSTOM Série Océanographie* **1975**, *13*, 267–321.
99. León-González, J.A. de Poliquetos de Fondos Blandos de La Costa Occidental de Baja California Sur, Mexico. I. Pilargidae. *Cah. Biol. Mar.* **1991**, *32*, 311–321.
100. Salazar-Vallejo, S.I.; Reyes-Barragán, M.P. *Parandalia vivianneae* n. sp. and *P. tricuspis* (Müller), Two Estuarine Polychaetes (Polychaeta: Pilargidae) from Eastern Mexico. *Rev. Biol. Trop.* **1990**, *38*, 87–90.
101. Struck, T.H.; Golombek, A.; Hoesel, C.; Dimitrov, D.; Elgetany, A.H. Mitochondrial Genome Evolution in Annelida—A Systematic Study on Conservative and Variable Gene Orders and the Factors Influencing Its Evolution. *Syst. Biol.* **2023**, *72*, 925–945. [CrossRef]
102. Britayev, T.A.; Zamishliak, E.A. Association of the Commensal Scaleworm *Gastrolepidia clavigera* (Polychaeta: Polynoidae) with Holothurians near the Coast of South Vietnam. *Ophelia* **1996**, *45*, 175–190. [CrossRef]
103. Ruff, R.E. A New Species of *Bathynoe* (Polychaeta: Polynoidae) from the Northeast Pacific Ocean Commensal with Two Species of Deep-Water Asteroids. *Ophelia Suppl.* **1991**, *5*, 219–230.
104. Martin, D.; Rosell, D.; Uriz, M.J. *Harmothoe hyalonemae* sp. nov. (Polychaeta, Polynoidae), an Exclusive Inhabitant of Different Atlanto-Mediterranean Species of *Hyalonema* (Porifera, Hexactinellida). *Ophelia* **1992**, *35*, 169–185. [CrossRef]

105. Tilic, E.; Rouse, G.W. Hardly Venus's Servant—Morphological Adaptations of *Veneriserva* to an Endoparasitic Lifestyle and Its Phylogenetic Position within Dorvilleidae (Annelida). *Org. Divers. Evol.* **2024**. [CrossRef]
106. Dimock, R.V.J. Intraspecific Agression and the Distribution of a Symbiotic Polychaete on Its Hosts. In *Proceedings of the Symbiosis in the Sea*; Vernberg, W.B., Ed.; University or South Carolina Press: Columbia, SC, USA, 1974; pp. 29–44.
107. Pernet, B.; Jaeckle, W.B. Size and Organic Content of Eggs of Marine Annelids, and the Underestimation of Egg Energy Content by Dichromate Oxidation. *Biol. Bull.* **2004**, *207*, 67–71. [CrossRef] [PubMed]
108. McHugh, D.; Fong, P.P. Do Life History Traits Account for Diversity of Polychaete Annelids? *Invertebr. Biol.* **2002**, *121*, 325–338. [CrossRef]
109. Rouse, G.W.; Scripps Institution of Oceanography, UCSD, La Jolla, CA, USA. Personal Observation, 2020.
110. Dall, W.H. On Some New or Interesting West American Shells Obtained from the Dredgings of the U.s. Fish Commission Steamer Albatross in 1888, and from Other Sources. In *Proceedings of the United States National Museum*; Smithsonian Institution Press; Washington, DC, USA, 1891; Volume 14, pp. 173–191.
111. Suzuki, K. Three New Species of Non-Marine Shells from the Tertiary Formations of Hokkaidō and Karahuto. *Jpn. J. Geol. Geogr.* **1941**, *18*, 53–58.
112. Taboada, S.; Silva, A.S.; Neal, L.; Cristobo, J.; Ríos, P.; Álvarez-Campos, P.; Hestetun, J.T.; Koutsouveli, V.; Sherlock, E.; Riesgo, A. Insights into the Symbiotic Relationship between Scale Worms and Carnivorous Sponges (Cladorhizidae, *Chondrocladia*). *Deep. Sea Res. Part I Oceanogr. Res. Pap.* **2020**, *156*, 103191. [CrossRef]
113. Eeckhaut, I.; Fievez, L.; Müller, M.C.M. Larval Development of *Myzostoma cirriferum* (Myzostomida). *J. Morphol.* **2003**, *258*, 269–283. [CrossRef]
114. Rouse, G.W.; Grygier, M.J. *Myzostoma seymourcollegiorum* n. sp. (Myzostomida) from Southern Australia, with a Description of Its Larval Development. *Zootaxa* **2005**, *1010*, 53–64. [CrossRef]
115. Salazar-Vallejo, S.I.; Harris, L.H. Revision of *Pilargis* de Saint-Joseph, 1899 (Annelida, Polychaeta, Pilargidae). *J. Nat. Hist.* **2006**, *40*, 119–159. [CrossRef]
116. Carr, C.M.; Hardy, S.M.; Brown, T.M.; Macdonald, T.A.; Hebert, P.D.N. A Tri-Oceanic Perspective: DNA Barcoding Reveals Geographic Structure and Cryptic Diversity in Canadian Polychaetes. *PLoS ONE* **2011**, *6*, e22232. [CrossRef] [PubMed]
117. Sjölin, E.; Erséus, C.; Källersjö, M. Phylogeny of Tubificidae (Annelida, Clitellata) Based on Mitochondrial and Nuclear Sequence Data. *Mol. Phylogenetics Evol.* **2005**, *35*, 431–441. [CrossRef] [PubMed]
118. Palumbi, S.R. Nucleic Acids II: The Polymerase Chain Reaction. In *Molecular Systematics*, 2nd ed.; Sinauer: Sunderland, MA, USA, 1996; pp. 205–247.
119. Palumbi, S.R.; Martin, A.; Romano, S.; McMillan, W.O.; Stice, L.; Grabowski, G. *The Simple Fool's Guide to PCR*; University of Hawaii: Honolulu, HI, USA, 1991.
120. Giribet, G.; Carranza, S.; Baguna, J.; Riutort, M.; Ribera, C. First Molecular Evidence for the Existence of a Tardigrada + Arthropoda Clade. *Mol. Biol. Evol.* **1996**, *13*, 76–84. [CrossRef]
121. Whiting, M.F.; Carpenter, J.C.; Wheeler, Q.D.; Ard, V. The Strepsiptera Problem: Phylogeny of the Holometabolous Insect Orders Inferred from 18S and 28S Ribosomal DNA Sequences and Morphology. *Syst. Biol.* **1997**, *46*, 1–68. [CrossRef]

Disclaimer/Publisher's Note: The statements, opinions and data contained in all publications are solely those of the individual author(s) and contributor(s) and not of MDPI and/or the editor(s). MDPI and/or the editor(s) disclaim responsibility for any injury to people or property resulting from any ideas, methods, instructions or products referred to in the content.